TECHNISCHE UNIVERSITÄT WIEN

VIENNA UNIVERSITY OF TECHNOLOGY

PhD Thesis

Dissertation

COMPONENTS FOR VISIBLE CURABLE FORMULATIONS WITH LOW OXYGEN INHIBITION

ausgeführt zum Zwecke der Erlangung des akademischen Grades eines Doktors der technischen Wissenschaften unter der Leitung von

Ao. Univ. Prof. Dr. Robert Liska

Institut für Angewandte Synthesechemie

Technische Universität Wien

von

Michael Höfer

9725703

Hötzendorfstraße 9

2231 Strasshof

Wien, am 10.12.2009

An dieser Stelle möchte ich meinem Betreuer Robert Liska meinen Dank ausdrücken, dessen Ideen, Motivation und Unterstützung maßgeblich zu meiner gesamten Arbeit beigetragen haben.

Bei Herrn Heinrich Gruber möchte ich mich für die Aufnahme am Institut für angewandte Synthesechemie und sein fortlaufendes Interesse an meiner Arbeit bedanken.

Insbesonders gilt mein Dank Simone Knaus für die Unterbringung und freundliche Duldung eines mit „Mikromengen“ arbeitenden Photochemikers in ihrem Stockwerk.

Des weiteren möchte ich meinen aktuellen und ehemaligen Stockwerks- und Instituts-Kollegen Katrin Fizor, Sabine Unger, Markus Adelwöhrer, Dzanana Dautefendic, Niklas Pucher, Christian Heller, Parichehr Esfandiari, Astrid Gugg, Claudia Dworak, Stefan Baudis, Andreas Mautner, Lidija Spoljaric-Lukacic, Gerald Ullrich, Bernhard Seidl, Thomas Verdianz, Stefan Kopeinig, Monika Schuster, Kadiriye Icten, Claudia Pich, Sonja Landertshamer und vielen anderen für das nette Arbeitsklima, Ratschläge und Hilfe, Kuchenspenden und die Ablenkung von der Arbeit danken.

Mein besonderer Dank gilt Alexander Liska, der mir die nötigen Fähigkeiten beigebracht hat auf einem „weiblich dominierten“ Stockwerk zu überleben, Walter Dazinger, der mir im Kampf gegen das Mysterium Software zur Seite gestanden hat, sowie meiner langjährigen und schmerzlich vermissten Laborkollegin Sigrid Jauk.

Für die finanzielle Unterstützung meiner Arbeit durch den FWF (P18623-N17), möchte ich mich herzlich bedanken.

Mein ganz spezieller Dank richtet sich schließlich an meine Eltern, die mir das Studium ermöglicht und mich immer vorbehaltlos unterstützt haben, an meine beiden Brüder Christian und Andreas, sowie an meine Großeltern, die mich in besonders stressigen Zeiten vor einem möglichen Hungertod bewahrt haben.

ABSTRACT

Inhibition of free radical polymerization by molecular oxygen is one of the most challenging problems in UV-Vis curable coatings. Apart from the utilization of an inert gas atmosphere, additives to reduce the oxygen inhibition due to production of new propagating centers are used to compensate the severe impact on curing speed and mechanical properties of cured surfaces. In comparison to the well established, omnipresent radical photocuring, one of the most tempting features of cationic photopolymerization is a total absence of inhibition by molecular oxygen. However, in the field of UV-Vis curing applications, cationic photopolymerization can be regarded as a niche technique and still demands additional efforts in research and development to enhance its potential.

The purpose of this research work was to meet both challenges in radical and cationic photopolymerization of UV-Vis curing applications. In regard to radical photocuring, a straightforward approach to reduce the oxygen inhibition by photosensitized generation of singlet oxygen and subsequent scavenging of this species by selective singlet oxygen trappers was investigated. For a possible application of this technique without use of colored sensitizers in UV-Vis curing, conjugated and bathochromic shifted furan derivatives were synthesized and tested on their reactivity as oxygen scavengers.

To enhance the field of possible initiating systems in cationic UV-Vis curing, a new class of onium salt initiators based on diphenyl(phenylethynyl)sulfonium and phenyl(phenylethynyl)iodonium salts as well as the new, photo-bleaching sensitizer 9,10-dibutylanthracene were examined. Apart from analysis of the photo-cleavage mechanism of the onium salts, the base structures as well as bathochromic shifted and conjugated derivatives were investigated on their reactivity as cationic photoinitiator systems in direct and sensitized irradiation.

KURZFASSUNG

Die Inhibierung der freien radikalischen Polymerisation durch molekularen Sauerstoff ist eine der größten Herausforderungen in der technischen Aushärtung von Beschichtungen mit sichtbarem- oder nahem UV-Licht. Abgesehen von der Verwendung von Schutzgas-Atmosphären werden Additive, die neue reaktive Zentren bilden eingesetzt, um die Inhibierung durch Sauerstoff - und die damit einhergehende starke Verringerung der Aushärtungsgeschwindigkeit und der mechanischen Eigenschaften - zu unterbinden. Im Vergleich zur gut etablierten, weit verbreiteten radikalischen Lichthärtung stellt die völlige Absenz der Inhibierung durch Sauerstoff eine der attraktivsten Eigenschaften der kationischen Polymerisation dar. In der technischen Anwendung lichthärtender Systeme muss die kationische Photopolymerisation jedoch als eine Nischen-Technik betrachtet werden, die noch immer zusätzliche Anstrengungen im Bereich der Forschung und Entwicklung benötigt um ihr Potential zu vergrößern.

Ziel und Zweck dieser Arbeit war die Weiterentwicklung sowohl radikalischer, als auch kationischer Polymerisationstechniken im Bereich der lichtinduzierten Härtung von Beschichtungen mit Lichtquellen für sichtbares- oder nahes UV-Licht. In Hinblick auf radikalische Lichthärtung wurde die photosensibilisierte Generierung von Singulett-Sauerstoff mit anschließender rascher chemischer Bindung durch selektive Singulett-Sauerstofffänger, als direkter Ansatz die Inhibierung durch Sauerstoff zu verringern, untersucht. Für einen möglichen Einsatz dieser Technik unter Verzicht auf stark gefärbte Sensibilisatoren wurden konjugierte und bathochrom verschobene Furanderivate dargestellt und auf ihre Reaktivität als Sauerstofffänger getestet.

Um das verfügbare Repertoire an photoinitiierenden Systemen für die kationische lichtinduzierte Härtung zu vergrößern, wurde eine neue Klasse von Onium-Initiatoren basierend auf Diphenyl(phenylethinyl)sulfonium und Phenyl(phenylethinyl)iodonium Salzen, sowie der neue, photo-bleichende Sensibilisator 9,10-Dibutylanthracen untersucht. Abgesehen von der Aufklärung des lichtinduzierten Spaltungsmechanismus der Onium-Salze wurden die Basisstrukturen sowie konjugierte und bathochrom verschobene Derivate auf ihre Reaktivität als Photoinitiator-Systeme in direkter und sensibilisierter Anregung getestet.

Table of Contents

		Experimental
Introduction	3	
Objective	22	
Results and Discussion	24	94
Part 1: Oxygen scavengers	24	94
1. State of the art	24	
2. Selection of oxygen scavengers for UV-Vis curing	27	
3. Synthesis of oxygen scavengers	29	94
3.1 Synthesis of 9,10-dibutyl-anthracene (**1**, **DBA**)	29	94
3.2 Synthesis of symmetrically substituted furan derivatives	30	95
3.2.1 Synthesis of 2,5-dibromo-furan (**2**)		95
3.2.2 Synthesis of 4-*N*,*N*-dimethylaminophenyl boronic acid (**3**)		96
3.2.3 Synthesis of 2,5-bis-[4-(*N*,*N*-dimethylamino)-phenyl]-furan (**4**)		98
3.2.4 Synthesis of 2,5-bis-(phenylethynyl)-furan (**5**)		99
4. Storage Stability	32	100
5. UV-Vis Spectroscopy	32	
6. Sensitized Steady State Photooxidation (SSSP)	34	101
7. Photopolymerization	36	102
Part 2: Cationic initiators	40	108
1. State of the art	40	
2. Onium salt base structures	47	108
2.1 Synthesis of onium salts as reference initiators (**TPS-T**)	47	108
2.2 Synthesis of diphenyl(phenylethynyl)sulfonium salts (**1T**)	48	109
2.3 Synthesis of phenyl(phenylethynyl)iodonium salts (**2T**)	50	111
2.4 Ion exchange	50	112
2.5 Quantification of ion exchange by IR spectroscopy	52	115
2.6 UV-Vis Spectroscopy	52	
2.7 Photolysis and thermal decomposition	53	117
2.7.1 Synthesis of decomposition products	55	120
2.7.1.1 Synthesis of phenyl(phenylethynyl) sulfide ($\mathbf{F_2}$)		120
2.7.1.2 Synthesis of phenyl(phenylethynyl) sulfoxide ($\mathbf{F_{2,OX}}$)		121

2.7.2 Photolysis of **1P** under inert gas ... 56
2.7.3 Photolysis and thermal decomposition of **2P** under inert gas ... 60
2.7.4 Photolysis of **1P** and **2P** under air ... 62
2.8 Photo-DSC ... 63 122
3. Broad band irradiation experiments ... 67 123
3.1 UV-Vis Spectroscopy ... 68
3.2 Photo-DSC ... 70 122
4. Bathochromic shifted and conjugated sulfonium salts ... 76 124
4.1 Synthesis of bathochromic shifted and conjugated sulfonium salts ... 79 124
4.1.1 Synthesis of precursors ... 80 124
4.1.1.1 Synthesis of 4-methoxyphenyl trimethylsilyl acetylene (**6**) ... 124
4.1.1.2 Synthesis of trimethylsilylacetylene (**7**) ... 125
4.1.1.3 Synthesis of 4,4'-dibromodiphenyl sulfide (**8**) ... 126
4.1.1.4 Sonogashira couplings for the synthesis of TMS-acetylene precursors (**9-11**) ... 127
4.1.2 Synthesis of sulfonium salts (**3P - 5P**, **6T** and **7P**) ... 82 130
4.1.2.1 Synthesis of sulfonium triflates (**3T-5T**) ... 130
4.1.2.2 Ion exchange ... 133
4.1.2.3 Synthesis of (2-isopropoxy-2-phenyl-vinyl)-diphenyl-sulfonium hexafluorophosphate (**7P**) ... 135
4.3 UV-Vis Spectroscopy ... 85
4.4 Photo-DSC ... 86 122
Materials and Methods ... 137
Conclusion ... 140
Abbreviations ... 144
References ... 146

Introduction

In curing of coating and resins, the development of tailor-made systems for the applied components is a prerequisite for an optimization of the procedure in respect to ecological and economical means. In the past decades, responsible management of natural, energetic and environmental resources has significantly increased in relevance in modern manufacturing processes. Therefore, research and industry are urged to adapt long-established techniques that do not meet the new demands or substitute them by enhanced methods. The current optimization of methods in coating technology is a paramount example for this dynamic process. A short overview of conventional curing processes of coatings is presented in Figure 1.

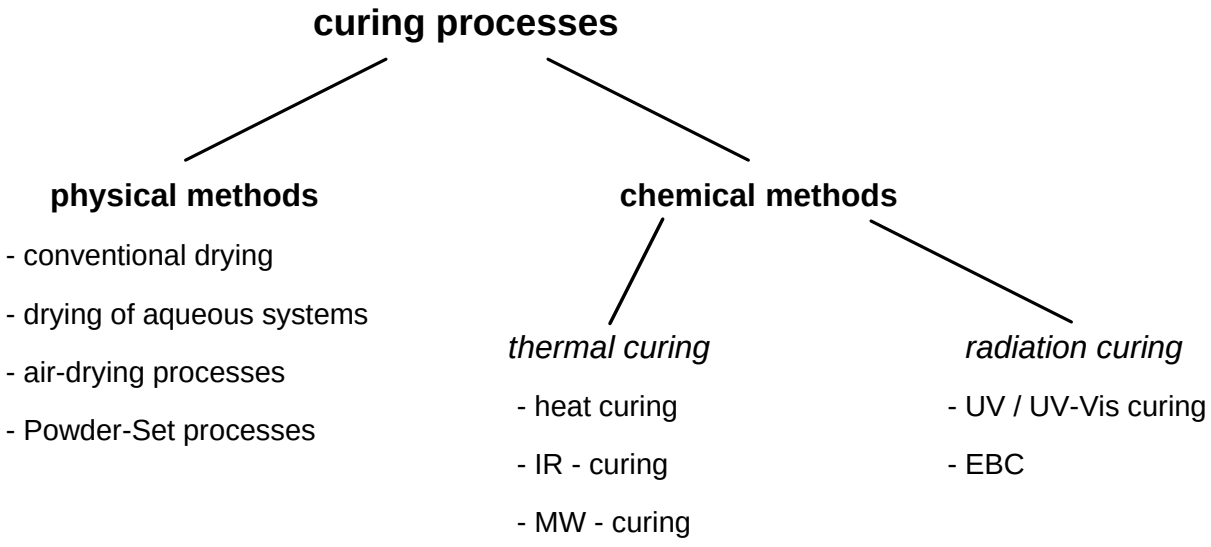

Figure 1: Curing techniques for coatings

Due to ecological and economical reasons, drying of aqueous systems and Powder-Set processes are the only physical methods left up to date. Long-established techniques like conventional drying by evaporation of organic solvents[1] were replaced by less environmentally harmful physical and chemical methods.

“Chemical Curing” is the polymerization process of a coating formulation containing an initiator and multifunctional monomers or oligomers with reactive groups. This

group of techniques contains thermal and radiation induced curing processes of polymerizable formulations,[2] but also oxidative drying (e. g. catalyzed by peroxide). EBC[3,4,5] (Electron beam curing), which exhibits an improved depth hardening and curing speed compared to common physical methods, has become an established technique in radiation curing apart from UV and UV-Vis curing. Moreover, EBC displays some significant advantages compared to UV / UV-Vis curing such as initiator free systems and enhanced rates of production. Unfortunately, high energy consumption and high expenditures on equipment often renders this method unprofitable.

The main advantages of UV / UV-Vis curing technologies are low expenditures on energy and place, the solvent-free process, high curing rates and an improved solvent resistance and mechanical properties of the film surface. These advantages are the reason for an increase of the application of UV curing techniques in spite of high investment costs for UV curing installations (Hg-medium-pressure and Hg-high-pressure lamps), shielding devices for eye and skin protection and air cleaning systems to reduce the level of generated ozone.[6]
UV and UV-Vis curable coating formulations are tailor-made systems which may contain the following components:[6]

- reactive oligomeres and polymers
  Unsaturated polyesters, acryloylated polyesters, polyethers, polyepoxides and polyurethanes

- reactive diluents
  Mono- and multifunctional (meth)acrylates and vinyl monomers
  Styrene

- UV or UV-Vis reactive components
  Photoinitiators
  Sensitizers

- Additives
  Stabilizers, inhibitors, fillers, plasticizers, antioxidants, sizing agents, wetting agents, matting agents, thixotroping agents, pigments

The reactive oligomers and polymers determine mechanical and optical properties like scratch resistance, flexural strength or adhesive strength as well as permeability and gloss. For an adjustment of the desired viscosity and as crosslinking agents, reactive diluents are applied. Apart from the cross-linking degree, flexibility and elasticity of the photo-cured film is determined by the reactive diluents.[6,7] In photo-curing, the same additives that are used in other chemical or physical curing methods are applied. In case of pigments, the maxima of light absorption must not coincide with the maximum of the photoinitiator which could impede the curing process.

The photoinitiator, that plays a key role in light induced radical polymerization, transfers irradiation to chemical energy and starts the chain reaction by formation of free radicals. This process can be subdivided into three different steps: [6]

1. Formation of a chemical reactive excited state of the initiator molecule by direct absorbance of light or by energy transfer by an excited photo-sensitizer. [8]

2. Formation of free radicals from an excited state by
   a) photo-cleavage[9,10]
   b) hydrogen abstraction from a hydrogen donor[11,12]
   c) electron transfer[13]

3. Start of the chain reaction initiated by reaction of free radicals with monomers or oligomers.[14,15]

A good match of the main emission bands of the light source with the absorption bands of the photoreactive molecule is a crucial factor for an efficient formation of excited states of a photoinitiator or a photosensitizer. For absorption of irradiation, chromophores (Table 1), which are unsaturated systems usually containing C=O - or C=N - double bonds that allow electronic excitation from $\pi \rightarrow \pi^*$ or $n \rightarrow \pi^*$ are a prerequisite.

Table 1: Absorption of chromophores

Chromophores	λ_{max} [nm] $\pi \rightarrow \pi^*$	λ_{max} [nm] $n \rightarrow \pi^*$
C=C	170	-
C=O	166	280
C=N	190	300
N=N	-	350
C=S	-	500

In a first step, an electron pair of singlet (ground) state ($\mathbf{S_0}$) is raised to an excited singlet state ($\mathbf{S_1}$*) by absorption of irradiation (hν).[16] This very short-lived excited state (<10^{-8} s) is hardly able to initiate photochemical reactions and energy degradation occurs via fluorescence or vibration relaxation. However, by "intersystem crossing" (ISC), the decisive transfer to an excited triplet state ($\mathbf{T_1}$*) (Figure 2) and relaxation to the triplet state $\mathbf{T_1}$ is possible.

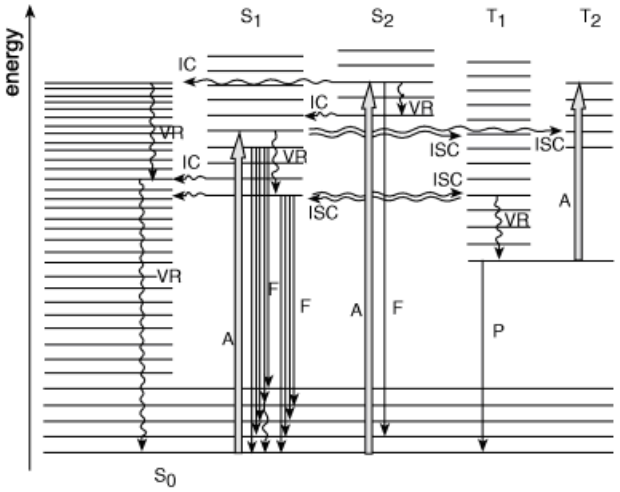

Figure 2: Simplified Jablonski-scheme:
A = absorption, excitation
F = fluorescence
P = phosphorescence
VR = vibration relaxation (radiationless deactivation)
IC = internal conversion
ISC = intersystem crossing

In the triplet states, which exhibit a significant enhanced life-time (ca. 10^{-6} s), the electron pairs possess unidirectional spin. Therefore, molecules in triplet state display distinctive features of a biradical. Inter system crossing to a triplet state may result in the formation of free radicals, but also in radiationless deactivation, phosphorescence or bimolecular quenching (for instance by oxygen). If free radicals are formed, a further degradation of the radical, recombination, termination of a chain reaction or an electron transfer as well as initiation of a new chain reaction is possible.[17]

In general, photoinitiators for radical polymerization can be divided in monomolecular (Type I) and bimolecular systems (Type II).[18] In case of Type I photoinitiators, homolytic photo-cleavage usually occurs adjacent to an aromatic carbonyl group. Thus, an aryl carbonyl radical is formed which initiates the polymerization. The most important representatives of this group of photoinitiators (Figure 3)[19] are benzoinethers (**I**), dialkoxyacetophenones (**II**), hydroxyalkylphenones (**III**), benzoylphosphineoxides (**IV**), und morpholinoketones (**V**).

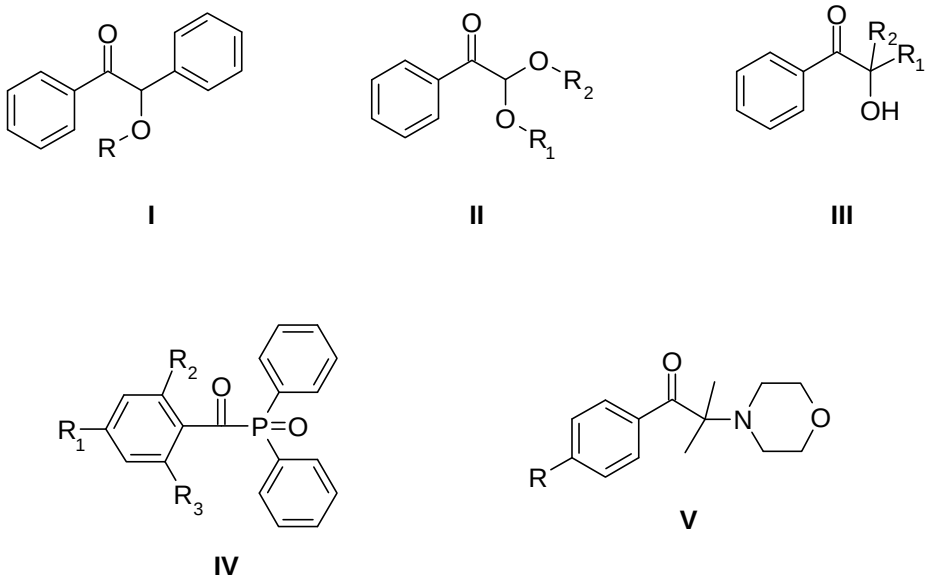

Figure 3: Type I photoinitiators

For an application in UV-Vis curable formulations, bisacylphosphinoxides are of significant importance due to their ability to absorb light in the visible part of the spectrum. An excellent overview for photoinitiators for visible light polymerization is presented by J. F. Rabek.[20]

In Figure 4, the photodecomposition scheme of the bisacylphosphinoxide Irgacure 819 is shown for illustration.

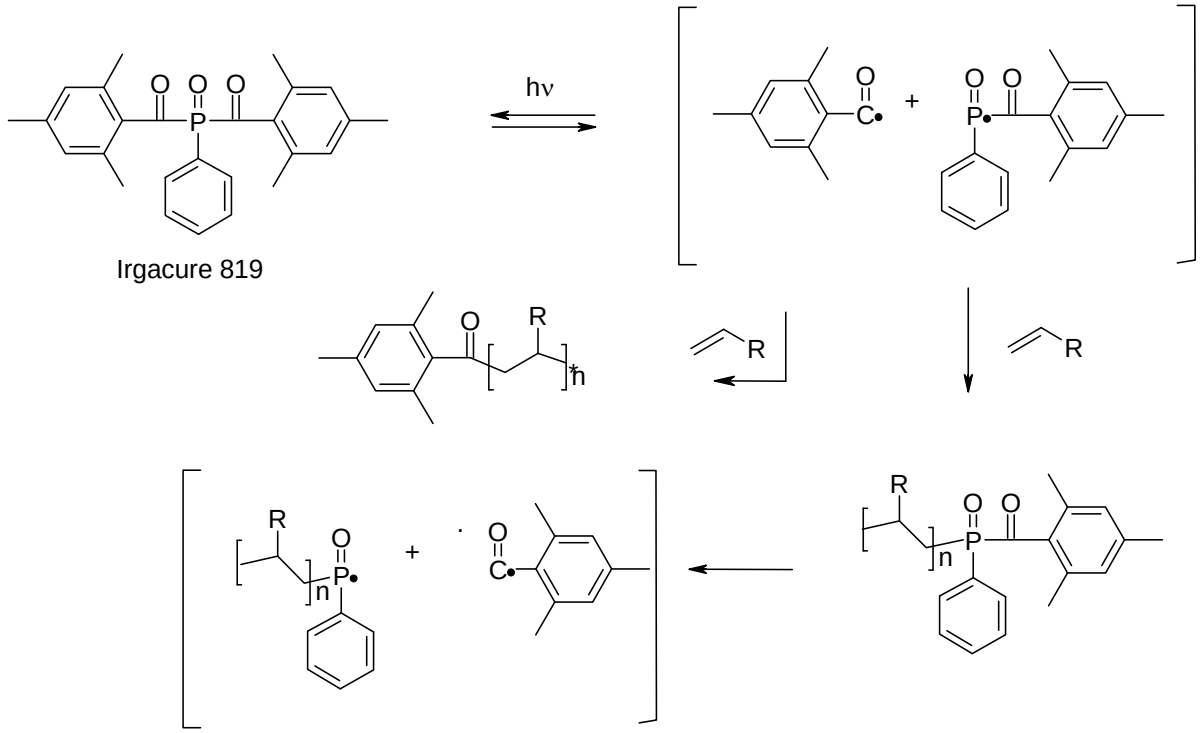

Figure 4: Photodecomposition scheme of bis(2,4,6-trimethylbenzoyl)phenylphosphinoxide (Irgacure 819)

As displayed in Figure 4, bisacylphosphinoxides decompose in two reaction steps, thus generating four radicals per molecule photoinitiator that are able to start the polymerization. Due to this decomposition mechanism, bisacylphosphineoxides are highly efficient initiators. [21]

Photoinitiators, which generate radicals by electron-proton transfer reactions or by direct hydrogen abstraction are classified as Type II, since their initiation process is bimolecular. In case of these initiators, hydrogen is usually transferred to an electronically excited ketone. Important Type II photoinitiators[19] like benzophenone (**BP**), camphorquinone (**CQ**) thioxanthones (**VI**), anthraquinones (**VII**), xanthones (**VIII**), benziles (**IX**) und ketocoumarines (**X**) are displayed in Figure 5.

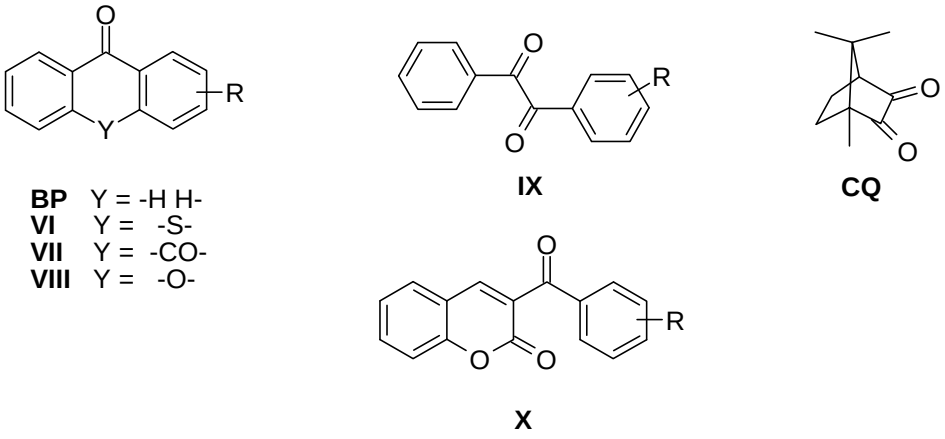

Figure 5: Type II photoinitiators

In case of electron-proton transfer reactions, electron donors like amines, which are able to transfer an electron to the photoinitiator by formation of two radical ions, are applied. In a second reaction step, radicals are generated by proton transfer. In Figure 6, this mechanism is illustrated for the system camphorquinone / ethyl 4-(dimethylamino)benzoate (**DMAB**). The initiation of the chain reaction is exclusively triggered by the amine-based radical.

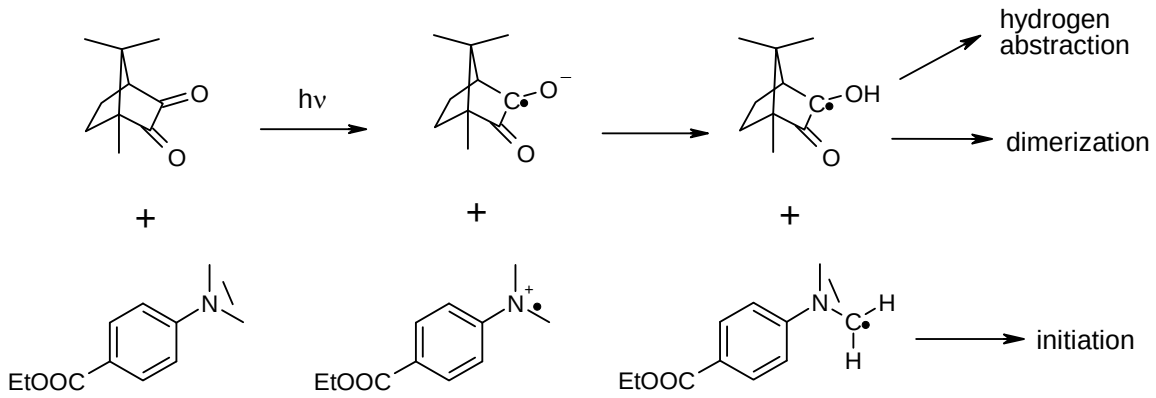

Figure 6: Electron and proton transfer of ethyl 4-(dimethylamino)benzoate to camphorquinone

As described above, Type II photoinitiators are also able to generate radicals by direct hydrogen abstraction (usually C-H adjacent to heteroatoms like N, S, O) from a coinitiator, the monomer or the growing polymer chain. In Figure 7 the mechanism of a direct hydrogen abstraction by camphorquinone is presented. In general, direct hydrogen abstraction is less efficient compared to electron-proton transfer reactions.

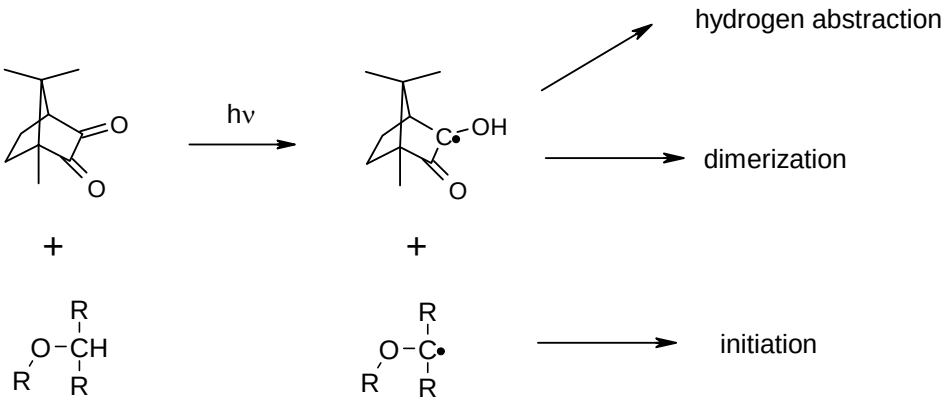

Figure 7: Direct hydrogen abstraction by camphorquinone

Due to an excellent absorption of light in the visible range of the spectrum, Type II initiators are still predominant as photoinitiators for Vis curable formulations. Unfortunately, Type II systems often display a reduced reactivity compared to Type I photoinitiators but share some fundamental problems in technical applications. One of these challenges is the **inhibition by molecular oxygen**, which is one of the most severe problems in thin film application of UV-Vis curable coatings.

Presence of oxygen in UV-curing has a severe impact on curing speed and mechanical properties of cured surfaces. In general, a prolonged inhibition period is observed, where free radicals are intercepted and the propagation of the polymer chain is inhibited. This inhibitory effect is caused by the biradical ground state of oxygen, making the molecule accessible to convert propagating radical centers to peroxy radicals (Figure 8).[22]

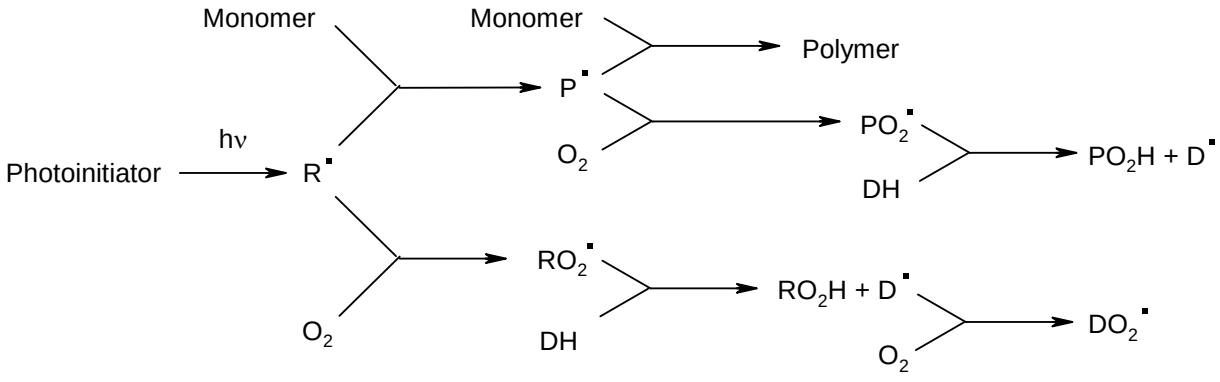

Figure 8: Oxygen inhibition in radical induced polymerization

These species show low reactivity towards polymerizable double bonds but are able to abstract hydrogen from secondary or tertiary carbon atoms. The new radical centers are significantly less reactive than the primary, propagating radicals and are able to react with oxygen in a chain process. Rather stable hydroperoxides and peroxides, which are generated by implementation of oxygen into the polymer chain, are formed and are nucleuses for an autooxidation process.

Due to the triplet ground state of molecular oxygen, an energy transfer with excited triplet states of the photoinitiator is also possible. Because of those quenching processes the average lifetime of the excited triplet states is reduced, impeding the polymerization in the initial stage, especially for Type II photoinitiator (PI) systems.

$$^1PI \xrightarrow{h\nu} {}^1PI^* \xrightarrow{ISC} {}^3PI^* \xrightarrow{^3O_2} {}^1PI + {}^1O_2^*$$

^{1}… singlet state; ^{3}… triplet state; *… excited state

The consequence of these inhibitory effects is a decrease of the rate of polymerization (R_p) and the double bond conversion (DBC) which results in the formation of tacky, insufficiently cured surfaces in thin film polymerization.[23] An excellent overview concerning oxygen inhibition in radiation curing and methods for a reduction of this effect are presented by C. Hoyle[24] and by A. B. Scranton. [25]

In the past decades, several techniques have been developed to reduce oxygen inhibition in UV-curing. A general differentiation of these techniques in physical and chemical methods is commonly used. The most efficient and commonly deployed ***physical method*** is the application of an inert gas atmosphere, usually nitrogen,[26] or in rare cases carbon dioxide[22,27] is used. The main requirement for these methods is a continuous flow of inert gas over the surface of the polymerizing monomer film, which involves high expenditures for materials and is in some cases not executable.

The application of wax or similar coatings with low permeability for oxygen is a physical method which can be utilized if a significant diffusion of oxygen from the

surrounding air into the monomer must be prevented. Under optimized conditions, this method is as efficient as the application of an inert gas atmosphere.[28] Unfortunately, a raise in temperature diminishes the barrier effect of the wax coating. An alternative method is the application of coatings of gelatine, which are more stable towards temperature and can be simply washed away with water after completion of the curing process. [29]

A very frequently used ***chemical method*** is the formation of new propagating centers by amine-based hydrogen donors like triethanolamine, *N*-methyldiethanolamine or *N*,*N*-dimethylethanolamin.[30] α-Hydrogen atoms of these amines react with peroxy radicals to form new α-aminoalkyl radicals which initiate more efficiently than radicals of tertiary carbon groups.[31,32] The general mechanistic aspects of this method are shown in Figure 9.[33]

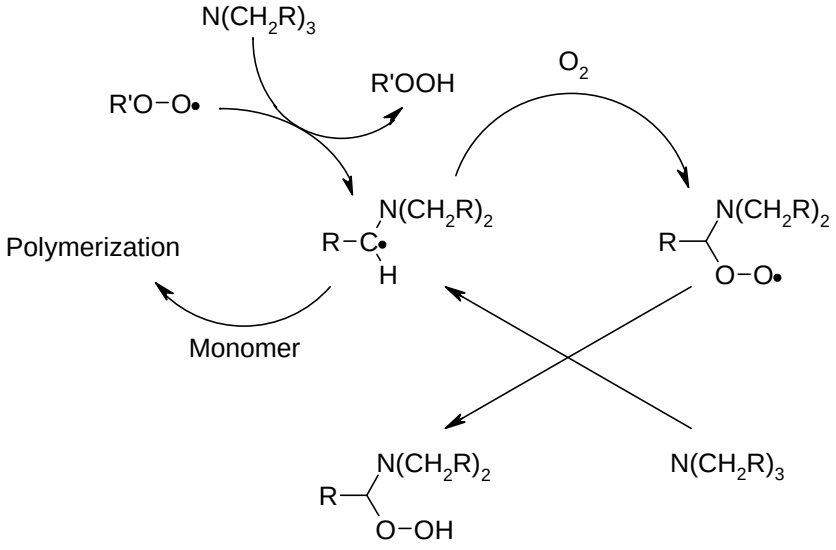

Figure 9: Amine-based hydrogen donors in radical polymerization

Cyclic *N*-vinylamides[34] which are applied as reactive diluents for photocuring formulations have been proposed to function similar to tertiary amines as hydrogen donors.

Trivalent phosphites and phosphines are well known as additives for a reduction of oxygen inhibition and as antioxidants.[35] A main disadvantage in the application of phosphites is a shelf-life of less than 24 hours in most monomer formulations.[36]

Addition of aromatic thiols[37] to acrylate formulations is also known to significantly reduce inhibition by molecular oxygen and photoinitiators containing aromatic thiol functions have been published in the past.[38] By donation of hydrogen to peroxy radicals formed by reaction of propagating centers with oxygen, thiols are transferred to highly reactive thiyl radicals. Generally, one of the main problems in both practical applications is their low shelf-life in monomer formulations.[36,37]

Another prevalent chemical method is the addition of benzophenone (**BP**) to sensitize the cleavage of hydroperoxides and peroxides to form hydroxy- and alkoxy-radicals that are able to act as new initiating centers. (Figure 10)

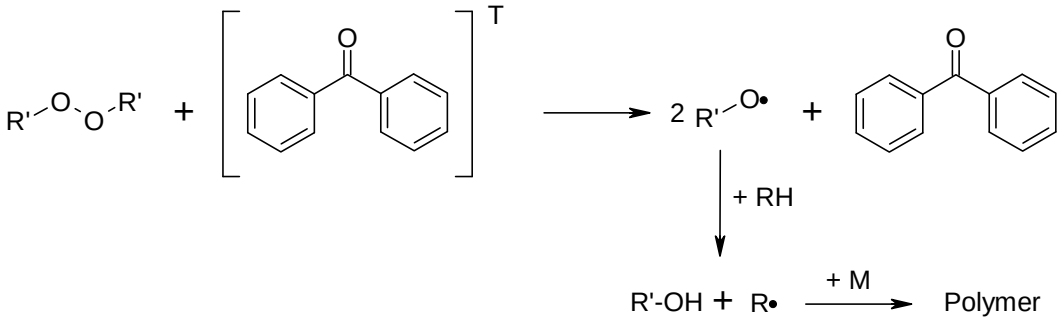

Figure 10: Photochemical cleavage of peroxides with triplet benzophenone

Furthermore, **BP** acts as a sensitizer for singlet oxygen, which unfortunately exhibits a very short lifetime (10^{-5} to 10^{-6} s) in monomer formulations, but is no longer able to react with propagating radical centers. An alternative, more straightforward approach is the **photosensitized generation of singlet oxygen and subsequent scavenging of this species**.

Another fundamental approach to completely evade the problem of inhibition by oxygen in thin film applications of UV-Vis curing formulations is a change of the polymerization technique. **Cationic photopolymerization** is the most dominant technique in UV-Vis curable coatings apart from free radical polymerization.
Nevertheless, cationic photopolymerization can be regarded as a niche technique compared to the well established, omnipresent radical photocuring and still offers a broad field in research and development to enhance its potential. In comparison with radical photocuring, significant differences as well as advantages and disadvantages are to be noted.

- First, cationic polymerization is to no extent inhibited by molecular oxygen, which is an important factor in thin film applications of UV-Vis curable coatings. In contrast to radical photocuring, water is a chain transferring agent and humidity is able to reduce the effectiveness of cationic curing formulations.

- Due to the initiation and propagation of the polymer chain by an acidic species, cationic polymerization is inhibited by bases. For this reason the effectiveness of cationic formulations might be influenced by the type of substrate in coating applications. Moreover, cured products may contain acids.

- Although photoinduced cationic polymerization can be regarded as a rapid curing process, curing times are in general significantly higher than those achieved by radical photopolymerization.

- Most formulations applied in cationic polymerization (especially epoxides) exhibit a reduced shrinking behavior compared to radical curing formulations. Partly due to the low shrinkage, these coatings possess an outstanding substrate adhesion.

- Another main advantage of cationic polymerization is the variety of polymers with different backbone structures that can be prepared.

Various types of cationically polymerizable monomers are known. From the group of ring opening heterocycles, epoxides are by far the most important monomers for industrial applications but also cyclic ethers, lactones, cyclic sulfides, acetals and siloxanes can be applied. A second group of important cationic polymerizable monomers are vinyl compounds like vinyl ethers. An overview of the possible monomers is presented in Figure 11 and two examples of commercially available difunctional epoxides are shown in Figure 12.

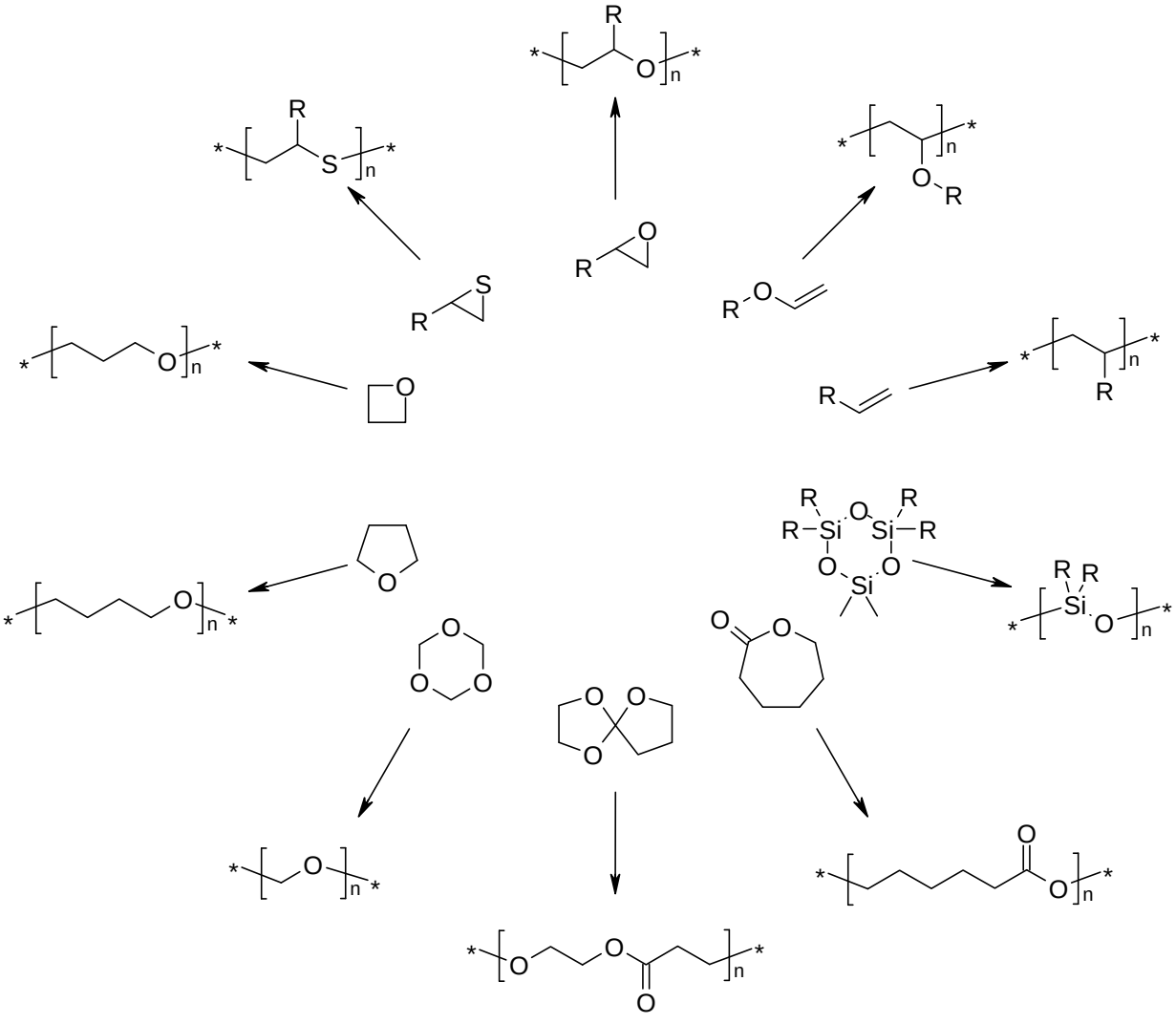

Figure 11: Cationically polymerizable monomers

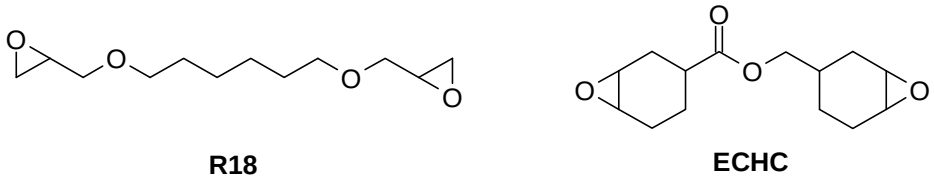

Figure 12: Two commercially available difunctional epoxides

As already mentioned above, ring opening polymerization of epoxides is by far the most important industrial application of cationic photopolymerization. As an example to display the general mechanism of cationic polymerization, the polymerization of an epoxide is shown in Figure 13.

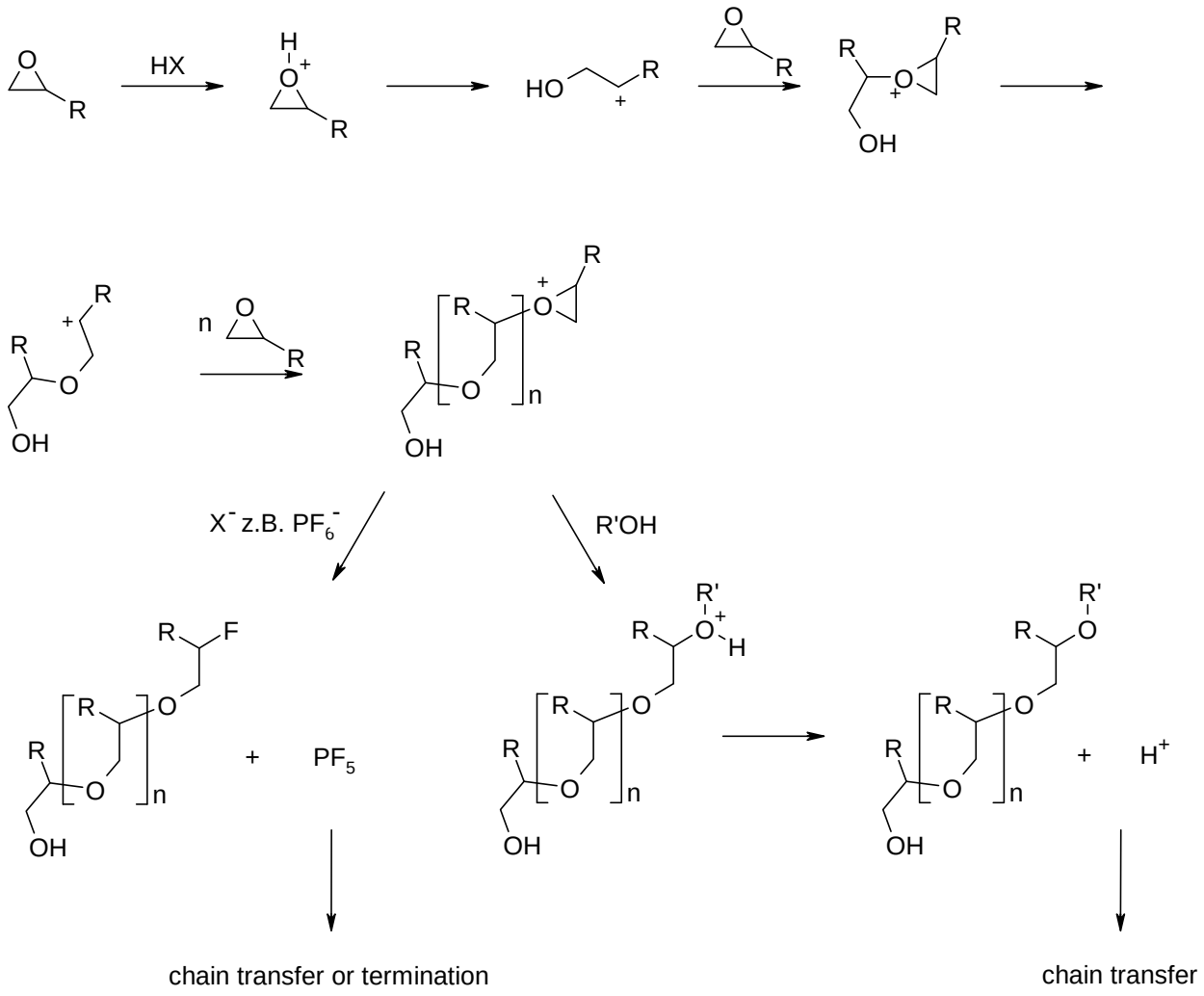

Figure 13: Cationic polymerization of an epoxide[18]

The initiating species in cationic photopolymerization is a free protonic acid. The chain reaction is started by a proton transfer to an epoxy group and subsequent ring opening that results in the formation of a carbenium ion. The carbenium ion immediately reacts with the next epoxy group and the repetition of this process generates a progressing polymer chain.
In case of halogen containing counterions like PF_6^-, termination reactions may occur by generation of the Lewis acid. In contrast to radical polymerization, recombination reactions with the initiator or of progressing polymer chains are not possible in cationic polymerization. Therefore, no significant termination takes place in absence of inhibitors like bases and nucleophiles. As a consequence, photo-induced cationic polymerization can proceed a significant amount of time in the absence of light once initiated. Alcohols can be applied as chain transfer reagents which reduce the kinetic chain length and therefore the average molecular weight of the polymer.

Like in radical photopolymerization, the photoinitiator plays the key role in curing processes of UV-Vis curable cationic coatings. Cationic photoinitiators are photo acid generators which decompose by formation of strong, non-nucleophile protonic acids. For this reason, these substances are also applied in imaging systems, containing dyes which change color as a function of the pH of the environment.

The transfer of irradiation to chemical energy by cationic photoinitiators is very similar to the radical initiators already mentioned. However, some differences have to be noted.

1. In contrast to radical polymerization, energy transfer sensitization is usually of little practical use. Instead, extension of the light sensitivity of cationic initiators towards the visible range relies heavily on the application of electron transfer type sensitizers.

2. Formation of free acids may occur by both homolytic[39] and heterolytic[40] cleavage of the initiator molecule.

In contrast to radical photoinitiation, photodecomposition of photoinitiators in cationic polymerization does not necessarily occur from an excited triplet state. Primary photochemical reactions of cationic photoinitiators may also occur predominantly from excited singlet states (S_1*), as revealed by sensitized[41] and photo-CIDNP[42] experiments.

In contrast to radical photopolymerization, thermal activation is needed in addition to photochemical initiation to convert the primary photoproduct into the initiating species. Therefore, the applied temperature has a significant effect on cure rates of cationic photo-resins.[43]

Major classes of photoinitiators for cationic polymerization (Figure 14)[43] are diaryliodonium salts (**XI**), triarylsulfonium salts (**XII**), ferrocenium-based salts (**XIII**), diazonium salts (**XIV**), dialkylphenacylsulfonium salts (**XV**), α-sulphonyloxy ketones (**XVI**) and silyl benzyl ethers (**XVII**).

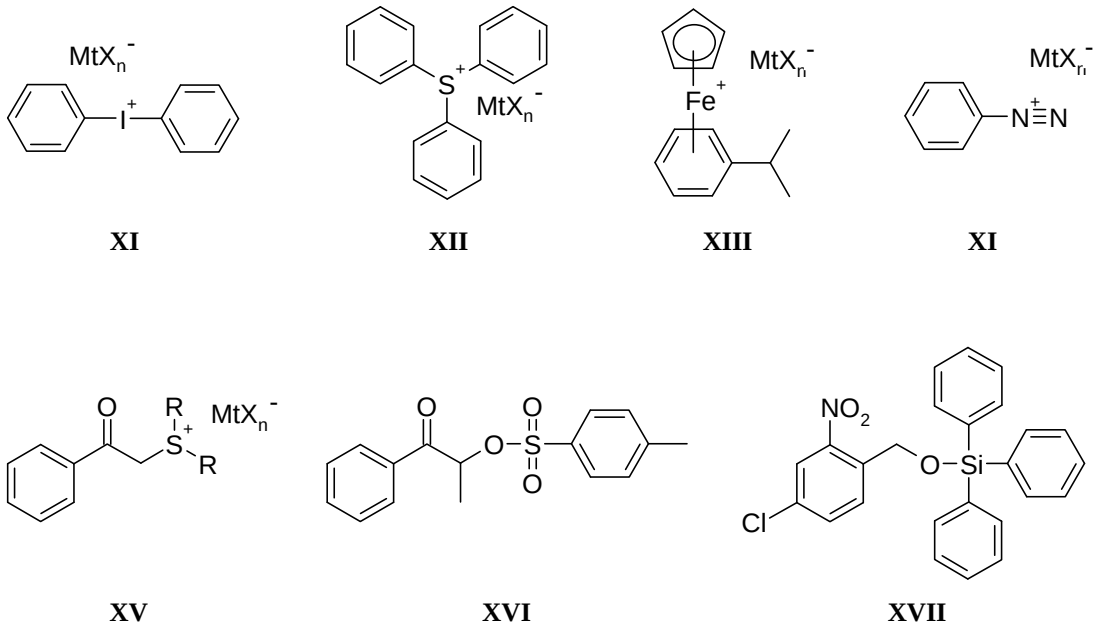

XI **XII** **XIII** **XI**

XV **XVI** **XVII**

Figure 14: Major classes of photoinitiators for cationic polymerization

Diaryliodonium and triarylsulfonium salts are, by far, the most important cationic photoinitiators applied in industrial coatings. Both structures can be easily synthesized on a large scale and exhibit an excellent thermal stability. Although iodonium salts

usually possess a higher reactivity, sulfonium salts are sometimes preferred in industrial applications due to a lower price and a reduced toxicity. Examples of commercially available diaryliodonium and triarylsulfonium salts for cationic polymerization are presented in Figure 15.

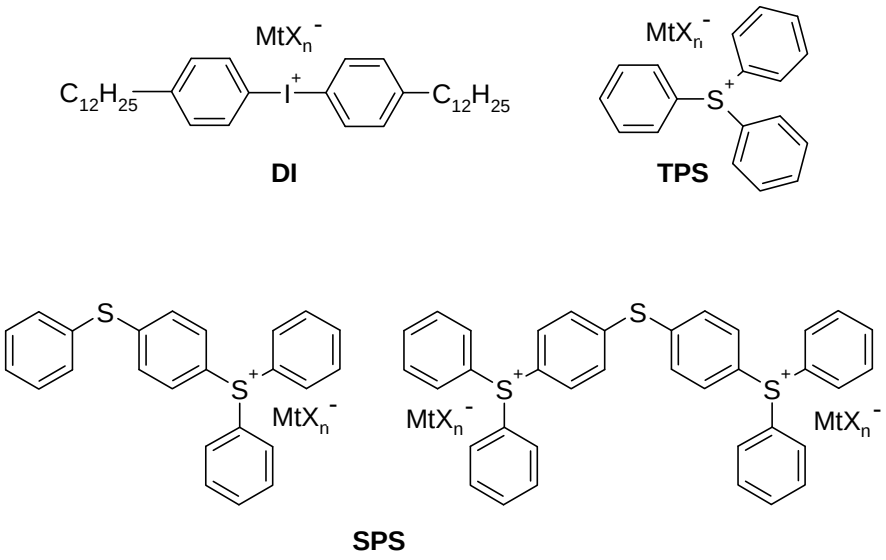

Figure 15: Examples of commercially available diaryliodonium and triarylsulfonium salt photoinitiators

The inorganic counterions of onium salts are not able to absorb light in UV-Vis and do not influence primary photochemical reactions. However, aside from the photochemistry of the organic chromophore, the counterion has the major influence on the initiation ability of cationic photoinitiators, since the reactivity is strongly dependent on the type of Brönsted acid formed.[18] Ions which possess nucleophilic characteristics, like halogenides, are able to undergo addition reactions with the cation of the propagating polymer chain. The order of reactivity of onium salts possessing the same cation, but different non-nucleophilic anions is generally $B(C_6F_5)_4^-$ > SbF_6^- > AsF_6^- > PF_6^- > BF_4^-. This effect is based upon the extent of separation in the propagating ion pair and the stability of the anion to fluoride abstraction (termination). Furthermore, the nature of the non-nucleophilic anion has a significant effect on secondary characteristics of photoinitiators like the solubility in apolar coating formulations.

The absorption spectrum of basic onium salts is usually in the range of UV-C. Fundamental change of the chemical structure to achieve a significant bathochromic shift like in case of **SPS** is a prerequisite for an enhancement of the absorption spectra. (Figure 16)

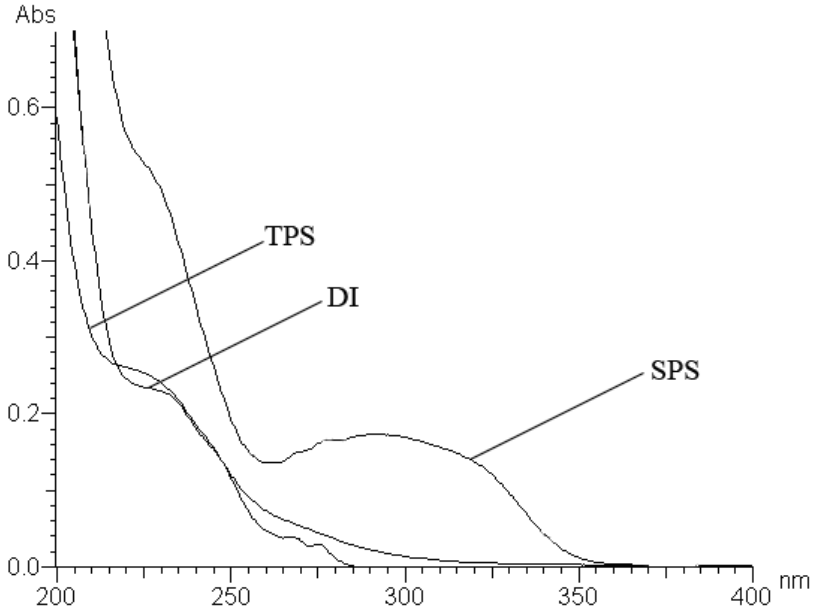

Figure 16: UV-Vis spectra of commercially available onium salt photoinitiators

In industrial applications of UV-Vis curable coatings, combinations of photoinitiators and sensitizers that absorb light in UV-Vis have to be utilized. In case of iodonium salts, photoredox induced decomposition[44] due to a combined application with radical photoinitiators is a possibility to enable UV-Vis curing. However, this method is far less suitable for sulfonium salts.[45] In contrast to cationic polymerization, energy transfer sensitization is of no practical use due to the high triplet energies of sulfonium and iodonium salts. However, electron transfer sensitization is applied extensively in thin film applications of UV-Vis curable formulations. This type of sensitization process does not occur via an excited state of the photoinitiator. Instead, electron transfer from the excited sensitizer to the onium salt results in a fast decomposition of the photoinitiator, preventing a back electron transfer. (Figure 17)

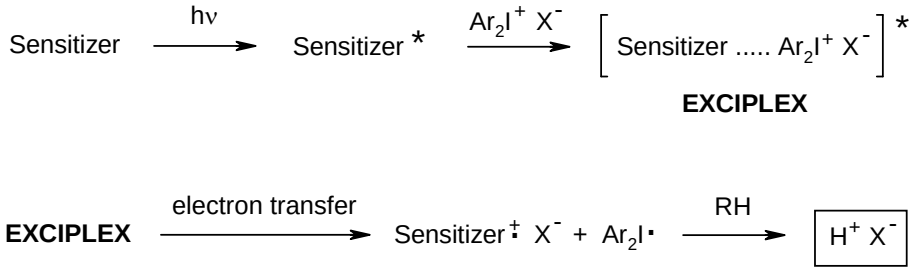

Figure 17: Electron transfer sensitization in the exciplex for a diaryliodonium salt

Major classes of electron transfer sensitizers like anthracenes (**XVIII**), perylenes (**XIX**), phenothiazines (**XX**), thioxanthones (**XXI**) and xanthones (**XXII**) are shown in Figure 18 for illustration.

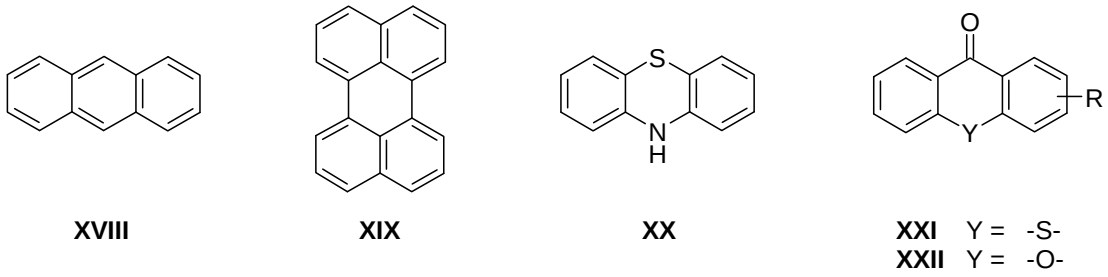

Figure 18: Major classes of electron transfer sensitizers

Polycyclic aromatic hydrocarbons and phenothiazines can be used as sensitizers for both iodonium and sulfonium salts. Since iodonium salts are more easily reduced (redox potential of the diphenyliodonium cation: -0.2 eV)[46] than sulfonium salts (redox potential of triphenylsulfonium cation: -1.2 eV)[47] a broader variety of sensitizers are applicable. In contrast to many aryl sulfonium salts, iodonium salts are capable of sensitization by xanthones and thioxanthones. A major drawback is the fact that most of the sensitizers have a limited solubility in typical cationic formulations. Furthermore most sensitizers are heavily colored and therefore not applicable in transparent coatings.

Objective

Inhibition of free radical polymerization by molecular oxygen is one of the most challenging problems in UV-Vis curable coatings due to a severe impact on curing speed and mechanical properties of cured surfaces. Apart from the utilization of an inert gas atmosphere, additives to reduce the oxygen inhibition due to production of new propagating centers are used. The photochemical scavenging of singlet oxygen is a more straightforward approach to reduce the oxygen inhibition by use of additives. However, only few attempts to establish this technology for UV-Vis curing systems can be found in literature. One reason for this discrepancy is the small number of substances that are known to undergo fast reactions with singlet oxygen in UV-Vis irradiation without application of heavily colored sensitizers.

In this work, new scavengers for singlet oxygen that are applicable in UV-Vis curing without a sensitizer are to be synthesized and tested on their

- storage stability and reactivity towards singlet oxygen in solution.
- ability to reduce oxygen inhibition under practical conditions.

These new scavengers are to be based on well known, highly reactive systems that are to be tuned in respect to the absorption wavelength by implementation of triple bonds or auxochromic groups.

A second, fundamental approach to completely evade the problem of inhibition by oxygen in UV-Vis curing is a change of the polymerization technique. Apart from free radical polymerization, the most dominant technique used in thin film applications of UV-curing systems is cationic polymerization. Unfortunately, most structures that are capable to initiate cationic photopolymerization only absorb light in UV-C. Therefore, colored sensitizers have to be applied to enable cationic polymerization in UV-Vis curing.

For this reason, new base structures that are capable of photo-acid-generation and therefore to initiate cationic polymerization are to be synthesized and tested on their

- decomposition pathway
- reactivity as photoinitiators for cationic polymerization
- applicability with sensitizers for UV-Vis curing that undergo photo-bleaching

These new structures are to be generated by implementation of triple bonds into existing photo-acid-structures based on iodonium and sulfonium salts to achieve a bathochromic shift of the UV spectra.

Based on these new structures, bathochromic shifted and conjugated derivatives are to be synthesized and tested on their applicability in UV-Vis curing.

Results and Discussion

Part 1: Oxygen scavengers

1. State of the art

In principal, photochemical reactions of organic molecules with singlet oxygen are based on two decisive steps:

- Photochemical generation of singlet oxygen by a sensitizer and
- a fast chemical (cyclo)addition reaction with an oxygen scavenger (OS)

Usually sensitizer and OS are two different organic molecules. However, several organic structures like polycyclic aromatic hydrocarbons are able to function as both sensitizers and OSs.

A selective excitation of a sensitizer is usually performed by UV-Vis irradiation and generation of singlet state oxygen is enabled by energy transfer from the excited, triplet state sensitizer to molecular, ground (triplet) state oxygen. Due to a high life time of the first excited singlet state ($1\Delta g$) of oxygen in solution and the specific electron configuration (Table 2) highly efficient oxidation reactions of OSs are possible.

Table 2: Excited states of singlet oxygen

state	highest orbitals	energy [kJ mol^{-1}]	life time in solution
$^1\sum g^+$	↑ ↓	155	10^{-12} s
$^1\Delta g$	↓↑	92	10^{-3} - 10^{-6} s
$^3\sum g^-$	↑ ↑	ground state	

The reaction mechanisms for the addition of singlet oxygen to organic molecules are fast *4 + 2* or *2 + 2* cycloadditions[48,49] or formation of allylhydroperoxides[50]. The *4 + 2* cycloaddition, an analogon to the Diels-Alder reaction, is applied in the most important methods for a fast chemical scavenging of singlet oxygen in literature.
Photochemical reactions with singlet oxygen are a valuable tool for synthetic and analytical methods. In both applications, mainly xanthenes, phenothiacines, porphyrines and phthalocyanines are utilized as very effective sensitizers, which exhibit triplet states with high life times and possess strong absorptions in the visible range of the spectrum.

First attempts to apply the fast scavenging of singlet oxygen as a method for a reduction of the oxygen inhibition in radical polymerization were accomplished by C. Decker[51] using 2,5-diphenyl-isobenzofuran (**DPBF**) as an OS and methylene blue (**MB**) as a sensitizer. (Figure 19) Excitation of the sensitizer was performed in a solution of acrylamides in 2-propanol with light in the range of 500 - 800 nm prior to the initiation of the polymerization by excitation of the photoinitiator (α,α-dimethoxy-α-phenylacetophenone) with UV-light.

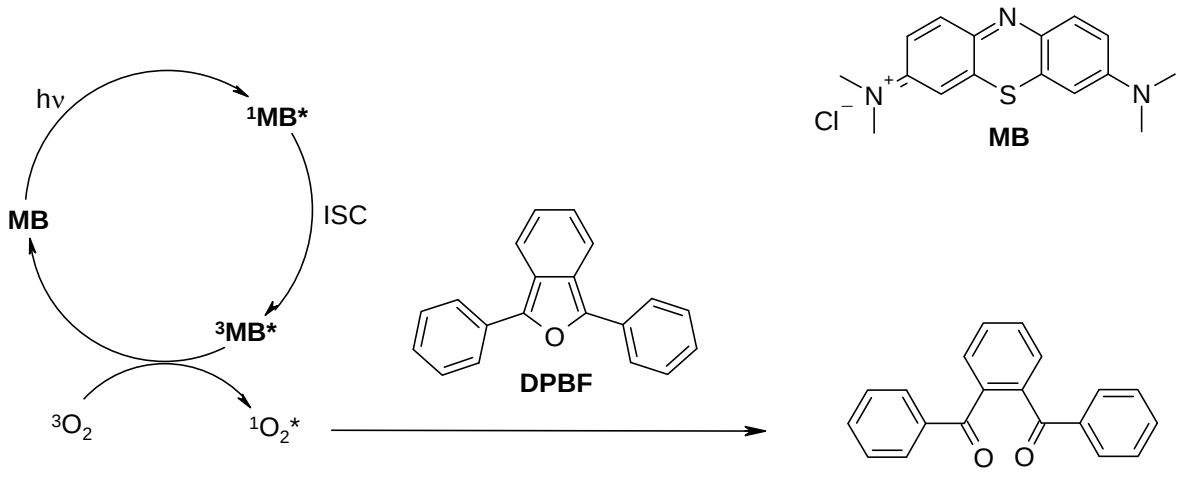

Figure 19: Reaction scheme of oxygen with **MB** / **DPBF**

In more recent publications by A. Scranton,[52,53,54,55] 9,10-dimethyl-anthracene (**DMA**) and 9,10-diphenyl-anthracene are applied as OSs and zinc porphyrins as well as zinc

phthalocyanines are used as sensitizers. (Figure 20) The formulations contained pentaerythritoltriacrylate or mixtures of pentaerythritoltriacrylate / dipentaerythritolpentaacrylate (1:1) as reactive components and were irradiated with light of 670 nm for a reduction of the oxygen level prior to the polymerization. The initiation was performed again by α,α-dimethoxy-α-phenylacetophenone as a photoinitiator (PI) by irradiation with UV-light.

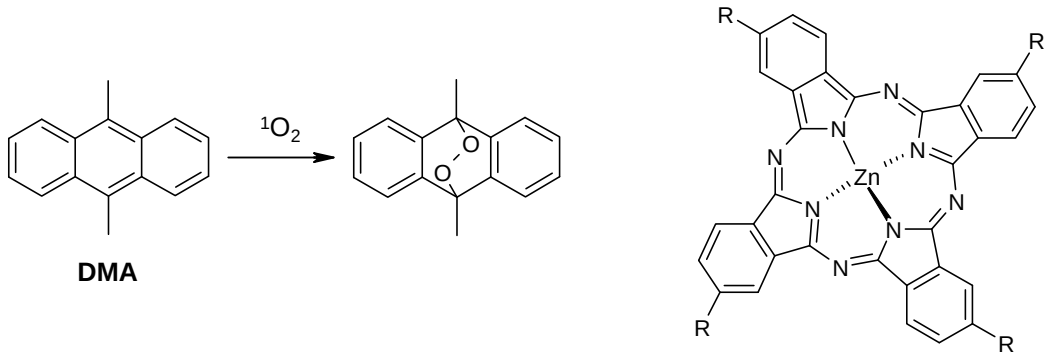

Figure 20: Reaction scheme of singlet oxygen with **DMA** and the phthalocyanine **Zn-ttp**

Furthermore, a German patent specification concerning the reduction of the oxygen inhibition by scavenging of singlet oxygen in dental applications[56] and a PCT-patent[57] have been published which specify on the whole on the methods discussed above.

Recently, first attempts have been made to simplify the described methods by application of just one light source for a concurrent reduction of the oxygen level and initiation of the photopolymerization.[58] Furthermore, different Type II PIs like camphorquinone (**CQ**) have been examined as sensitizers for singlet oxygen and OSs like 9,10-dibutyl-anthracene (**DBA**) and 2,5-diphenylfuran (**DPF**) which are able to sensitize their own oxidation have been successfully tested in UV-curing of methacrylate formulations.[58] (Figure 21)

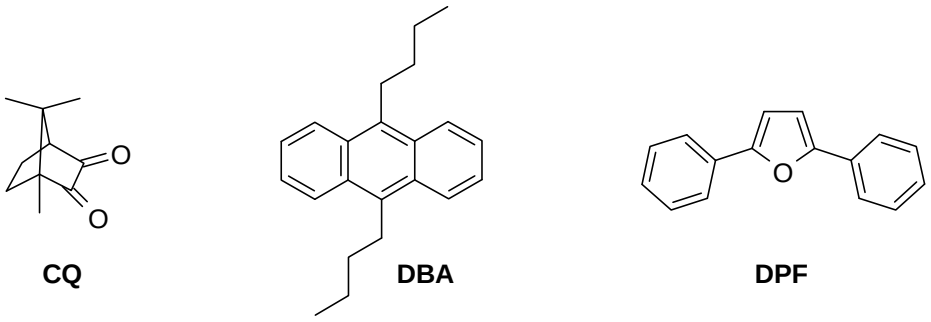

Figure 21: The PI / sensitizer **CQ** and the OS / sensitizer systems **DBA** and **DPF**

2. Selection of oxygen scavengers for UV-Vis curing

From the group of substances that are able to undergo fast cycloadditions with singlet oxygen, 2,5-diphenyl-isobenzofuran (**DPBF**) and polycyclic aromatic hydrocarbons like anthracenes or perylenes are able to absorb light in the visible part of the spectrum and are also known to function as sensitizers. However, **DPBF** exhibits an insufficient stability against autooxidation reactions with oxygen in the dark[58,59] and readily undergoes cycloaddition reactions with carbon-carbon double bonds as found in acrylates and methacrylates.[58] (Figure 22)

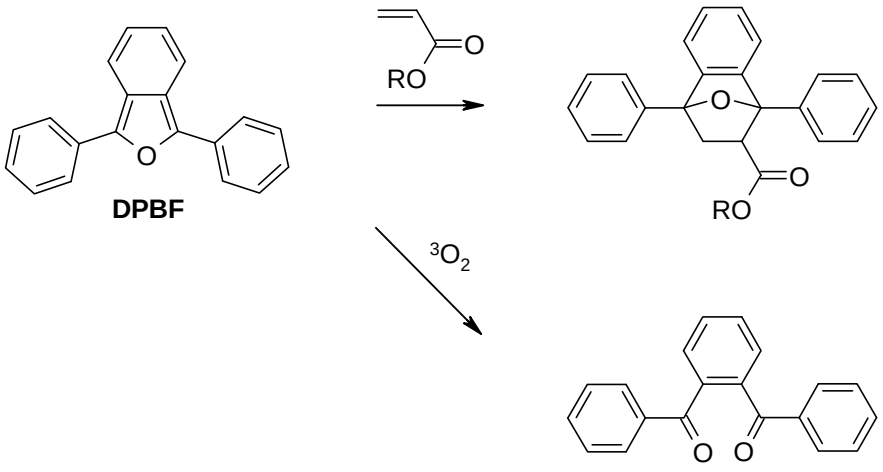

Figure 22: Thermally induced cycloaddition of **DPBF** with acrylates and autooxidation in the dark

Polycyclic aromatic hydrocarbons usually exhibit an insufficient solubility in coating formulations, with the exception of alkyl-substituted anthracenes like **DMA**, **DBA** and 9,10-diheptyl-anthracene that have already been used extensively as OSs in literatur.[52,58]

However, 2,5-diphenylfuran (**DPF**) has been successfully tested in UV-curing of methacrylate formulations[58] and furans, in general, are known for a high reactivity towards singlet oxygen.[60] Unfortunately, simple furans including **DPF** are not able to absorb light in the visible part of the spectrum. For this reason, bathochromic shifted furan derivates based on the structure of **DPF** have to be synthesized as possible new OSs. Especially **DPF** derivatives with auxochromic groups in *p* - position of the phenyl rings and furan derivatives with enhanced conjugation like 2,5-bis-phenylethynyl-furans are promising new OSs with an improved absorption behavior. (Figure 23)

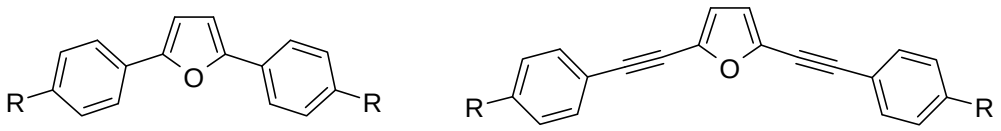

R... auxochromic group

Figure 23: Bathochromic shifted **DPF** derivatives

Due to the implementation of auxochromic groups or an enhancement of the conjugation, the electronic state in the positions 2 and 5 of the furan ring might be significantly altered. Therefore, it can not be excluded that the reactivity towards singlet oxygen might significantly change. For this reason, only two new structures, 2,5-bis-(4-dimethylamino-phenyl)-furan (**4**) and 2,5-bis-phenylethynyl-furan (**5**) were chosen for first tests. In case of a high reactivity of these structures towards singlet oxygen, other derivatives with a broad selection of different auxochromic groups are to be synthesized.

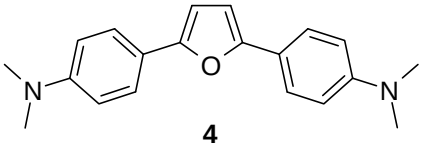

4

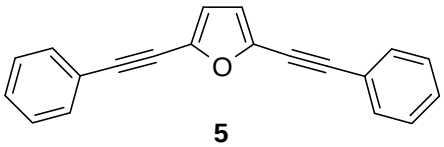

5

The OSs **DPF** and **DBA** have already been found to function both as sensitizers and scavengers and are suitable reference structures for tests in solutions and under practical conditions.

3. Synthesis of oxygen scavengers

3.1 Synthesis of 9,10-dibutyl-anthracene (1, DBA)

9,10-Disubstituted anthracene derivatives can be synthesized by conversion of anthraquinone with organometallic reagents[61] and subsequent reductive dehydration with tin dichloride[62] in concentrated hydrochloric acid.

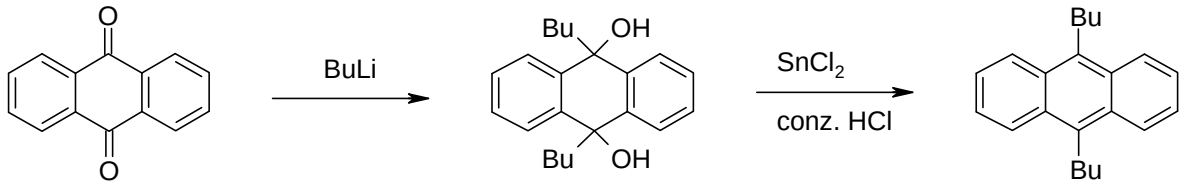

1

Therefore, 9,10-dibutyl-anthracene (**DBA**, **1**) was synthesized in an optimized procedure[58] by conversion of anthraquinone with 4 equivalents of *n*-butyllithium at 0 °C in dry THF and subsequent extraction. The raw intermediate product 9,10-dibutyl-9,10-dihydro-anthracene-9,10-diol was reduced without isolation with an excess of tin dichloride in conc. HCl. After extractive workup and chromatographic purification, the anthracene **DBA** was received in 36% yield.

3.2 Synthesis of symmetrically substituted furan derivatives

Established synthetic routes for the preparation of 2,5-substituted diphenylfuran derivatives with congeneric substituents are either synthesis of the corresponding butane diones and subsequent ring closure to the furan[63,64] or coupling techniques[65] of phenyl reagents with furan dihalogenides.

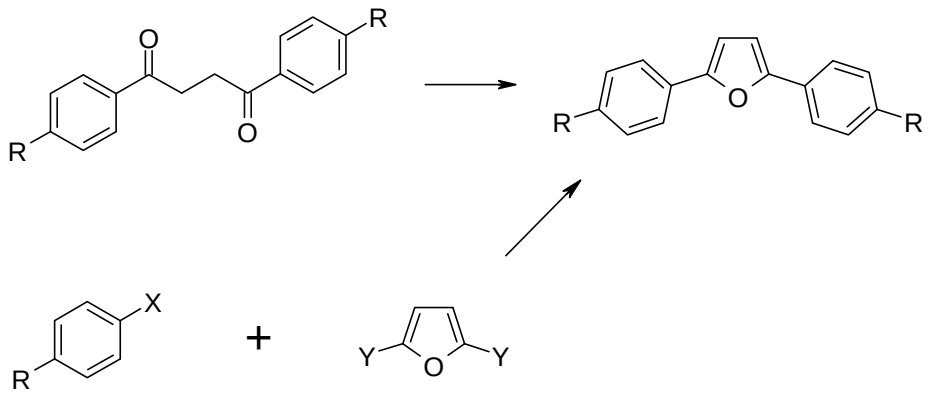

X, Y = reaktive groups for coupling

Since both target substances should be efficiently and selectively accessible by coupling reactions with 2,5-dibromofuran, the second synthetic route was chosen. 2,5-Dibromo-furan (**2**) was obtained by bromination of furan with 2.05 equivalents of NBS in a synthesis based on the experiments of Prugh *et al* [66] in carbon tetrachloride at reflux.

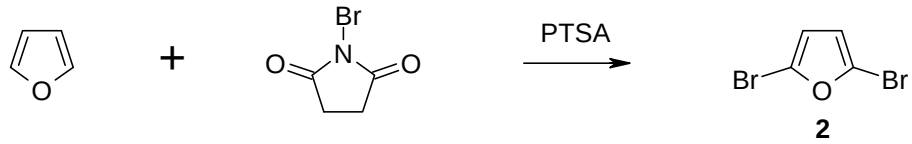

2

After extractive workup, vacuum distillation and subsequent column chromatography, the bromo furan **2** was received as a colorless oil in 44% yield.

The coupling reagent 4-*N*,*N*-dimethylaminophenyl boronic acid was obtained from 4-bromo-*N*,*N*-dimethylaniline by conversion with 2 equivalents of lithium at 0 °C and subsequent reaction with 1.25 equivalents of tributyl borate in THF.

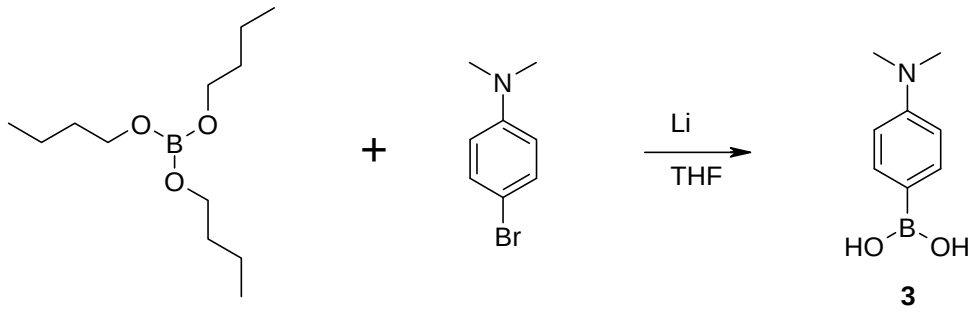

3

After extractive workup, column chromatography and subsequent washing with diisopropyl ether, the boronic acid **3** was received as colorless crystals in a yield of 48%.

Preparation of new symmetrically 2,5-disubstituted furan derivatives as potential OSs was performed by Pd-catalyzed coupling reactions with 2,5-dibromo-furan.

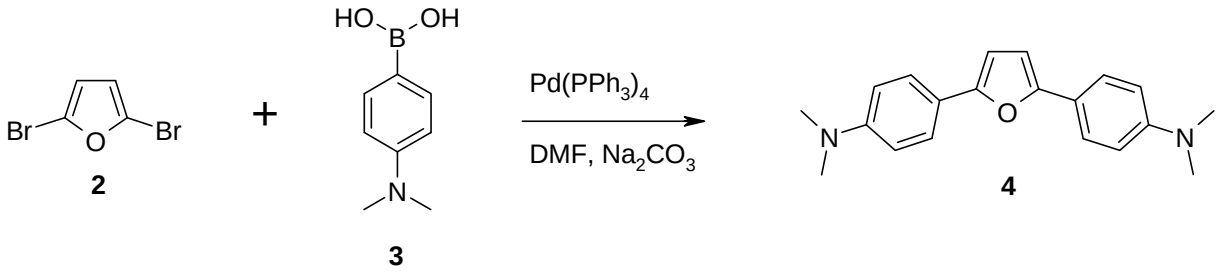

2 **3** **4**

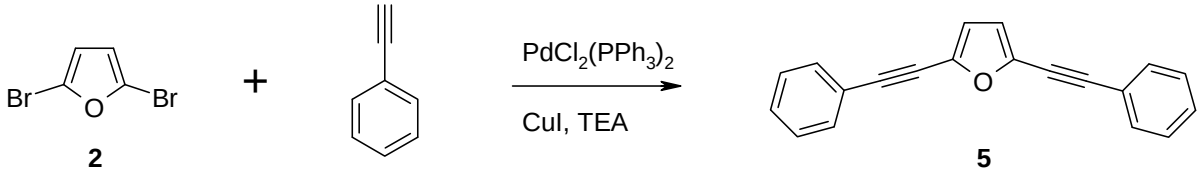

2 **5**

The bathochromic shifted diphenylfuran derivative 2,5-bis-(4-dimethylamino-phenyl)-furan[67] (**4**) was prepared by coupling with 2.67 equivalents of the boronic acid **3** (Suzuki-coupling) in a degassed mixture of DMF and aqueous 1 M Na_2CO_3 solution with $Pd(PPh_3)_4$ as catalyst. After extraction and chromatographic purification, the

diphenyl derivative **4** was received in 53% yield. The diphenylfuran derivative with an expanded conjugated system due to the implementation of triple bonds, 2,5-bis-phenylethynyl-furan (**5**) was synthesized by coupling with 2.4 equivalents of phenylacetylene (Sonogashira-coupling) using copper (I) iodide / $PdCl_2(PPh_3)_2$ as catalyst in degassed triethylamine. After extractive workup, column chromatography and recrystallization from petroleum ether, the 2,5-substituted furan **5** was obtained as colorless crystals in 75% yield.

4. Storage Stability

OSs that react with singlet oxygen in a [4 + 2] cycloaddition reaction are inevitably capable to undergo thermally induced pericyclic reactions with acrylic or methacrylic double bonds. Furthermore, the well reputed OS **DPBF** was found to be susceptible to oxidation by triplet oxygen in the dark.[59] For these reasons the storage stability of the new potential furan based OSs (1×10^{-3} mol L^{-1}) was determined in air saturated MeCN and MeCN / dodecyl acrylate (1×10^{-2} mol L^{-1}) under nitrogen atmosphere at rt in the dark. The samples were investigated for the concentration of OS as well as for decomposition and reaction products by HPLC analysis. In contrast to **DPBF**, which exhibits a half life of approximately 14 days under oxygen and is totally consumed by cycloaddition with dodecyl acrylate within 72 h under the chosen conditions[58], the anthracene derivative **DBA** and the furan derivatives **DPF**, **4** and **5** exhibited no significant decomposition reactions in both formulations within 30 days.

5. UV-Vis Spectroscopy

UV-Vis spectroscopy is an important tool to gain an overview of the range of wavelength an OS / sensitizer system is able to absorb. Without application of an additional sensitizer, a good light absorption of the OS / sensitizer system to generate a

sufficient level of singlet oxygen is a key factor in the reduction of the oxygen inhibition. In case of **DPF**, absorption tails out at a lower wavelength than the emission maximum of high pressure mercury lamps (ca. 365 nm), which is a severe disadvantage for photo-reactive substances. The new furan derivatives **4** and **5** possess functional groups that should cause a bathochromic shift compared to the base structure **DPF**, which was used as a reference in UV-Vis spectroscopy.

Actually, UV absorption of both furan derivatives **4** and **5** in MeCN shows strong absorptions near 365 nm which is very useful for a possible application as OS / sensitizer systems for UV-Vis photopolymerization (Figure 24).

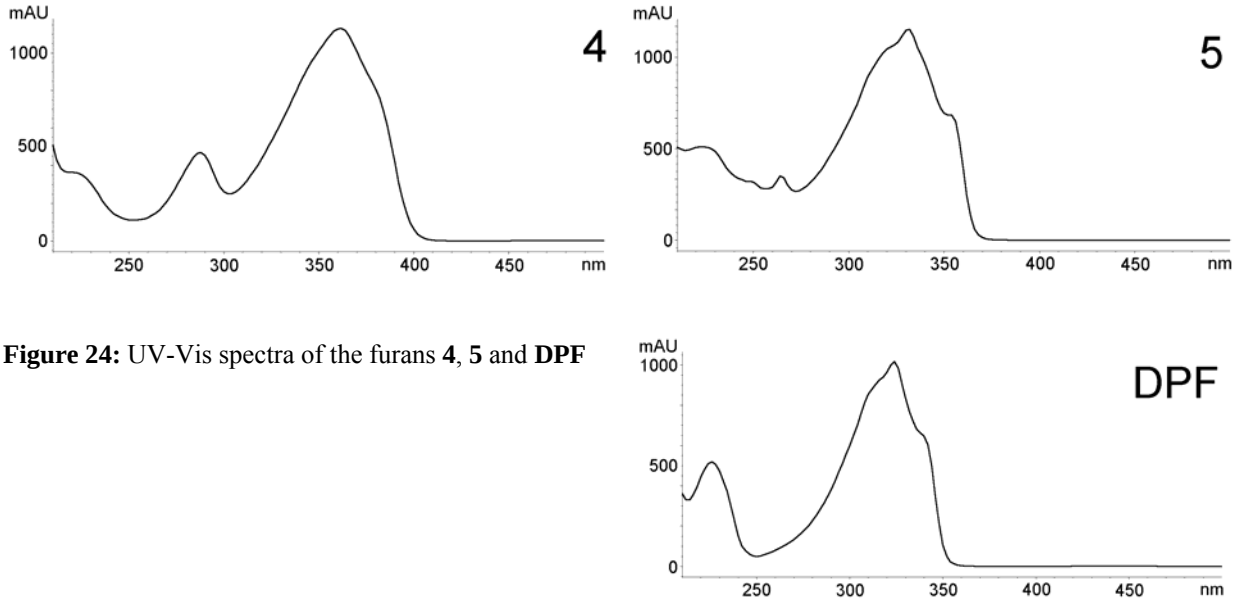

Figure 24: UV-Vis spectra of the furans **4**, **5** and **DPF**

Although a significant red shift compared to **DPF** was expected due to the implementation of 2 triple bonds in case of the furan **5**, the λ_{max} of the new furan derivative is almost identical to **DPF**. In comparison to the UV absorption of **DPF**, the tail out of the furan **5** is shifted from approximately 355 to 370 nm. In contrast to **5**, the λ_{max} of the dimethylamino substituted furan **4** is red shifted for approximately 35 nm compared to the base structure **DPF** due to the implementation of the dimethylamino groups which are strong electron donors. The UV absorption of **4** tails out at approximately 410 nm and is therefore significantly shifted in comparison to **DPF**.

.

6. Sensitized Steady State Photooxidation (SSSP)

SSSP combined with subsequent HPLC analysis is a perfect tool for preliminary reactivity tests in photooxidation chemistry, since the time-dependency of the concentration of reactive species, the OS, sensitizer and photooxidation products can be easily investigated throughout the process. Photooxidation of furans[68] by singlet oxygen occurs via fast [4 + 2] cycloaddition reactions, resulting in ozonoide-like primary photoproducts that decompose at rt to diketones in case of 2,5-disubstituted furans (Figure 25). 9,10-Dialkyl-anthracenes[48] react in an analogous way with singlet oxygen to yield endoperoxides that are stable at rt. Additionally, photobleaching is observed.

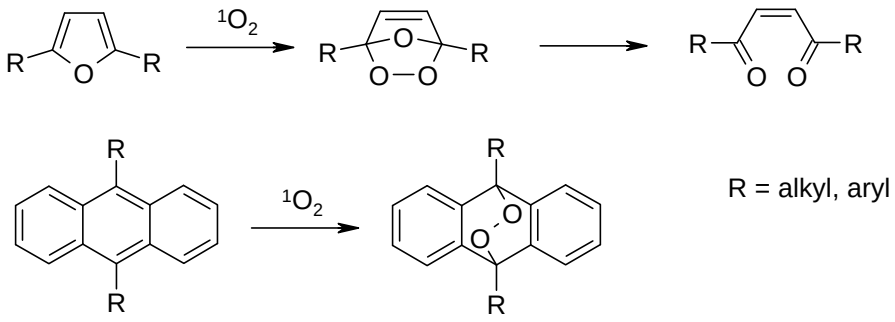

Figure 25: Photooxidation of disubstituted furans and anthracenes

Due to the high selectivity of the photooxidation reactions of the selected OSs that yield just one major product in SSSP, the chromatograms can be easily interpreted. Data obtained from the whole wavelength spectrum (200 - 500 nm) was used for the monitoring of sensitizers and photoproducts and to exclude the occurrence of colored side products, unwanted in respect to a possible technical application. Interpretations of the chromatograms were always performed at the wavelength of maximum absorption of the selected OS. From the integral of the UV-Vis absorption signal of the OS vs time, the reaction rate of decomposition (R_v) can be calculated.

In a first set of experiments, the relative reactivity of the selected OSs was reviewed in SSSP experiments at 400 - 500 nm using **MB** (1 x 10^{-4} mol L^{-1}) as a sensitizer (Figure 26) and the anthracene **DBA** and the furan **DPF** as reference OSs. The reference OS **DBA** definitely displayed the highest reactivity and the reference furan **DPF** approximately half the R_v of **DBA**. Unfortunately, the furans **4** and **5** which possess expanded conjugated electron systems compared to **DPF** displayed a significantly reduced reactivity towards singulett oxygen.

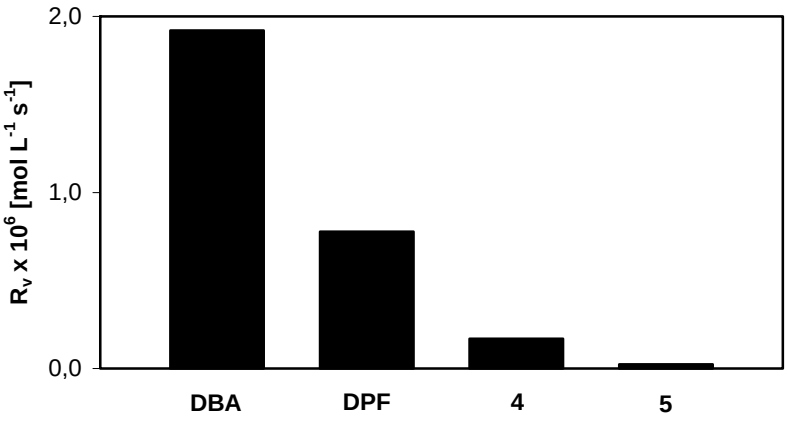

Figure 26: SSSP experiments (400 - 500 nm): R_vs of OSs **1**, **DPF, 4** and **5** with **MB** as a sensitizer (1 x 10^{-4} mol L^{-1})

It has to be noted that in this set of experiments the 400 - 500 nm filter was carefully selected to avoid direct excitation of OSs and to ensure that only the sensitizer is able to be triggered by light. Without application of a filter, the anthracene **DBA** and the conjugated furans **DPF**, **4** and **5** would have been able to sensitize their own oxidation reactions.

Therefore, the capability of the furans **4** and **5** to function both as sensitizer and OS and their corresponding relative R_vs were reviewed in another SSSP experiment at 320 - 500 nm without application of an additional sensitizer (Figure 27).

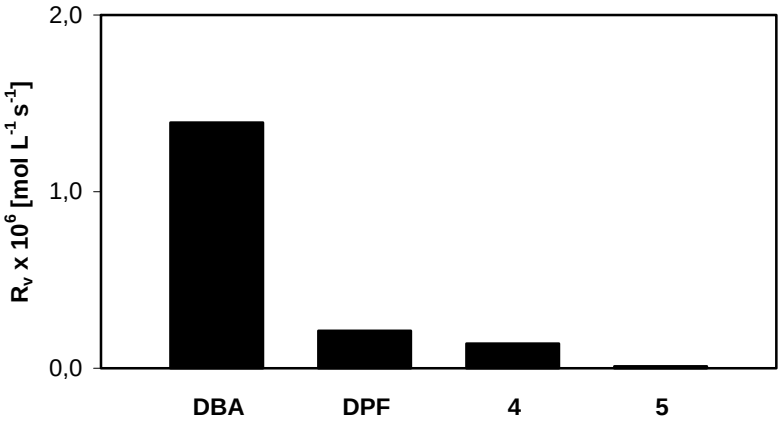

Figure 27: SSSP experiments (320 - 500 nm): R_vs of OSs **DBA**, **DPF**, **4** and **5** without sensitizer

In this reaction setting, the reference anthracene **DBA** displayed a high efficiency to function both as sensitizer and OS. The R_v is in the same order of magnitude than the R_v determined in the experiment with **MB** as sensitizer at 400 - 500 nm. The R_v of **DPF** is significantly higher than the R_v of **5** attesting again a reduced reactivity of this furan to react with singlet oxygen. However, the reactivity of the furan **4** was hardly reduced compared to the experiment with **MB** as sensitizer in contrast to the reference furan **DPF**. In photooxidation without application of a sensitizer, **4** exhibits a reactivity that is well comparable to the established OS **DPF**.

7. Photopolymerization

The main objective of the project was to evaluate the applicability of the new OS / sensitizer systems (45.0 mmol L^{-1}) to reduce oxygen inhibition in photopolymerizable methacrylate formulations. The most practical method is the analysis of the chemical composition of the surface layer of polymerized films by ATR IR spectroscopy. Although differential scanning photocalorimetry (photo-DSC) is an appropriate method for the fast and accurate evaluation of the performance of a UV-Vis curing system, it is not the method of choice for the analysis of the polymerization of thin films. Due to the minimum mass needed for a sufficient signal strength and accuracy, the thickness of the irradiated formulation (~ 300 µm) is higher than usually applied for most coatings. Nevertheless, photo-DSC (320 - 500 nm, 1000 mW cm^{-2}) is a good

tool to indicate possible differences between bulk and thin layer polymerization and was therefore used to permit a rough comparison to the results of the ATR IR spectroscopic surface analysis of photo-cured films (60 µm, medium pressure mercury lamp, 50 W cm^{-1}, 15 cm distance).

Thin films of 1,6-bis(methacryloxy-2-ethoxycarbonylamino)-2,4,4-trimethylhexane (**UDMA**) containing a 1:1 mixture of **CQ** / ethyl 4-(dimethylamino)benzoate (**DMAB**) (each 27.8 mmol L^{-1}) as a PI- and sensitizer-system were polymerized under nitrogen and air and the surface layer of the cured films was investigated by ATR IR spectroscopy.

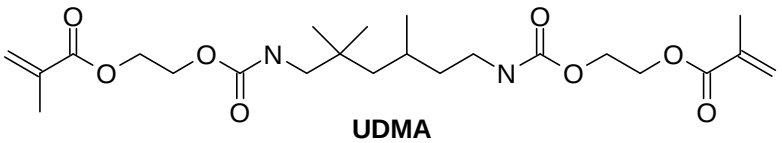

UDMA

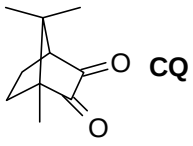

CQ

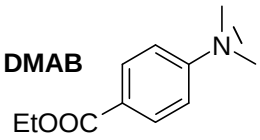

DMAB

The double bound conversion (DBC) was calculated from the ratio of the area of the signal of the C=O stretching vibration band (1706 cm^{-1}) to the area of the signal of the CH_2 - torsion vibration (815 cm^{-1}) or the C=C stretching vibration band (1638 cm^{-1}) of the methacrylic double bond. Photo-DSC measurements were carried out with the same monomer formulation under nitrogen and air and the double bonds converted were calculated from the area below the trace. The rate of polymerization (R_p) was calculated from the height of the peak, the density and the theoretical heat of polymerization from the monomer.

A first screening of the new structures in thin film polymerization exhibited no reactivity for the furan **5** as OS, which was already indicated before by the low R_v values of this substance in the SSSP experiments. In contrast to **DBA** or **DPF,**

investigation of the DBC of the polymerized films containing **5** gave virtually the same values that were found for the formulation without OS (Figure 28).

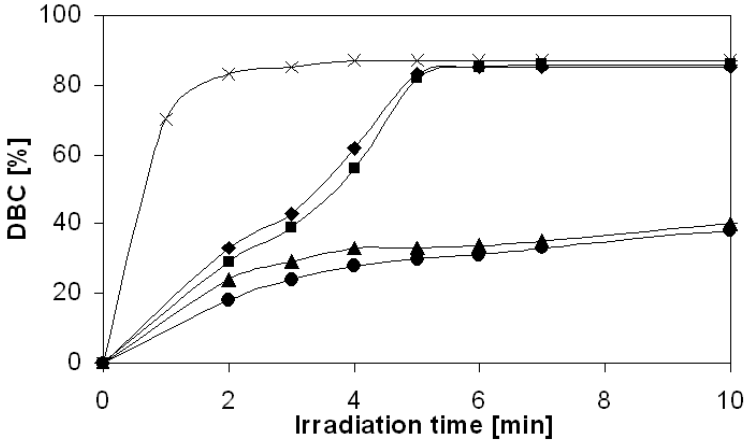

Figure 28: Dependency of the surface DBC under addition of ♦… **DPF**, ■… **DBA**, ●… **4**, ▲… without OS or with **5**, ✕… N_2 atmosphere without OS

Since the results of the SSSP experiments without addition of a sensitizer were very well comparable for the furan **4** and **DPF**, an improvement of the DBC in the thin film experiments was to be expected. Nevertheless, the DBC of the cured films containing **4** was measurably reduced compared to the formulation without OS. Since the furan **4** possesses dimethylamino groups, this structure is a possible coinitiator for **CQ**. Therefore, it was assumed that this reduction of the reactivity of the formulation was due to an interference of the new OS with the **CQ** / **DMAB** initiator system. For this reason, photo-DSC experiments of formulations containing **DMAB, DMAB** / **4** and only **4** as coinitiator (each 27.8 mmol L^{-1}) were conducted (Figure 29, Table 3).

Table 3: Photo-DSC data of **UDMA** using **DMAB**, **4**, and **DMAB** / **4** as coinitiators

Coinitiator	t_{max} [s]	$R_p \times 10^3$ [mol $L^{-1}s^{-1}$]	EGC [%]
DMAB	10	55	57
4	50	17	46
DMAB / **4**	12	42	56

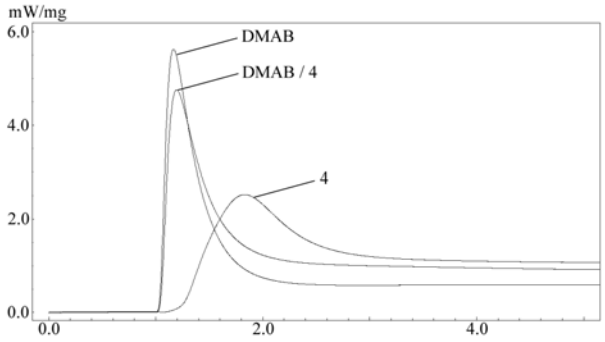

Figure 29: Photo-DSC of **UDMA** using **DMAB**, **4**, and **DMAB** / **4** as coinitiators for **CQ**

Obviously the dimethylamine **4** is able to function as a coinitiator for **CQ**, although this PI system is significantly less reactive than **CQ** / **DMAB**. In comparison to the formulation containing **CQ** / **DMAB**, t_{max} is enhanced approximately 5 times and the R_p values and DBC are significantly decreased. The formulation containing both **DMAB** and **4** as coinitiators also exhibits a measurable decrease of R_p and t_{max} compared to the formulation containing only **CQ** / **DMAB**. Therefore, the reduced reactivity of **4** to function as coinitiator for **CQ** is obviously not only an effect of a less effective redox system. Probably, **4** is able to form radicals that are significantly more stable than those of **DMAB** and is therefore able to reduce the reactivity of the **CQ** / **DMAB** initiator system. This reduction of reactivity of the PI obviously outweighs the positive effects of a presumably reduced oxygen inhibition. For this reason, the addition of **4** as OS is no option to enhance the reactivity of formulations containing PI / Coinitiator redox systems like **CQ** / **DMAB**.

Part 2: Cationic initiators

1. State of the art

Diaryliodonium and triarylsulfonium salts are, by far, the most important cationic photoinitiators applied in industrial coatings. Various synthetic strategies have been developed for the preparation of both types of photoinitiators (PIs). Diaryliodonium salts are usually prepared by electrophilic aromatic substitution reactions. In Figure 30 the two most prevalent methods in industrial applications are shown for illustration.

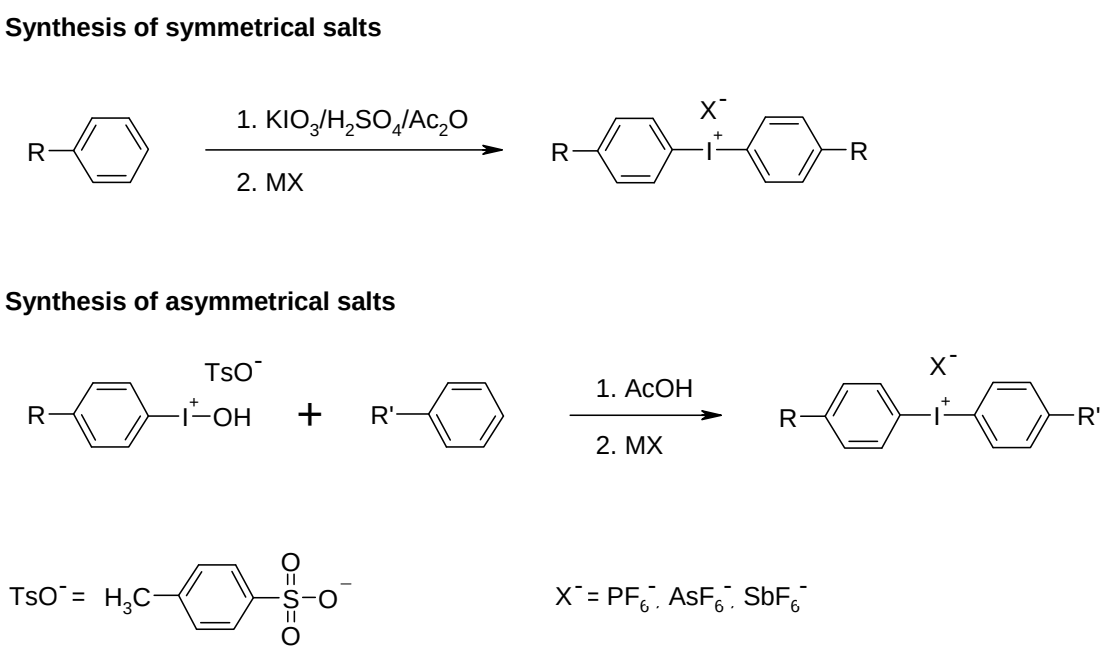

Figure 30: Synthesis of iodonium salts

Symmetrical iodonium salts are usually prepared by reaction of aromatic precursors with potassium iodate in the presence of sulphuric acid and acetic acid anhydride.[69] As an intermediate product an iodonium bisulphate salt is obtained that is changed to the target salt that contains a non-nucleophilic counterion in a metathesis reaction. In case of the preparation of asymmetrical iodonium salts, aryliodoso derivatives are converted to iodonium salts by reaction with a second aromatic compound and acetic

acid. The obtained iodonium tosylate is again converted to the target structure by exchange of the anion.

Furthermore, several other synthetic routes by means of electrophilic aromatic substitution reactions and modifications of the methods described above have been presented in literature. A direct preparation of symmetric iodonium salts from aromatic precursors is possible by reaction with $(IO)_2SO_4$ or $(CF_3CO_2)_3I$ in combination with acids.[70,71] Alternative synthetic routes to asymmetric iodonium salts apply aryl iodates or aryl iodides in combination with $K_2S_2O_8$ as educts.[70,72] Additionally, both symmetric and asymmetric iodonium initiators can be synthesized by organometallic mediated displacement reactions from phenyllithium compounds. [73,74,75,76]

Similar to iodonium salts, sulfonium initiators are prepared by two different prevalently applied methods. Complex mixtures of triarylsulfonium salts are prepared on a commercial scale from benzene.[77] (Figure 31)

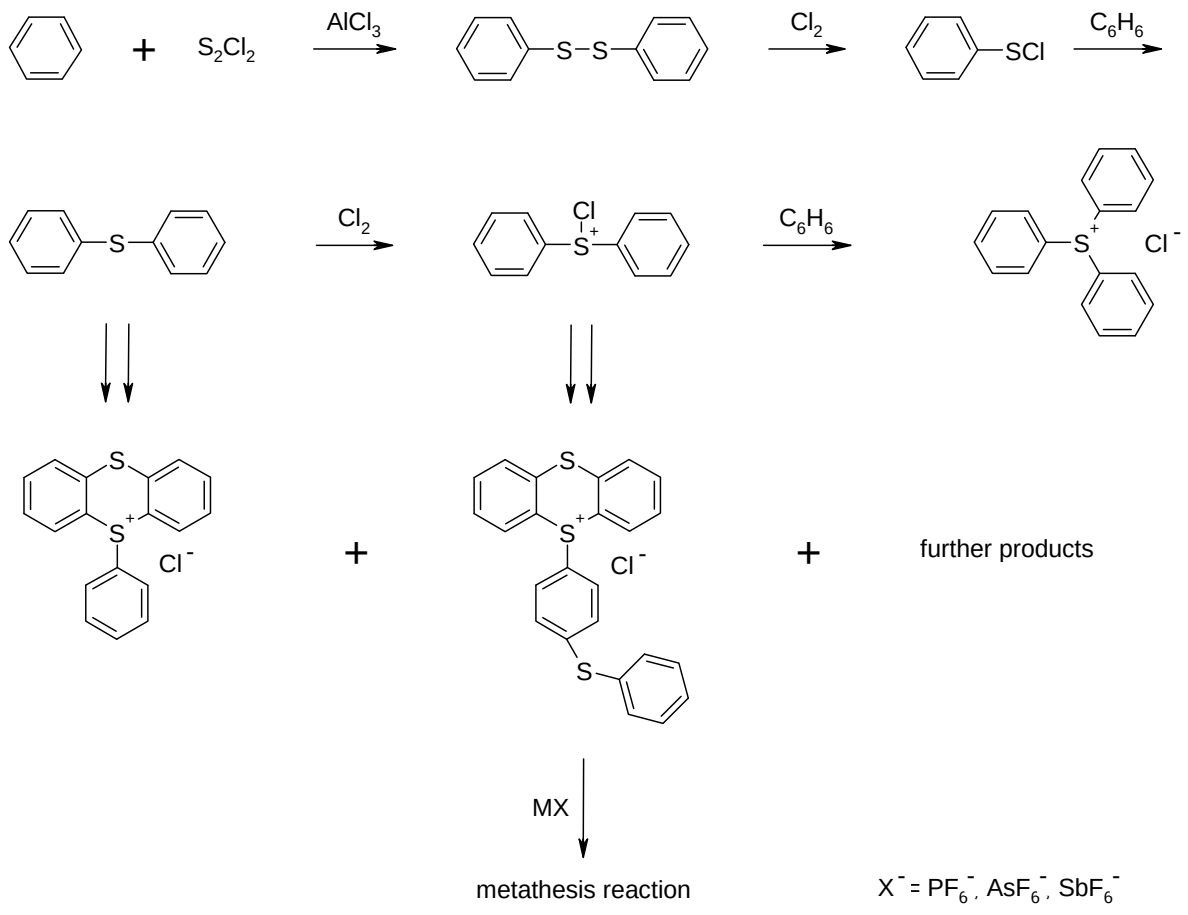

Figure 31: Synthesis of mixtures of triarylsulfonium salts

The occurrence of an impure product by synthesis via the Friedel-Crafts reaction is not a drawback for an application as a cationic PI, since higher substituted derivatives absorb at longer wavelengths. Therefore, product mixtures are more reactive than the pure compounds and are used without further purification.

A second important approach to the synthesis of both symmetrical and asymmetrical triarylsulfonium PIs is based on the copper (II) catalyzed conversion of diarylsulfides with iodonium salts.[78] (Figure 32)

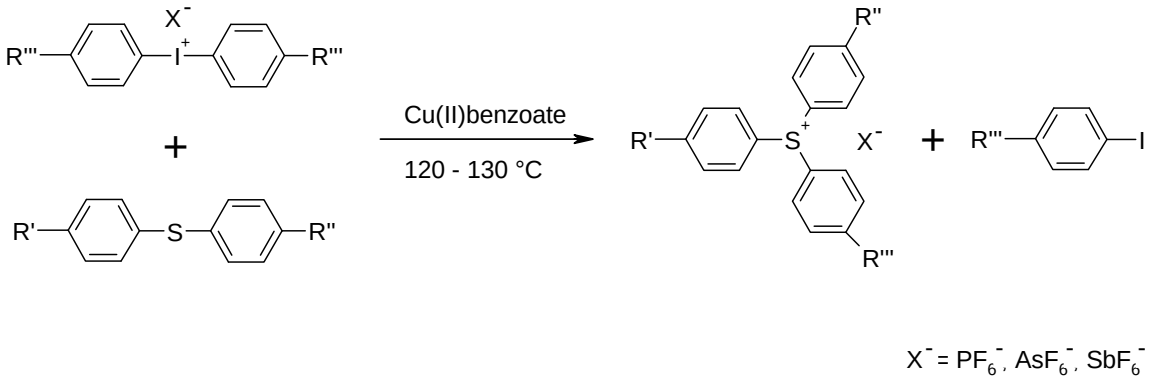

Figure 32: Synthesis of asymmetrical triarylsulfonium salts

This method can be readily used on a laboratory scale, since the iodonium salts are easily available and no further metathesis reaction to change the counterion is necessary. Apart from the two methods described above, examples for further synthetic routes to sulfonium PIs are conversion of diarylsulfoxides with aromatic Grignard reagents[79] or with $AlCl_3$ and aromatic compounds[80] and conversion of aromatic compounds with thionylchloride.[81]

Synthesis of iodonium and sulfonium salts usually yields derivatives with a nucleophilic anion like HSO_4^-, Cl^- or TsO^-. For a subsequent application as a cationic PI, the counterion has to be exchanged in a metathesis reaction to a non-nucleophilic anion such as SbF_6^-, AsF_6^-, PF_6^- or BF_4^- that is unable to perform addition reactions to the propagating polymer chain. Most applied methods are equilibrium processes in the presence of an acid or alkali metal salt containing the desired anion.[82] Nevertheless, excellent yields can be obtained since the target salts precipitate from solution due to

their insolubility in water. In case of chlorides, silver salts can be used in the metathesis reactions which generate insoluble silver (I) chloride.[83,84]

The photolytic cleavage reactions of base structures like triphenylsulfonium salts and diphenyliodonium salts have been investigated in detail in the past (Figure 33).[39,40,85,86] Homolytic and heterolytic cleavage of the C-S^+ or C-I^+ bond may occur, although heterolytic cleavage seems to be the predominant pathway. For both mechanisms, recombination of the primary cleavage products in the solvent cage have been specified, either by direct recombination to the PI or by molecular rearrangement to form phenylthiobiphenyl (**a**) or phenyliodobiphenyl isomers.

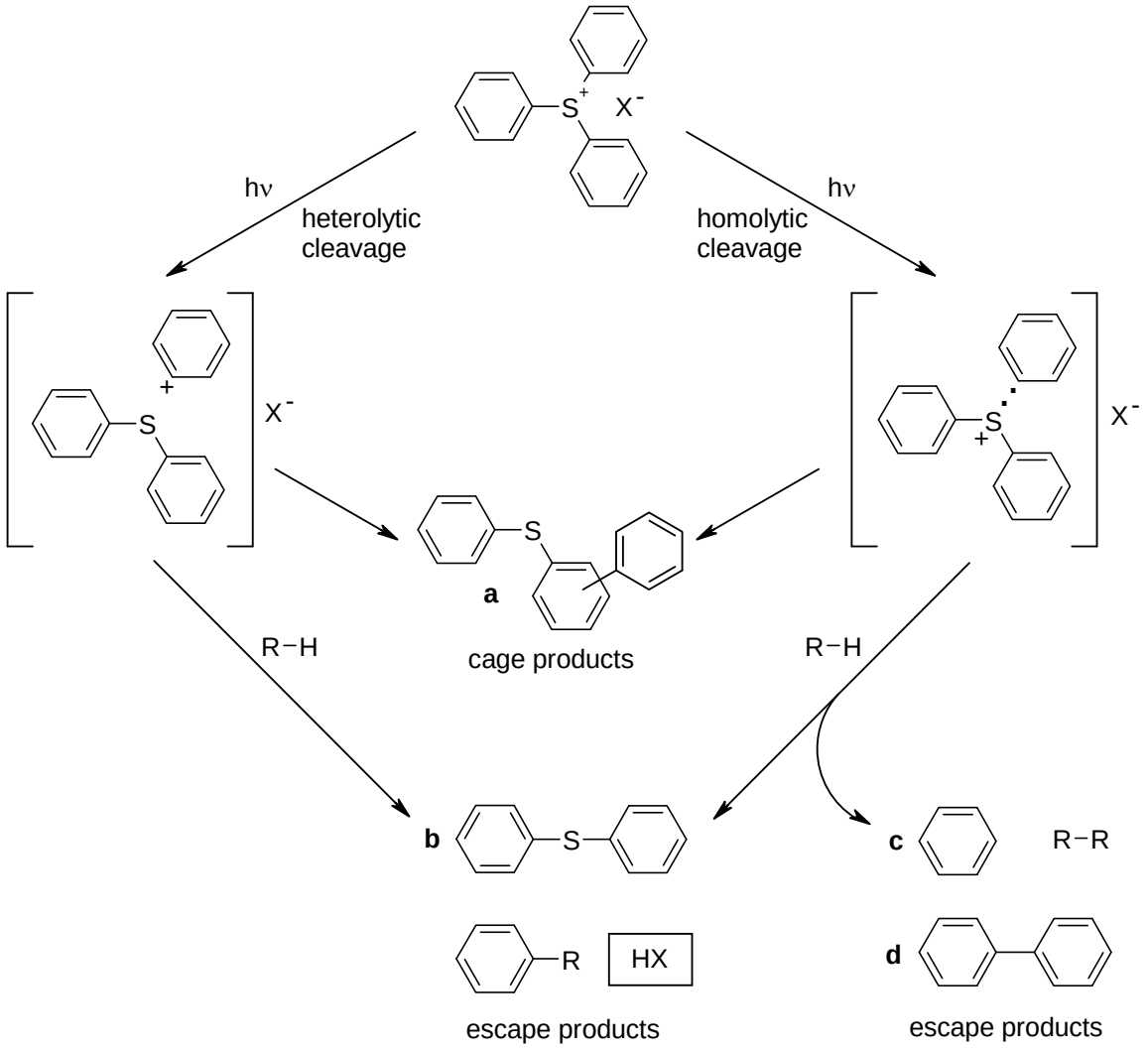

Figure 33: Photochemical decomposition of triphenylsulfonium salts

The main photoproducts of triphenylsulfonium salts are all three isomers **a**, which account in polar solvents for 60 to 70% of the total photoproducts with the *o*-isomer at top priority,[85] diphenylsulfide (**b**) and exclusively for the homolytic cleavage benzene (**c**) and biphenyl (**d**). Diphenyliodonium salts follow a similar reaction pathway, with corresponding photoproducts, but produce only 10 to 25% of the cage products.[86]

The improvement of absorption behavior of aryl onium salts has definitely been the main focus of research work for customization in the past. Apart from bathochromic shifted aryl onium salts due to the implementation of auxochromic substituents like in the commercial mixture **SPS** or expanded conjugation of the aryl systems, completely new aryl onium salt base structures like thioxanthonium -, dibenzothiophenium - or phenoxathiinium[87] salts as well as stable dialkyl onium salts like dialkylphenacylsulfonium salts have been developed.[88] (Figure 34)

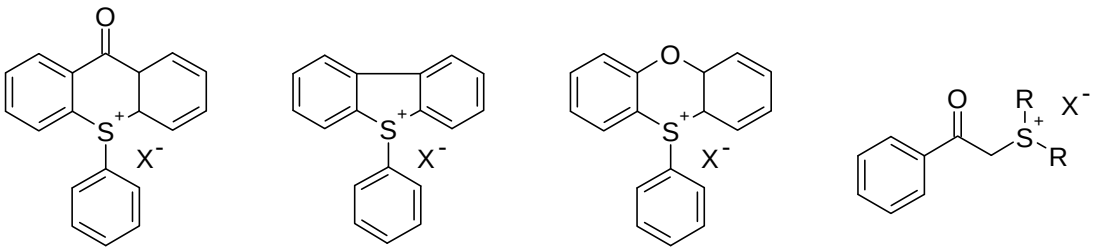

Figure 34: Thioxanthonium -, dibenzothiophenium -, phenoxathiinium - and dialkylphenacylsulfonium salts

However, few of those new PIs are commercially available and used in technical applications. Far more preferred is the utilization of sensitizers to compensate for the low absorption of elementary aryl onium salts.

Polycyclic aromatic hydrocarbons like anthracenes are able to sensitize both diaryliodonium and triarylsulfonium salts. Unfortunately, most anthracenes exhibit a poor solubility in typical cationic coating formulations and are readily oxidized to anthraquinones which are heavily colored or phenylated in the electron transfer sensitization process. (Figure 35)

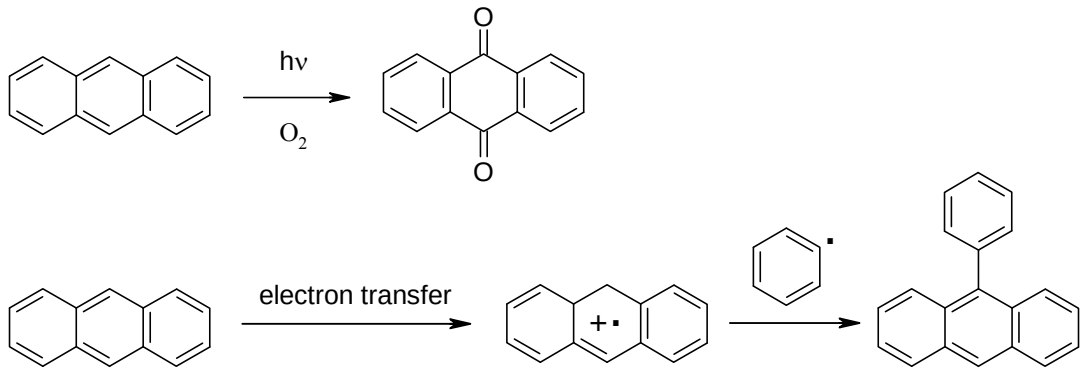

Figure 35: Oxidation and phenylation of unsubstituted anthracenes

In case of 9,10-disubstituted anthracenes like 9,10-dimethylanthracene (**DMA**) the formation of these colored side products is significantly reduced since the positions of the anthracene ring which possess the highest reactivity are already blocked. Due to a stop of the oxidation process at the endoperoxide, the conjugation is reduced and a photo-bleaching effect occurs. (Figure 36)

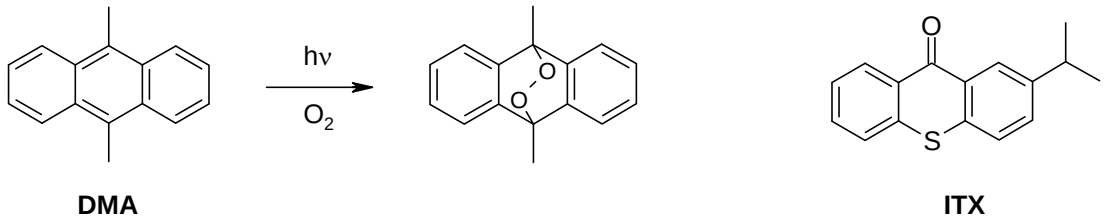

Figure 36: Oxidation of **DMA** and the commercial sensitizer **ITX**

In contrast to many aryl sulfonium salts, iodonium salts are capable of sensitization by thioxanthones like 2-isopropylthioxanthone (**ITX**, Figure 36), which is probably the most commonly used sensitizer for aryl iodonium salts. **ITX** is heavily colored and application of this sensitizer results in discoloration of the product. Unfortunately, aryl onium salts are not capable to be sensitized by ketones like benzophenone.

In 2003, a synthetic route to a sulfonium salt with a new base structure, diphenyl(phenylethynyl)sulfonium tetrafluoroborate, has been published.[89] For the synthesis of analogous phenyl(phenylethynyl)iodonium salts, several other synthetic routes have been developed in the past.[90,91,92,93,94] (Figure 37)

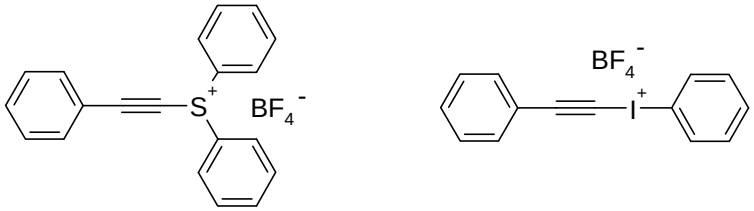

Figure 37: Diphenyl(phenylethynyl)sulfonium and phenyl(phenylethynyl)iodonium tetrafluoroborate

Both ethenylphenyl onium structures should assumedly meet most properties essential for a cationic onium salt initiator. Due to the implementation of the triple bond, a red-shift of UV-absorption, slightly improved solubility, change of the redox potential and an alteration of the cleavage mechanism producing less benzene compared to phenyl onium salts are possible. Although these new structures are very likely to compensate for one or more of the disadvantages of common aryl onium PIs, both ethenylphenyl onium structures have not been prepared as salts containing a highly non-nucleophilic anion and tested as PIs yet.

2. Onium salt base structures

2.1 Synthesis of onium salts as reference initiators (TPS-T)

The onium salt base structures diphenyliodonium hexafluorophosphate (**DPI-P**) and triphenylsulfonium hexafluorophosphate (**TPS-P**) were prepared as standards of comparison for reactivity tests.

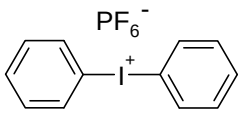

DPI-P

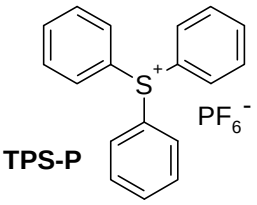

TPS-P

DPI-P was prepared from commercially available diphenyliodonium bromide by ion exchange. For the preparation of **TPS-P**, activation of diphenyl sulfoxide, reaction with phenylmagnesium bromide and subsequent exchange of the counterion is probably the most suitable method for laboratory purposes,[95] although a variety of other synthetic routes have been described in the past.[77,78,80,81]

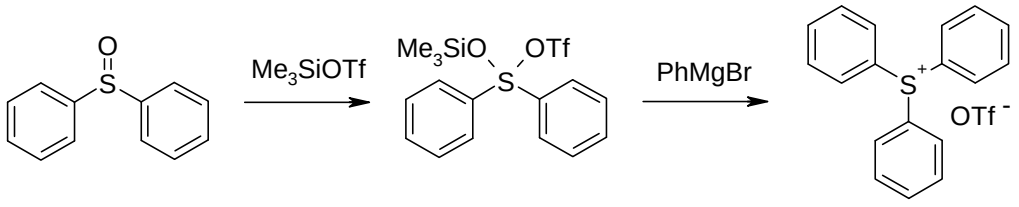

TPS-T

Therefore, phenylmagnesium bromide was prepared by Grignard reaction of bromobenzene with magnesium in anhydrous THF. Diphenyl sulfoxide was activated by reaction with trimethylsilyl triflate and converted to the sulfonium salt by reaction with 2.7 equivalents of the Grignard reagent. After extraction and recrystallization from 2-propanol **TPS-T** was obtained as colorless crystals in a yield of 49%.

2.2 Synthesis of diphenyl(phenylethynyl)sulfonium salts (1T)

From the literature it is well known that diphenyl(phenylethynyl)sulfonium tetrafluoroborate can be prepared by conversion of a 1-alkynyl-(phenyl)-λ**3**-iodane salt with diphenylsulfide.[89]

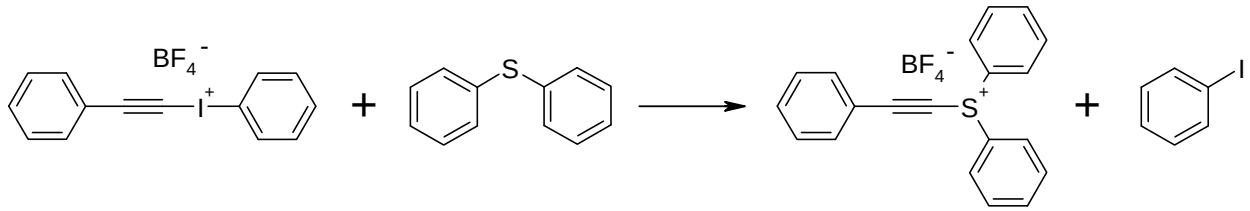

Unfortunately, this synthetic approach has two severe drawbacks: First, the general concept is not suitable as an approach that can be easily adapted for the synthesis of more complex (phenylethynyl)sulfonium salts. Furthermore, a synthesis that yields a (phenylethynyl)sulfonium triflate would enable more convenient methods for the ion exchange to non-nucleophilic anions that are inevitable for a sufficient photoreactivity as a PI. Therefore, a first attempt was made to transfer the concept of the synthesis of **TPS-T** to (phenylethynyl)sulfonium salts. Diphenyl sulfoxide was activated by reaction with trimethylsilyl triflate and phenylethynyllithium was applied as organometallic reagent for a direct synthesis of **1T**.

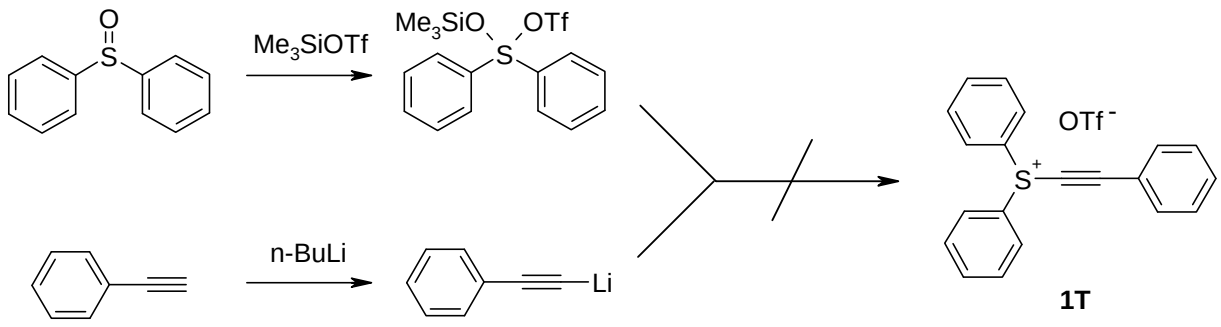

Unfortunately, the target substance could not be detected in the mixture of products. Therefore, another method was chosen analogue to the synthesis of dimethyl(phenylethynyl)sulfonium trifluoromethane sulfonate.[96]

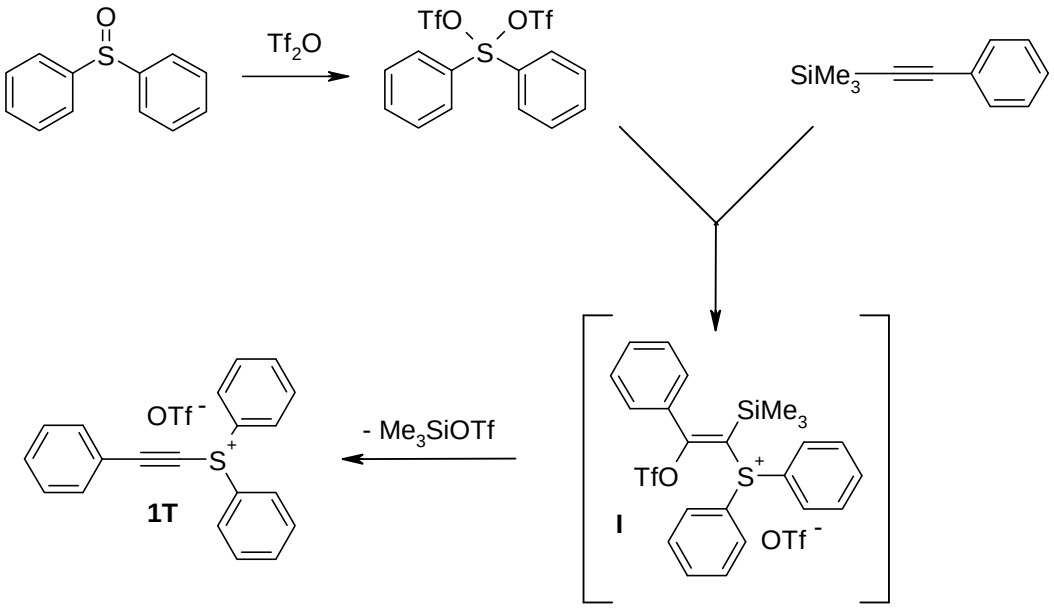

Diphenyl sulfoxide was activated by reaction with 1 equivalent of trifluoromethanesulfonic acid anhydride to give diphenyl sulfide ditriflate. Subsequent reaction with trimethylsilyl(phenyl)acetylene presumably proceeds via an unstable intermediate (**I**) that decomposes to give **1T**. Attempts to purify this sulfonium salt by crystallization or by column chromatography using mixtures of CH_2Cl_2 and alcohols that are usually applied in the purification of triarylonium salts failed due to addition reactions of alcohols to the triple bond of **1T**. From an attempt to purify the product by recrystallization from 2-propanol, (2-isopropoxy-2-phenyl-vinyl)-diphenylsulfonium triflate was isolated and characterized by NMR as a mixture of isomers E : Z = 1 : 16.

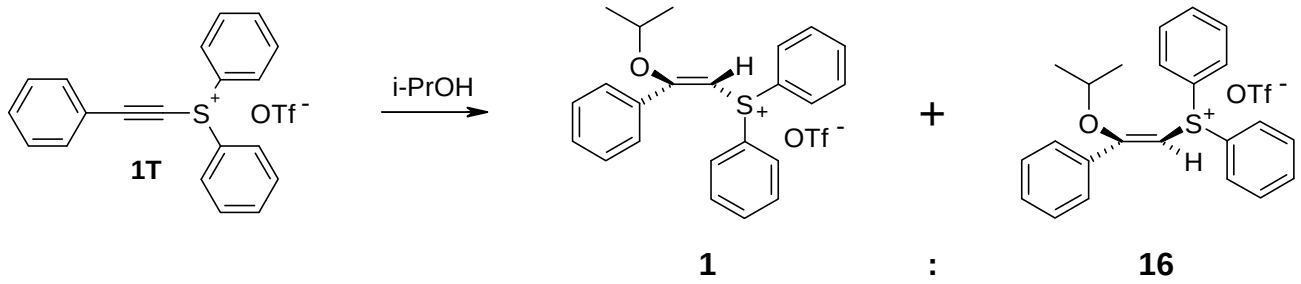

Finally, **1T** was obtained after column chromatography with CH_2Cl_2 / MeCN as a yellow oil (57%) that partially crystallized in a time span of several month.

2.3 Synthesis of phenyl(phenylethynyl)iodonium salts (2T)

In contrast to the synthesis of phenylethynyl sulfonium salts, several pathways for the preparation of phenylethynyl iodonium salts have already been published.[90,91,92,93,94] For the synthesis of the iodonium salt **2P**, a method for the direct preparation of the corresponding phenylethynyl iodonium triflate salt **2T** by conversion of (diacetoxyiodo)benzene with trimethylsilyl(phenyl)acetylene was chosen.[92]

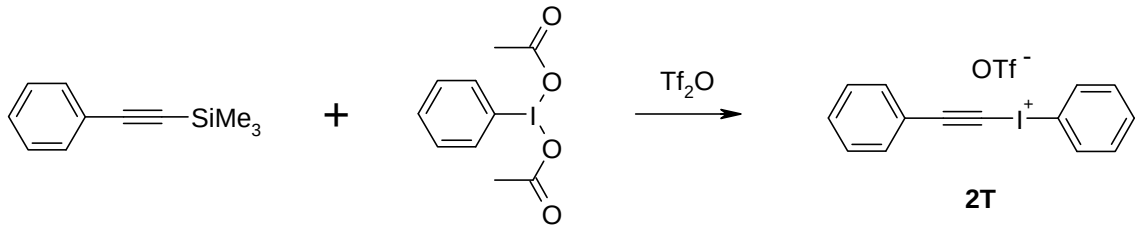

2T

(Diacetoxyiodo)benzene was activated with 1 equivalent of trifluoromethanesulfonic acid anhydride and converted by subsequent reaction with 1.5 equivalents of trimethylsilyl(phenyl)acetylene. After extraction and column chromatography of **2T** with pure CH_2Cl_2, a small amount of crystals was obtained that were utilized to start crystallization of the oil at -20 °C. Subsequent washings with ether gave **2T** in 65% yield.

2.4 Ion exchange

The last synthetic step in the preparation of sulfonium and iodonium salts as PIs for cationic photopolymerization is the ion exchange of the anionic counterion. The synthesized iodonium- and sulfonium salts were received as triflates. However, onium triflates exhibit a low photoreactivity as initiators due to the relative high nucleophility of the anion and are not suitable for an application as cationic PIs. For this reason, the anion was changed to hexafluorophosphate, which exhibits a high stability and a low nucleophilic character, to prepare the PIs **1P**, **2P**, **TPS-P** and **DPI-P**. Additionally, the

corresponding hexafluoroantimonates **1Sb**, **2Sb**, **TPS-Sb** and **DPI-Sb**, which should exhibit an even higher reactivity compared to hexafluorophosphates, were synthesized. Apart from the purpose of comparison of NMR and IR spectroscopy of the structures, the more reactive hexafluoroantimonates should be utilized in case that the hexafluorophosphates exhibit an insufficient reactivity for the performance of photo-DSC studies.

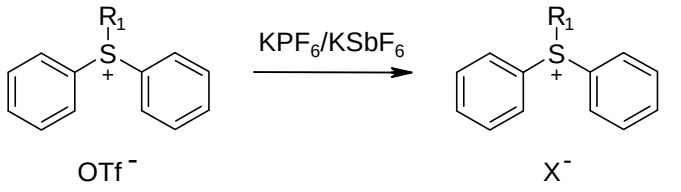

1P: $R_1 = C_8H_5$, X = PF_6

1Sb: $R_1 = C_8H_5$, X= SbF_6

TPS-P: $R_1 = C_6H_5$, X = PF_6

TPS-Sb: $R_1 = C_6H_5$, X= SbF_6

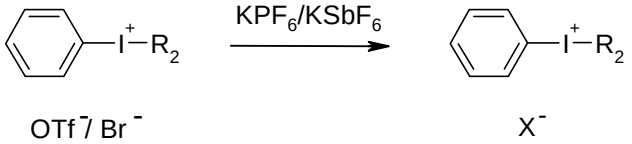

2P: $R_2 = C_8H_5$, X = PF_6

2Sb: $R_2 = C_8H_5$, X= SbF_6

DPI-P: $R_2 = C_6H_5$, X = PF_6

DPI-Sb: $R_2 = C_6H_5$, X= SbF_6

Generally, ion exchange was performed by suspending the onium salt in a concentrated solution of 10 equiv. potassium hexafluorophosphate or -antimonate or in a two phase system of CH_2Cl_2 / 5 equiv. concentrated solution of potassium salt depending on the solubility of the onium salts in both solvents. In case of the iodonium salts **2P** and **2Sb** the ion exchange and the subsequent purification had to be performed at 0 °C due to the low thermal stability of these structures. All other ion exchanges were performed at rt. The new PIs were received in yields from 60 to 95%. The degree of residual nucleophilic anions was analyzed by IR spectroscopy, in case of a concentration of triflate > 5 mol%, the ion exchange process was repeated.

2.5 Quantification of ion exchange by IR spectroscopy

Since residual nucleophilic anions, like triflate ions, have an impact on the performance of the cationic PI, an entire conversion of the counterion is a crucial factor in the synthesis. Although many methods for ion exchange exist that are generally dependent on the nature of the counterions,[82,83,84] a sufficient quantification of the residual concentration of the nucleophilic anion is usually not possible by standard analytical methods used for substance verification like NMR, HPLC or GC MS. However, IR spectroscopy combined with a subsequent mathematical peak deconvolution of the IR spectrum is a perfect tool for the monitoring of the ion exchange process. Especially for the exchange of anionic counterions that exhibit strong absorptions in IR like triflates and most counterions conventionally used for cationic PIs, the degree of ion exchange can be determined with a sufficient accuracy. The determination of the residual concentration of the nucleophilic anion can be performed by mathematical peak deconvolution of IR spectra using calibration curves or internal standards. ATR IR spectra with ATR correction were utilized for estimation purposes only, for an exact determination of the degree of ion exchange, FT IR spectroscopy in CH_2Cl_2 in a sealed cell with NaCl windows was used.

2.6 UV-Vis Spectroscopy

The UV-Vis absorption spectra of the PIs **1P** and **2P** were measured in the range of 1×10^{-3} to 1×10^{-6} mol L^{-1} in MeCN as solvent (Figure 38, Table 4). The UV-Vis spectra of the well known base structures, the triphenylsulfonium salt **TPS-P** and the diphenyliodonium salt **DPI-P**, are shown for comparison. Similar to common phenyl onium salts, the nature of the inorganic counterion does not have any significant impact on the UV-Vis absorption spectra of phenylethynyl onium salts. UV-Vis spectra of **1T** and **1Sb** as well as **2T** and **2Sb** can be regarded as almost identical to the spectra of the hexafluorophosphates that are shown for illustration.

Table 4: UV-Vis data of PIs **1P**, **2P**, **TPS-P** and **DPI-P** in MeCN (1 x 10^{-5} mol L^{-1})

PI	λ_{max} [nm]	$\varepsilon_{max} \times 10^{-3}$ [L mol^{-1} cm^{-1}]
TPS-P	226	23.4
1P	274	16.9
	221	40.4
DPI-P	222	19.4
2P	243	13.7
	229	16.3

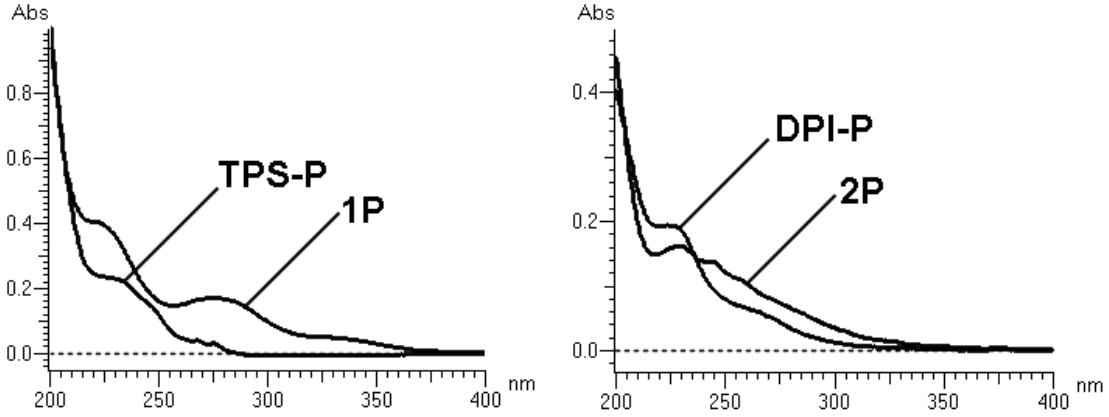

Figure 38: UV-Vis spectra of **1P**, **2P**, **TPS-P** and **DPI-P** (1 x 10^{-5} mol L^{-1}) in MeCN

Due to the implementation of the triple bond, a significant red-shift in the absorption spectrum of **1P** compared to **TPS-P** was observed. As usually found for triple bonds, the wavelength of maximum absorption (λ_{max}) of the new chromophore is shifted approximately 50 nm in comparison to the λ_{max} of the triphenyl sulfonium chromophore. Tail out of the absorption was shifted from 280 nm (**TPS-P**) to above 350 nm (**1P**) which is of significant importance for the direct excitation of the chromophore. In contrast to **1P**, the bathochromic shift of λ_{max} due to the implementation of the triple bond is less significant in the UV-Vis spectrum of **2P**. A new λ_{max} becomes apparent at 243 nm and absorption tails slowly out between 300 and 350 nm.

2.7 Photolysis and thermal decomposition

Due to the implementation of a triple bond into the base structures of typical cationic PIs like **TPS-P** and **DPI-P**, phenylethynyl sulfonium and -iodonium salts like **1P** and

2P may exhibit a different photochemistry than usual aryl onium salts. The most convenient method to investigate the decomposition pathway is to draw conclusions from the analysis of the corresponding photoproducts. In case that the photodecomposition occurs in analogy to phenyl onium salts like **TPS-P** and **DPI-P** as well in a heterolytic as in a homolytic pathway, a significant amount of different photoproducts are to be expected. (Figure 39) Diphenylsulfide and phenyl(phenylethynyl) sulfide as well as iodobenzene and phenylethynyl iodide are most probably main photoproducts. In case that homolytic decomposition is as important for phenylethynyl onium salts as it is for **TPS-P** and **DPI-P**, significant amounts of benzene, phenylacetylene and, due to recombination of radicals, biphenyl, 1,2-diphenylacetylene, and 1,4-diphenyldiacetylene have to be expected. Furthermore, in-cage-rearrangements products similar to the photodecomposition of to **TPS-P** and **DPI-P** may occur.

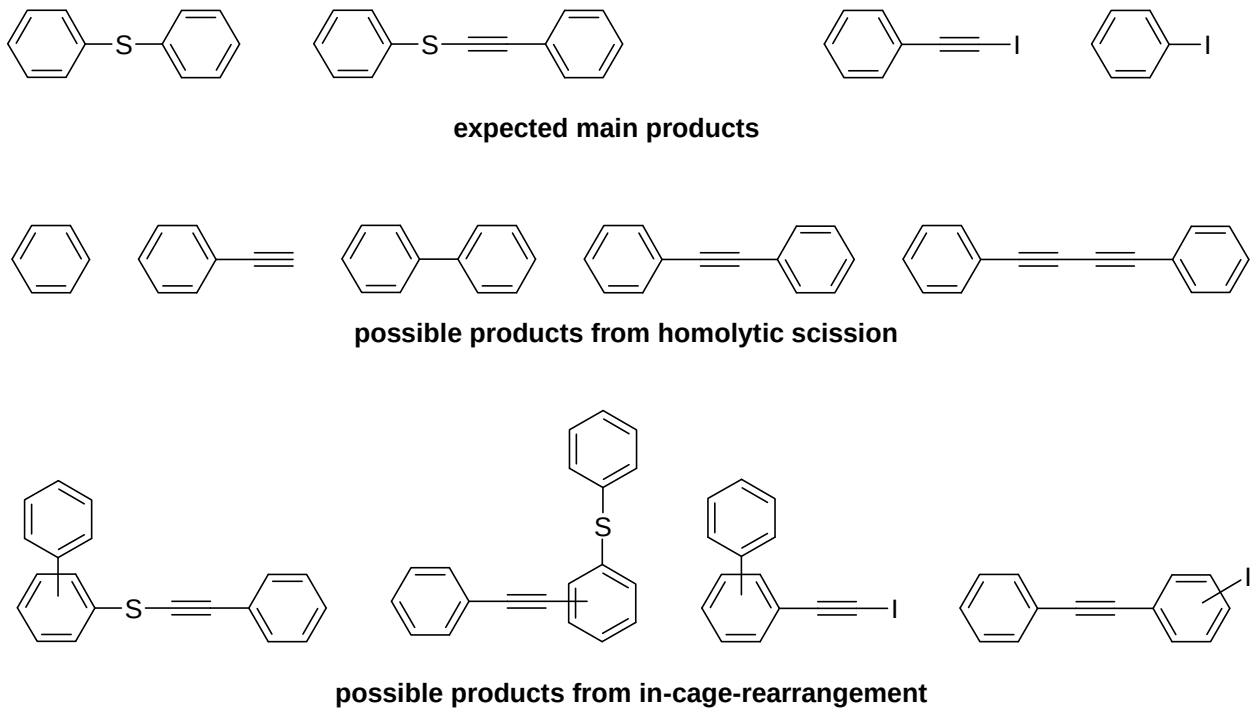

Figure 39: Possible photodecomposition products of **1P** and **2P**

Reversed phase HPLC with UV detection and GC MS analysis are a perfect combination for a qualitative and quantitative analysis of photoproducts of aryl sulfonium and aryl iodonium salts. Due to the large amount of information gained by

both chromatographic methods, the UV and MS spectrum, photoproducts can be easily identified and quantified. However, ionic residues and the strong acids that are formed during photolysis have a negative impact on the separation of the organic photoproducts and on the analytical equipment and must be separated before analysis. Photolysis of **1P** and **2P** (1 x 10^{-2} mol L^{-1}) was carried out in MeCN under argon and under air with filtered UV-Vis light (1000 mW cm^{-2}; 250 - 450 nm). Residues of the PIs, acids and ionic compounds were separated by column chromatography from the photolysis solution. As it could not be excluded that important photolysis products are lost by this separation technique, an identical photolysis of the PIs was carried out in CH_2Cl_2 with subsequent removal of ions and acids by extraction with water. In both solvents, photolysis yielded virtually the same distribution of photoproducts, negligible differences were only found due to reaction of the solvents with cations.

2.7.1 Synthesis of decomposition products

Most possible decomposition products of **1P** and **2P** are commercially available for an application as internal standards for GC MS or HPLC analysis. However, one of the main decomposition products to be expected, phenyl(phenylethynyl) sulfide (**F_2**), had to be synthesized. A first attempt was made to obtain **F_2** by coupling of phenylacetylene with diphenyl disulfide in the presence of copper (I) iodide and potassium carbonate in DMSO as described in literature.[97]

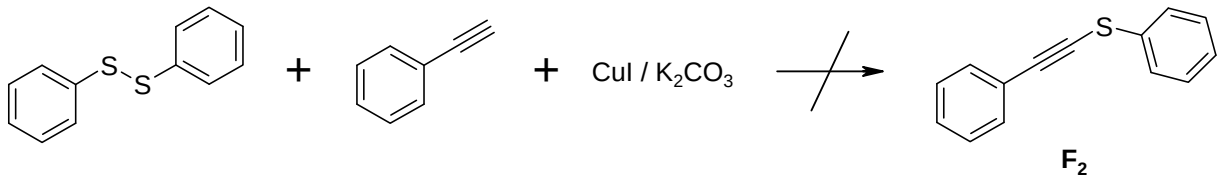

However, the desired product could not be isolated or detected in the mixture of reaction products and also variation of reaction conditions gave no satisfying results. An alternative synthesis of **F_2** is the reaction of diphenyl disulfide with phenylethynyllithium.[98]

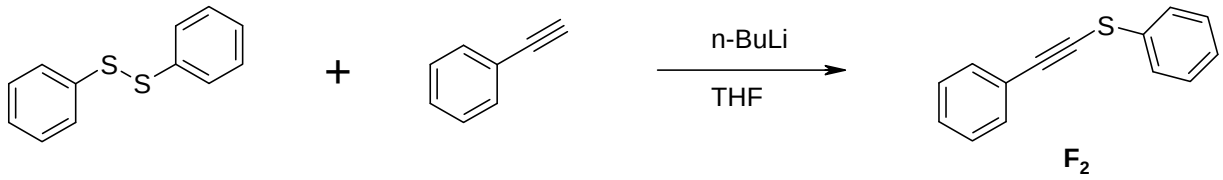

F₂

After conversion of phenylacetylene with 1.05 equiv. of n-butyllithium and subsequent reaction with diphenyl disulfide in THF, extractive purification gave pure **F₂** as a yellowish oil in 99% yield.

Organic sulfides are known to be oxidized to the corresponding sulfoxides by reaction with singlet oxygen.[99] In contrast to radical polymerization, cationic polymerization is usually not performed under an inert gas atmosphere in technical applications and generation of singlet oxygen is therefore an inevitable process that may result in a conversion of photo-cleavage products. For this reason phenyl(phenylethynyl) sulfoxide (**F$_{2, ox}$**) was synthesized to serve as a standard for GC MS and HPLC analysis for photodecomposition tests under air.

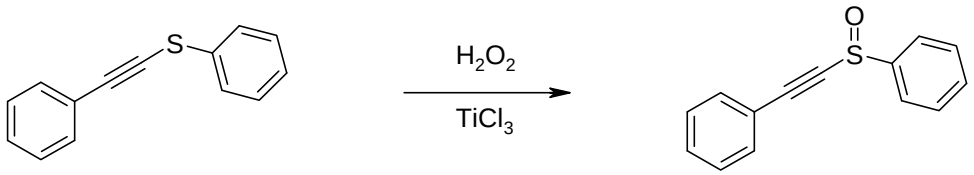

F₂ **F$_{2, ox}$**

F$_{2, ox}$ was synthesized, analogue to a reaction procedure for the synthesis of diphenyl sulfoxide from diphenyl sulfide,[100] by oxidation of **F₂** with hydrogen peroxide in the presence of titan (III) chloride in a mixture of methanol and water at 5 °C. After column chromatographic purification, **F$_{2, ox}$** was obtained as a colorless oil (89%).

2.7.2 Photolysis of 1P under inert gas

In the photolysis of **1P,** two major photoproducts could be observed. MS and UV spectra gave some strong indication to diphenylsulfide (**F₁**) and 2-phenylethynyl

phenyl sulfide (**F$_2$**) (Figure 40). Therefore, **F$_2$** was prepared according to literature,[98] and the two substances (**F$_1$** is commercially available) were used as standards in HPLC analysis to verify identity and to determine the distribution of the products. In both solvents (MeCN and CH_2Cl_2), photolysis yielded a molar ratio of **F$_1$** : **F$_2$** of approximately 8 : 1. In contrast to the photolysis of **TPS-P**, analysis of the photoproducts gave no evidence of traces of cage-products (Figure 39) formed by rearrangement reactions. Traces (< 1%) of only two side products (**F$_3$** and **F$_4$)** that were most likely formed by rearrangement and recombination of organic radicals could be identified by HPLC and GC MS. Apart from **F$_1$ - F$_4$**, only minor, secondary photoproducts originating from reactions of cations with the solvent could be detected.

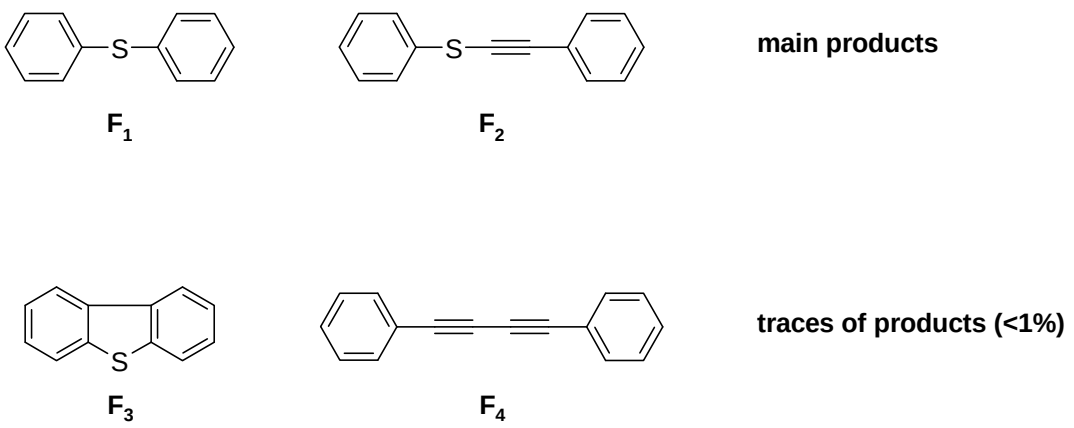

Figure 40: Main photodecomposition products **F$_1$** and **F$_2$** and recombination and rearrangement products **F$_3$** and **F$_4$** in the photolysis of **1P**

Obviously, the diversity of photoproducts of **1P** is clearly restricted in comparison to **TPS-P**. Due to the total lack of cage-products, occurrence of in-cage-rearrangements in the photodecomposition of **1P** is obviously insignificant. Although **F$_4$** was found as a trace product and phenylacetylene was detected in the photolysis of **1P** in CH_2Cl_2, no other products derived from radicals like benzene, biphenyl or 1,2-diphenylacetylene could be verified. This absence of significant amounts of recombination products of radicals indicates a preference of a heterolytic photodecomposition pathway. According to the detected photoproducts, the main decomposition pathway of **1P** in direct irradiation seems to be a heterolytic cleavage, preferably of the ethynyl carbon-

sulfur bond (Figure 41) which is presumably a direct consequence of a reduced bond-strength.

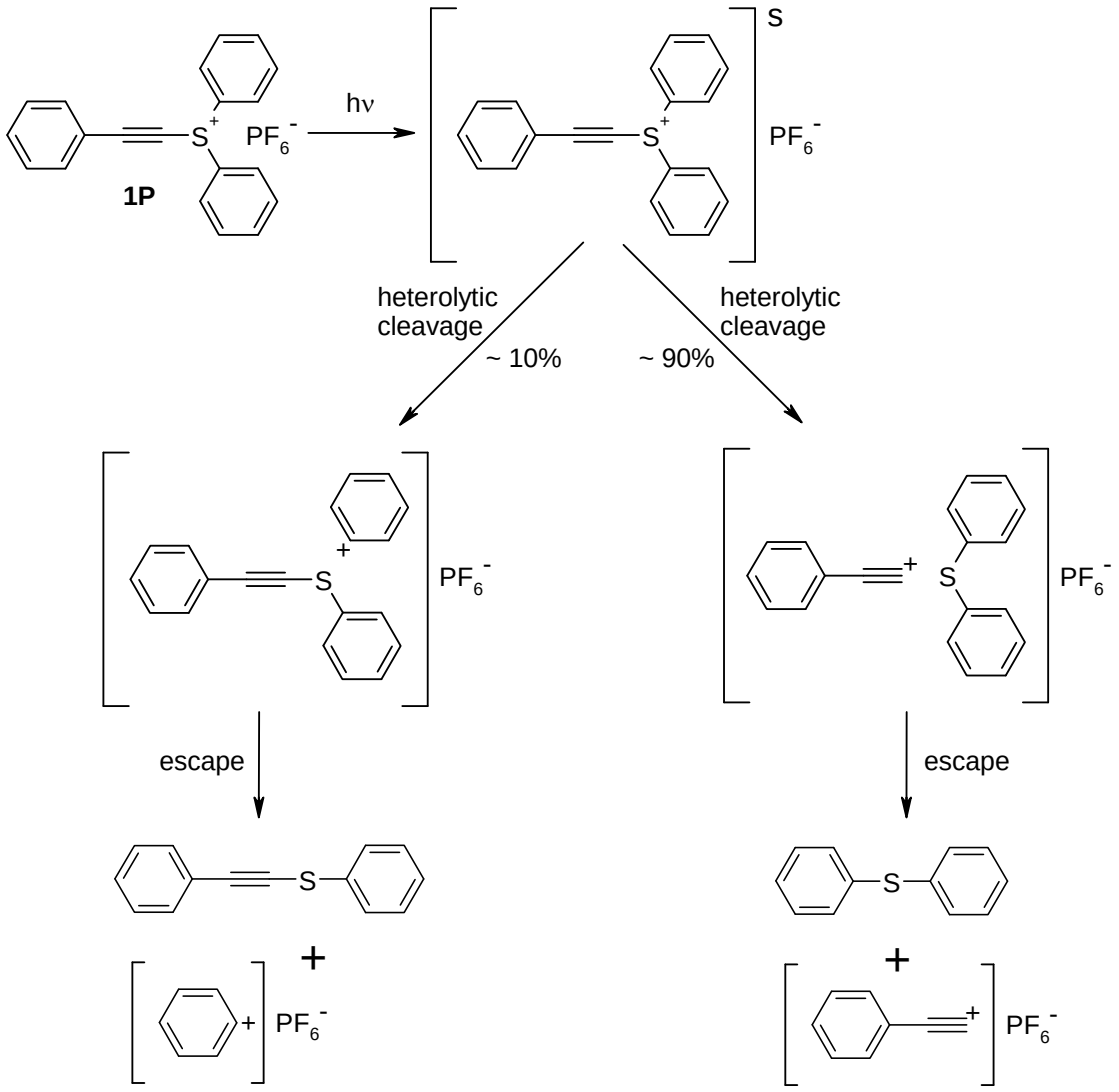

Figure 41: Heterolytic (main) photochemical decomposition pathway of **1P**

Due to the formation of the recombination product **F4**, homolytic photochemical decomposition or in cage rearrangements that form phenylacetylene radicals from phenylacetylene cations in the solvent cage obviously occur to some extent. The yield of phenylacetylene radicals formed in the photodecomposition is necessarily more than twice the concentration of the photoproduct **F4**. Furthermore, not every phenylacetylene radical generated will result in the formation of the recombination product **F4**. However, due to the low concentration of recombination products of

phenylacetylene radicals the heterolytic decomposition pathway is obviously predominant. Nevertheless, homolytic cleavage can be proposed as a minor, secondary photodecomposition pathway for **1P** (Figure 42).

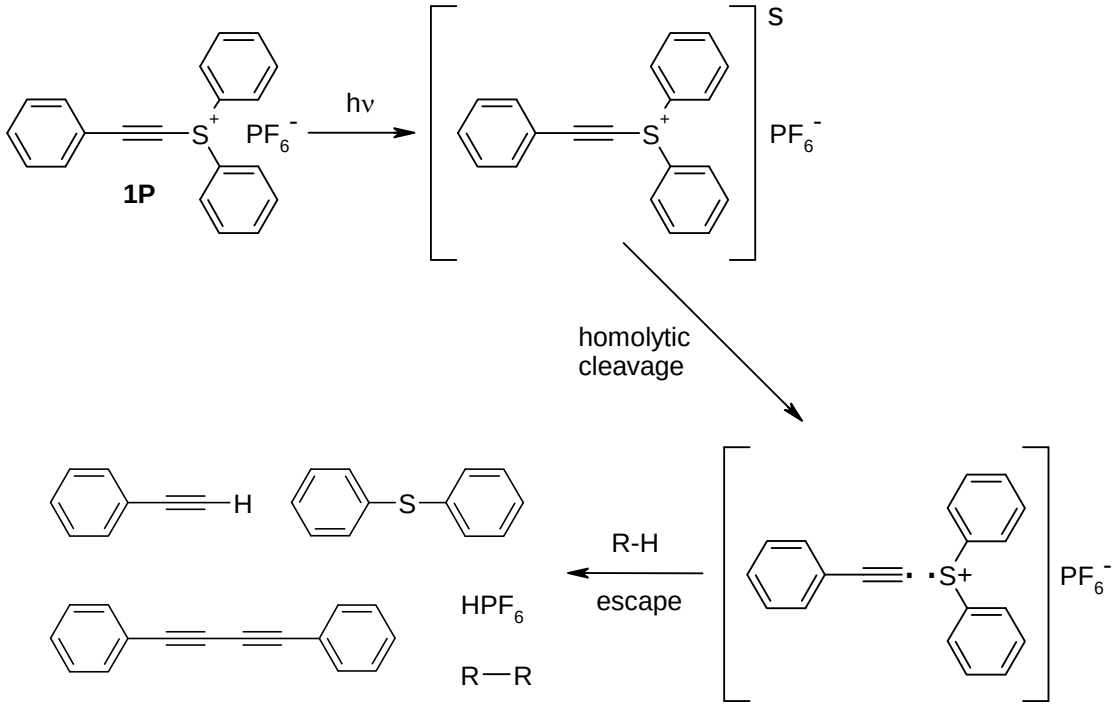

Figure 42: Homolytic (minor) photochemical decomposition pathway of **1P**

It is very probable, that a corresponding homolytic decomposition also occurs by scission of the sulfonium-phenyl bond which yields benzene, biphenyl and in combination with the presented homolytic pathway 1,2-diphenylacetylene. However, since no traces of these products were detectable, this second homolytic decomposition pathway is obviously insignificant.

It is not totally clear, how the second trace product **F_3** is formed in the photodecomposition of **1P**. The formation of **F_3** is not recorded in the photolysis of **TPS-P** in literature. Nevertheless it must be presumed that **F_3** is probably evolved from diphenyl sulfide by reaction with cations or radical cations.

2.7.3 Photolysis and thermal decomposition of 2P under inert gas

In the case of the iodonium salt **2P** it can be expected that the ethynyl carbon-iodine bond is significantly weaker in comparison to the sulfonium salt **1P**. Therefore, an even more definite preference of the scission of the ethynyl carbon-iodine bond could be expected. In photodecomposition experiments of phenyl(phenylethynyl)iodonium tosylate, iodobenzene (**F_5**) and phenylethynyl iodide (**F_6**) (Figure 43) have been found as major products in a molar ratio of 2.5 : 1 in literature.[101]

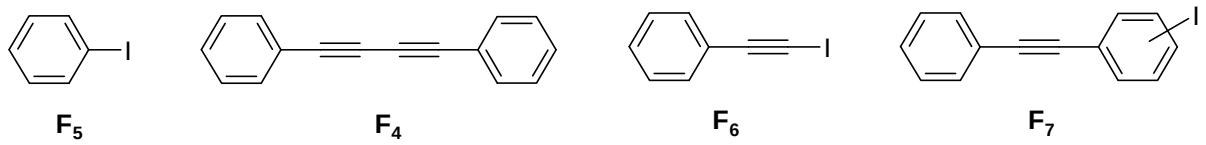

Figure 43: Photochemical (**F_5**, **F_6**) and thermal (**F_4** - **F_7**) decomposition products of **2P**

However, photolysis of **2P** in MeCN and CH_2Cl_2 yielded only **F_5** as a main photoproduct and only minor amounts (<5%) of **F_6**. Similar to the photodecomposition of **1P**, no evidence of traces of cage-products formed by rearrangement reactions analogous to **DPI-P** could be found. Furthermore, no traces of rearrangement and recombination products of organic radicals analogous to **F_3** and **F_4** were detectable. Obviously, the iodonium salt **2P** exhibits an even more defined, simple photodecomposition pathway in comparison to the sulfonium salt **1P** (Figure 44).

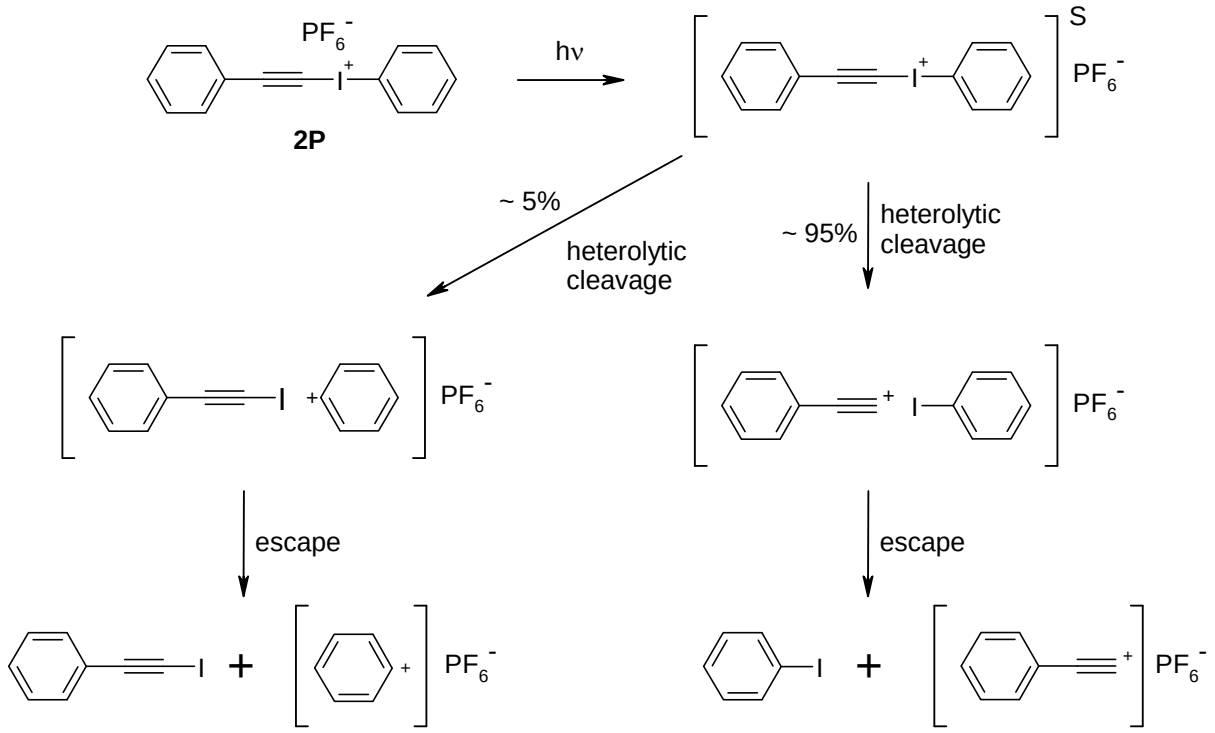

Figure 44: Heterolytic (main) photochemical decomposition pathway of **2P**

In contrast to **1P** which is stable at rt, crystalline **2P** exhibits only a limited stability at rt due to the high reactivity of the phenylacetylene-iodonium bond. In form of an undercooled melt or in concentrated polar solutions, **2P** may thermally decompose within several hours. Apart from the main product $\mathbf{F_5}$, several side products in the thermal decomposition of a sample of **2P** (50 wt%) in trifluoromethane sulfonic acid at rt were detected in HPLC and GC MS (Figure 43). The side product $\mathbf{F_6}$ was observed to account for less than 5 mol% of the decomposition products and $\mathbf{F_4}$ for 2 - 4 mol%. The iodo-(phenylethynyl)benzene isomers $\mathbf{F_7}$ only occurred as trace products.

Since phenylacetylene was also detected in traces in photochemical decomposition in CH_2Cl_2 as well as more pronounced in thermal decomposition, it must be presumed that homolytic cleavage occurs to some extent in both decomposition pathways. However, since no traces of other possible recombination products of radicals like benzene, biphenyl or 1,2-diphenylacetylene could be verified, it can be proposed that in both photochemical and thermal decomposition a heterolytic pathway is dominant.

2.7.4 Photolysis of 1P and 2P under air

In the photolysis of the sulfonium salt **1P** under air, a new minor product could be observed in comparison to photolysis under an inert gas atmosphere. MS and UV spectra gave some strong indication to diphenylsulfoxide (**$F_{1,\ Ox}$**) which was used as standard in HPLC analysis to verify identity and determine the distribution of the products. To exclude the existence of unrecognized phenyl(phenylethynyl) sulfoxide (**$F_{2,\ Ox}$**) in the product mixture, this substance was synthesized and applied as an additional standard. However, no oxidation product **$F_{2,\ Ox}$** could be detected in both HPLC and GC MS analysis.

The distribution of the major photoproducts and their oxidation products (**F_1** + **$F_{1,\ Ox}$**) : (**F_2**) was approximately 8 : 1, the same distribution as under inert gas. At first glance, it seems to be possible that the sulfide **F_1** was conversed to the sulfoxide due to oxidation by singlet oxygen (Figure 45).

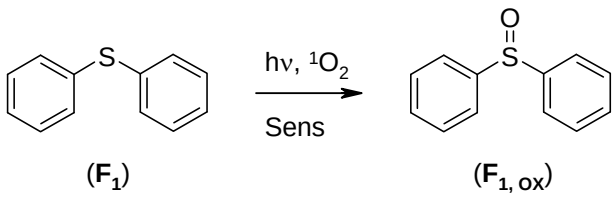

Figure 45: Oxidation of **F_1** by singlet oxygen

However, sulfide oxidation by singlet oxygen mechanism is known to be sluggish in aprotic media, especially in case of aryl alkyl and diaryl sulfides[99] and in contrast to common photooxidation reactions, no effective sensitizer for singlet oxygen was applied in the photolysis. A probable resolution to this antagonism can be found in the mechanism of electron transfer sulfoxidation of diphenyl sulfide.[102] In electron transfer oxidation of sulfides, the conversion is proposed to proceed via a reaction of the diphenyl sulfide radical cation with molecular oxygen. Due to homolytic cleavage reactions, diphenyl sulfide radical cations are generated as intermediates in photodecomposition of sulfonium salts.

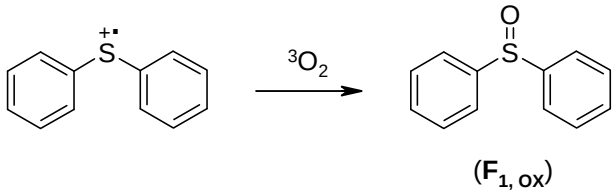

Figure 46: Oxidation of diphenyl sulfide radical cation by molecular oxygen

For this reason, it is very likely that $\mathbf{F_{1,\ Ox}}$ is formed to some part by oxidation with molecular oxygen during homolytic photo-cleavage. (Figure 46)

In contrast to the sulfonium salt **1P**, in the photolysis of **2P** no change in the distribution of photoproducts and no new photo-cleavage or photooxidation products could be detected.

2.8 Photo-DSC

Differential scanning photocalorimetry (photo-DSC) is a unique method for obtaining a fast and accurate indication of the performance of a UV-curing system. With a single measurement, various important parameters are accessible. Apart from t_{max}, which reveals information about the photoinitiator activity, the EGC can be calculated from the area below the trace and R_p can be determined from the height of the exothermic peak.

The present photo-DSC study was carried out to investigate the photoreactivity of the onium salts **1P** and **2P** in comparison to **TPS-P** and **DPI-P**. The PIs (2.5×10^{-2} mol L^{-1}) were applied as 50 wt% solutions in propylene carbonate in 3,4-epoxycyclohexenylmethyl-3',4'-epoxycyclohexenyl carboxylate (**ECHC**)**.** Since sensitizers to enhance the performance of onium salts are commonly used in technical applications, the experiments focused on the enhancement of the performance of the different systems by addition of **DBA**, **ITX** and **BP** (1×10^{-2} mol L^{-1}). Although the latter one is described to show no activity for classical systems like **TPS-P** and **DPI-P**, we were interested to see if there is an effect on the performance of **1P** and **2P**. All

experiments were carried out with filtered UV-Vis light (280 - 450 nm) in isothermal mode at 30 °C under a nitrogen atmosphere to exclude humidity.

The comparison of the t_{max} values of different cationic curing systems is an adequate method for the determination of the photoinitiation activity and for an indication of sensitization or inhibitory effects (Figure 47).

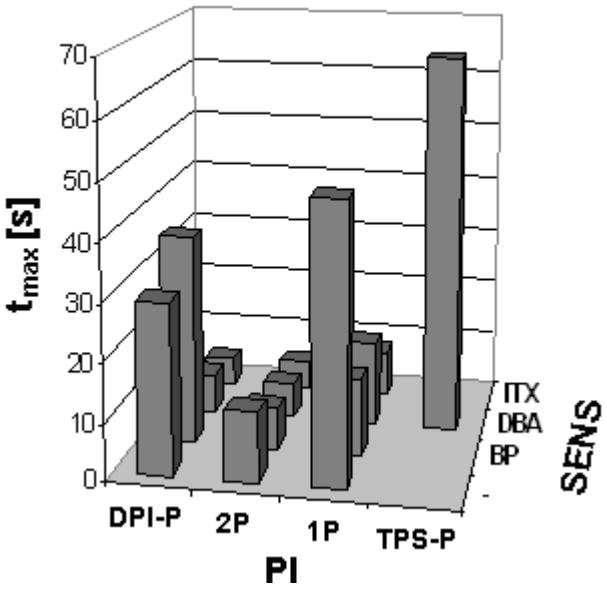

Figure 47: t_{max} values of **ECHC** with different PI / sensitizer systems

In comparison to all other PIs, the phenylethynyl sulfonium salt **1P** possesses a higher UV absorption above 280 nm. Nevertheless, the more reactive iodonium salts **DPI-P** and **2P** provide significantly lower t_{max} values without application of a sensitizer. The formulation containing the phenylethynyl iodonium salt **2P** exhibits less than half of the t_{max} value of **DPI-P**. Obviously, the t_{max} value of **2P** is already in the order of magnitude of formulations containing efficient sensitizer / PI combinations. In contrast to **1P** that shows some moderate photoreactivity, **TPS-P** was not capable to initiate photopolymerization without application of a sensitizer due to the wavelength range of the applied light source.

In accordance with the literature,[103] **TPS-P** can not be sensitized by the thioxanthone **ITX** or by **BP**, but some moderate reactivity can be found with the anthracene **DBA**,

which is still significantly poorer than any other systems in these studies. All other PIs provide a significant decrease of t_{max} together with **DBA** or **ITX** compared to the samples without a sensitizer, which is a strong evidence for a sensitization process.
Independent of the choice of sensitizer (except **BP**) the t_{max} values of formulations with the sulfonium salt **1P** are approximately twice as large as those containing the iodonium salts **DPI-P** or **2P**. The t_{max} of both iodonium salts are approximately in the same order of magnitude except in combination with **BP** or in direct excitation. As described in literature, the iodonium salt **DPI-P** exhibits no efficient sensitization by **BP** although the calculated ΔG value is slightly negative ($\Delta G = -2$ kcal mol^{-1}).[46] With **BP** as sensitizer, a minor increase of t_{max} of **ECHC** compared to the sample without sensitizer was detected, probably caused by a light screening effect. In contrast to **DPI-P,** both phenylethynyl onium salts **1P** and **2P** exhibit significantly lower t_{max} values when applied together with **BP** as sensitizer, a strong indication of some type of sensitization process. Presumably the incorporation of the triple bond into the aryl-onium system causes a significant change of the redox potential thus enabling the application of new sensitizers like **BP** that are not capable to sensitize common onium salts (Table 5).

Table 5: Sensitization of the onium salts **TPS-P**, **DPI-P**, **1P** and **2P**

	TPS-P	**DPI-P**	**1P**	**2P**
DBA	✓	✓	✓	✓
ITX	-	✓	✓	✓
BP	-	-	✓	✓

It can be concluded that the corresponding order of reactivity of the chosen PIs is obviously **2P** > **DPI-P** > **1P** >> **TPS-P**. The analogue order of reactivity for the sensitizers under the chosen experimental conditions is **ITX** > **DBA** / **BP** >> no sensitizer. Additionally, this trend is also distinctly visualized by the corresponding EGC and R_p values (Figure 48). It has to be noted that the EGC values have to be considered with care, as this values are determined from the area below the trace during the time of irradiation. Post polymerization effects, that are of significant relevance in cationic polymerization, are not considered.

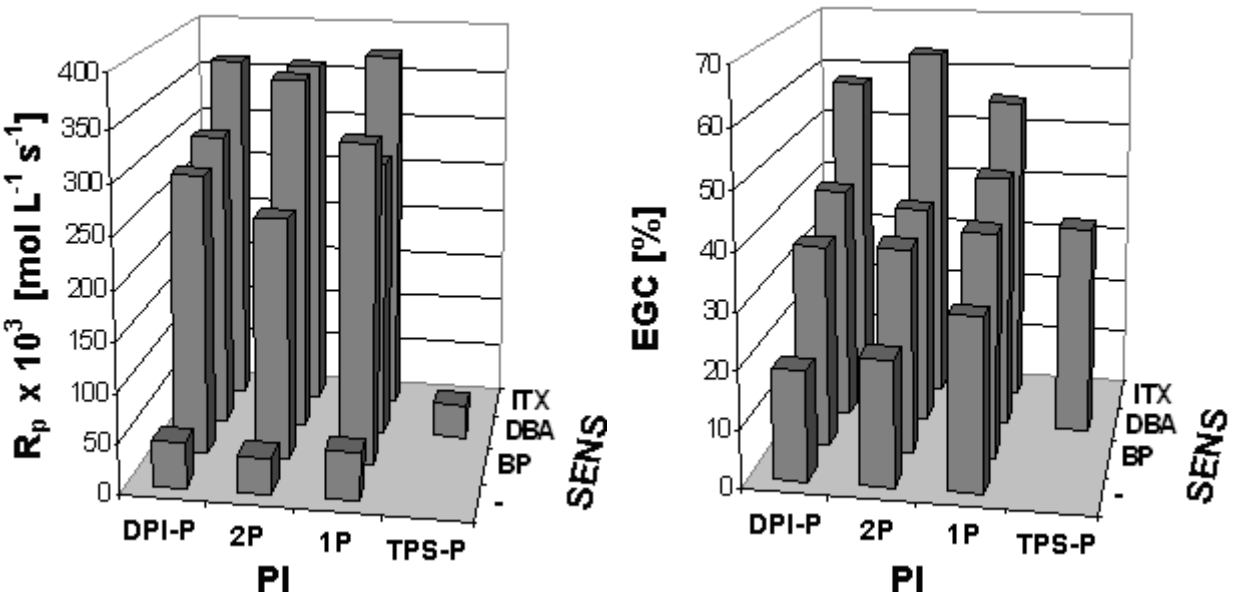

Figure 48: EGC and R_p values of **ECHC** with different PI / sensitizer systems

EGC and R_p values for formulations containing the phenylethynyl onium salts **1P** and **2P** are significantly increased by application of **BP** as sensitizer and are in the same order of magnitude than those of formulations containing the anthracene **DBA**. Furthermore, the overall performance of **1P** and **2P** together with **BP** as sensitizer in photo-DSC is evidently comparable to formulations containing the iodonium salt **DPI-P** and **DBA**, which is again a strong indication that unlike common aryl-sulfonium salts, phenylethynyl onium salts are capable of sensitization by **BP**. It has to be noted that **BP** is able to increase the EGC and R_p values in the case of **DPI-P** although it is commonly described that **BP** is not able to efficiently act as a sensitizer.

3. Broad band irradiation experiments

In combination with electron transfer sensitizers, the performance of a cationic PI gets increasingly independent of the direct absorption of the onium-chromophore. Onium salt formulations usually rise significantly in performance with already low admixtures of sensitizers and exhibit an optimal sensitizer-concentration. In the previous chapter, 9,10-dibutylanthracene (**DBA**) proved to be a promising new sensitizer which possesses an activity comparable to **ITX**. In contrast to most commercially used sensitizers like **ITX**, **DBA** is able to sensitize sulfonium salts.

Anthracenes, for example 9,10-dimethylanthracene (**DMA**), exhibit their strongest absorptions in UV-C, significantly below 280 nm. **DBA** should exhibit an absorption spectrum very similar to **DMA**, since the exchange of dimethyl- to dibutyl-substituents should most probably have only a minor influence on the absorption of the chromophore. Although the results of the photo-DSC experiments (280 - 450 nm) showed a high activity for **DBA**, the experimental conditions were obviously not suitable to show the full potential of this new sensitizer.

In contrast to iodonium salts, very few sensitizers exist for sulfonium salts that can be used in technical applications, for instance in apolar coating formulations. Polycyclic aromatic hydrocarbons like anthracenes or perylenes are probably the most well-known sensitizers for sulfonium salt PIs but usually suffer from a whole series of different disadvantages. Most derivatives exhibit an insufficient solubility in monomer formulations and can be phenylated by phenyl radicals which are generated in cationic polymerization due to homolytic cleavage reactions. Furthermore, reaction with singlet oxygen which is inevitably generated during a photo-curing process under air results in the formation of quinones, which are heavily colored. Contrary to most commercially available condensed aromatic hydrocarbons, 9,10-dibutylanthracene (**DBA**) exhibits an excellent solubility in common monomer formulations due to flexible hydrocarbon side chains in position 9 and 10 of the anthracene system. Furthermore, **DBA** is not oxidized to a quinone, but forms a stable endoperoxide by reaction with singlet oxygen and therefore undergoes a photo bleaching effect.

Because of these interesting attributes, the ability of **DBA** to act as a sensitizer for cationic PIs was examined in more detail in broad band irradiation experiments together with commercially available cationic PIs. (Figure 49)

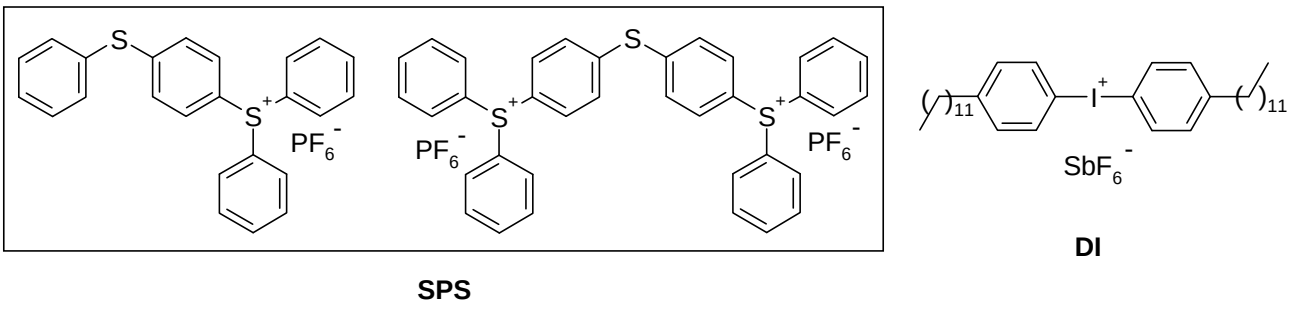

SPS **DI**

Figure 49: (4-Dodecyl)bis(diphenyliodonium) hexafluoroantimonate (**DI**) and a mixture of diphenyl(4-phenylthio)phenyl sulfonium and (thiodi-4,1-phenylene)bis(diphenylsulfonium) hexafluorophosphate (**SPS**)

The iodonium salt **DI** and the physical mixture of hexafluorophosphates **SPS** are two commercially available cationic PIs that are very frequently used in practical applications. Therefore, they are appropriate standard PIs for the analysis of the reactivity of **DBA** as a sensitizer. However, commercial PIs may still contain side products from the synthesis that can function as a sensitizer and are deliberately not completely purified in this case. Furthermore, commercial PIs may already contain admixtures of sensitizers. Therefore, **SPS** and **DI** were purified by column chromatography and the relation of single to double salt (1 : 3) was determined for **SPS** by NMR analysis.

3.1 UV-Vis Spectroscopy

UV-Vis absorption of **DBA** in MeCN shows two maxima near the emission maximum of high pressure mercury lamps (ca. 365 nm) and tails out in the visible region of the light spectrum at approximately 425 nm (Figure 50). Both attributes are very useful for a possible application of **DBA** as a sensitizer for UV / Vis-photopolymerization.

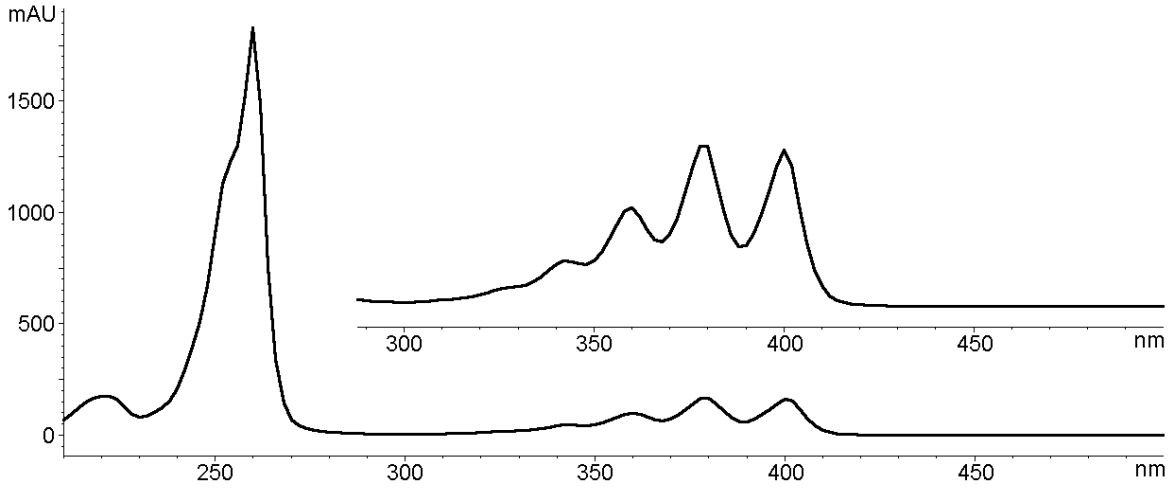

Figure 50: UV-Vis spectra of **DBA**

As proposed, the anthracene **DBA** exhibits the strongest absorptions in the region of UV-C with a λ_{max} at approximately 260 nm. Since those higher energetic absorptions tail out very sharp below 280 nm, excitation possibilities of the sensitizer **DBA** were not used to their full potential in the previously conducted photo-DSC experiments (filtered UV-Vis light, 280 - 450 nm). For this reason, all further photo-DSC experiments with **DBA** as a sensitizer were carried out with light sources that exhibit a broader emission spectrum (250 - 450 nm).

The UV-Vis absorption spectra of the PIs **DI** and **SPS** were measured in the range of 10^{-3} to 10^{-6} mol L^{-1} in MeCN as solvent (Figure 51, Table 6). The UV-Vis spectrum of **1P** is also shown for comparison.

Table 6: UV-Vis data in MeCN of PIs **1P**, **SPS** and **DI** (10^{-5} mol L^{-1})

PI	λ_{max} [nm]	ε_{max} x 10^{-3} [L mol^{-1} cm^{-1}]
1P	275	16.9
SPS	293	17.3
DI	229	24.4

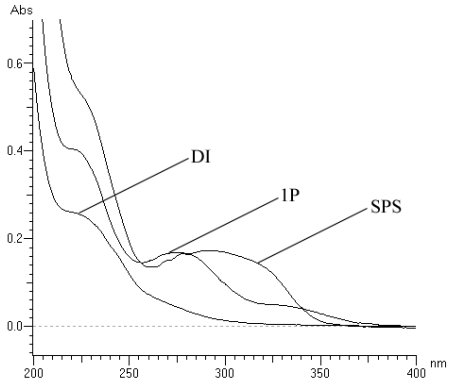

Figure 51: UV-Vis spectra in MeCN of PIs **1P**, **SPS** and **DI** (10^{-5} mol L^{-1})

As expected, **SPS** exhibits the highest λ_{max} of the selected PIs and absorption tails out at more than 350 nm. The λ_{max} is shifted approximately 70 nm in comparison to the triphenylsulfonium base structure **TPS-P** (Figure 38, Table 4) and 20 nm in comparison to **1P** due to p-substitution with a phenyl sulfide. In contrast to **1P** and **SPS**, **DI** exhibits no λ_{max} above 250 nm. The absorption spectrum is almost identical with the spectrum of **DPI-P** (Figure 38, Table 4). Although tail out of absorption is well beyond 300 nm, **DI** is usually applied with a sensitizer in practical applications.

3.2 Photo-DSC

Photo-DSC measurements were carried out with 5.7 ± 2 mg sample weight of 1,6-bis(2,3-epoxypropoxy)hexane (**R18,** UPPC) in isothermal mode at 30 °C under air. Filtered UV-Vis light (1000 mW cm^{-2}; 250 - 450 nm) was applied by a light guide (Efos-Novacure). The given PI concentrations are related to reactive groups to permit a comparison of PIs with a different number of reactive centers within a molecule. All presented data was measured with a PI concentration of 2.5 x 10^{-2} mol reactive groups / L as well as a sensitizer concentration of 2.5 x 10^{-2} mol L^{-1}. The PIs were applied as 50 wt% formulations in propylene carbonate.

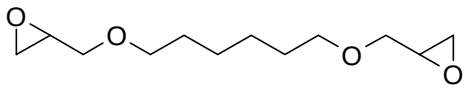

R18

The ability of **DBA** to function as a sensitizer for cationic PIs under this experimental assembly was first verified by application of the reference initiator **1P**. For a comparison of the activity of the anthracene **DBA**, the thioxanthone **ITX** was applied in the photo-DSC experiments as reference sensitizer (Figure 52, Table 7).

Table 7: Photo-DSC data of **R18** using **1P** as PI and **DBA**, **ITX** or no sensitizer

sensitizer	t_{max} [s]	$R_p \times 10^3$ [mol $L^{-1}s^{-1}$]	EGC [%]
-	193	43	88
ITX	63	139	97
DBA	62	204	95

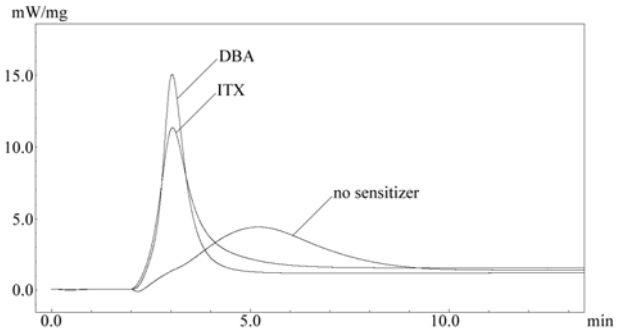

Figure 52: Photo-DSC of **R18** using **1P** as PI and **DBA**, **ITX** or no sensitizer

Due to the determined EGC value, **1P** already displays a sufficient reactivity for a complete curing process of **R18** without application of a sensitizer. However, t_{max} and consequently the curing speed of the formulation is significantly enhanced by application of a sensitizer. In combination with **DBA** or **ITX**, t_{max} values are reduced to approximately one third in comparison to the sample without a sensitizer, Rp is increased by a factor of 3 due to sensitization by **ITX** and a factor of 4 with **DBA** and EGC is slightly enhanced. In contrast to the previous photo-DSC experiments at an irradiation wavelength of 280 - 450 nm (Figures 47 and 48), **DBA** exhibits an improved sensitizer activity. Performance of the formulation containing **DBA** is equal to **ITX** in comparison of the determined t_{max} and EGC values and exceeds **ITX** in R_p in sensitized photopolymerization of **R18** with **1P** as PI.

SPS is a high reactive commercial sulfonium hexafluorophosphate salt mixture that can also be applied without a sensitizer. Although many sulfonium salts are not susceptible to sensitization by thioxanthones like **ITX**, a sensitization by anthracenes like **DBA** is possible (Figure 53, Table 8).

Table 8: Photo-DSC data of **R18** using **SPS** as PI and **DBA**, **ITX** or no sensitizer

sensitizer	t_{max} [s]	$R_p \times 10^3$ [mol $L^{-1}s^{-1}$]	EGC [%]
-	70	131	86
ITX	68	119	82
DBA	57	165	88

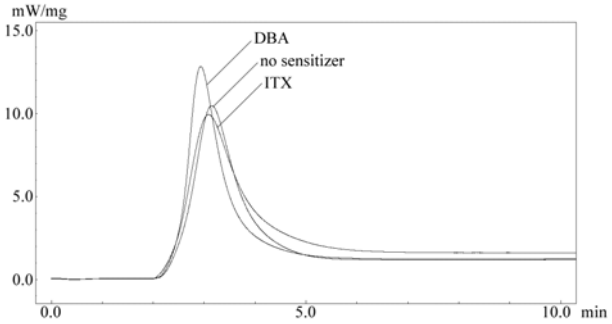

Figure 53: Photo-DSC of **R18** using **SPS** as PI and **DBA**, **ITX** or no sensitizer

Obviously no sensitization effect occurs in combination with **ITX** in case of **SPS**. Quite the contrary, performance of the photocuring formulation with admixture of the thioxanthone seems to be slightly reduced in R_p and EGC in comparison to the formulation without a sensitizer, presumably due to a filter effect. Although the commercial mixture **SPS** is already maximized on reactivity and displays a high reactivity in **R18** even without a sensitizer, the performance of the curing system is further improved by admixture of **DBA**. The t_{max} of the formulation is reduced by approximately 20% and R_p is increased by 10%.

The iodonium antimonate salt **DI** is a PI that is especially suitable for application in apolar coating formulations such as epoxy functional silicones. Due to the UV absorption characteristics, **DI** relies heavily on sensitization for an improved performance in photo-DSC (Figure 54, Table 9).

Table 9: Photo-DSC data of **R18** using **DI** as PI and **DBA**, **ITX** or no sensitizer

sensitizer	t_{max} [s]	$R_p \times 10^3$ [mol $L^{-1}s^{-1}$]	EGC [%]
-	242	21	76
ITX	111	37	78
DBA	118	48	90

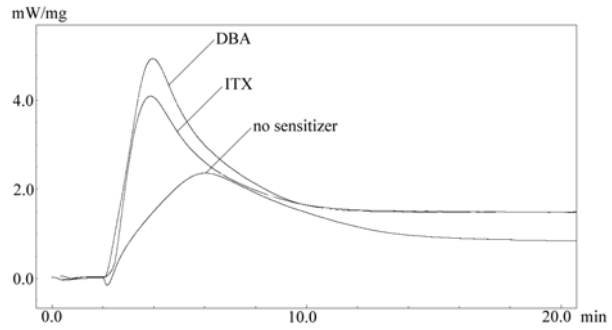

Figure 54: Photo-DSC of **R18** using **DI** as PI and **DBA**, **ITX** or no sensitizer

Obviously, the formulations containing **DI** are far less reactive than the formulations containing **1P** in combination with a sensitizer or **SPS**. However, application of **ITX** or **DBA** significantly enhances polymerization. In combination with both **DBA** and **ITX**, t_{max} is approximately halved and R_p is approximately doubled for **ITX** and raised for the factor 2.5 for **DBA**. The anthracene **DBA** enhances polymerization of the photocuring system considerably more significant than **ITX**, especially in regard to a higher EGC value.

For a visual comparison of effectivity of the sensitizers **DBA** and **ITX**, but also to allow a comparison of the reactivity of the PIs with each other, all results are summarized. (Figure 55)

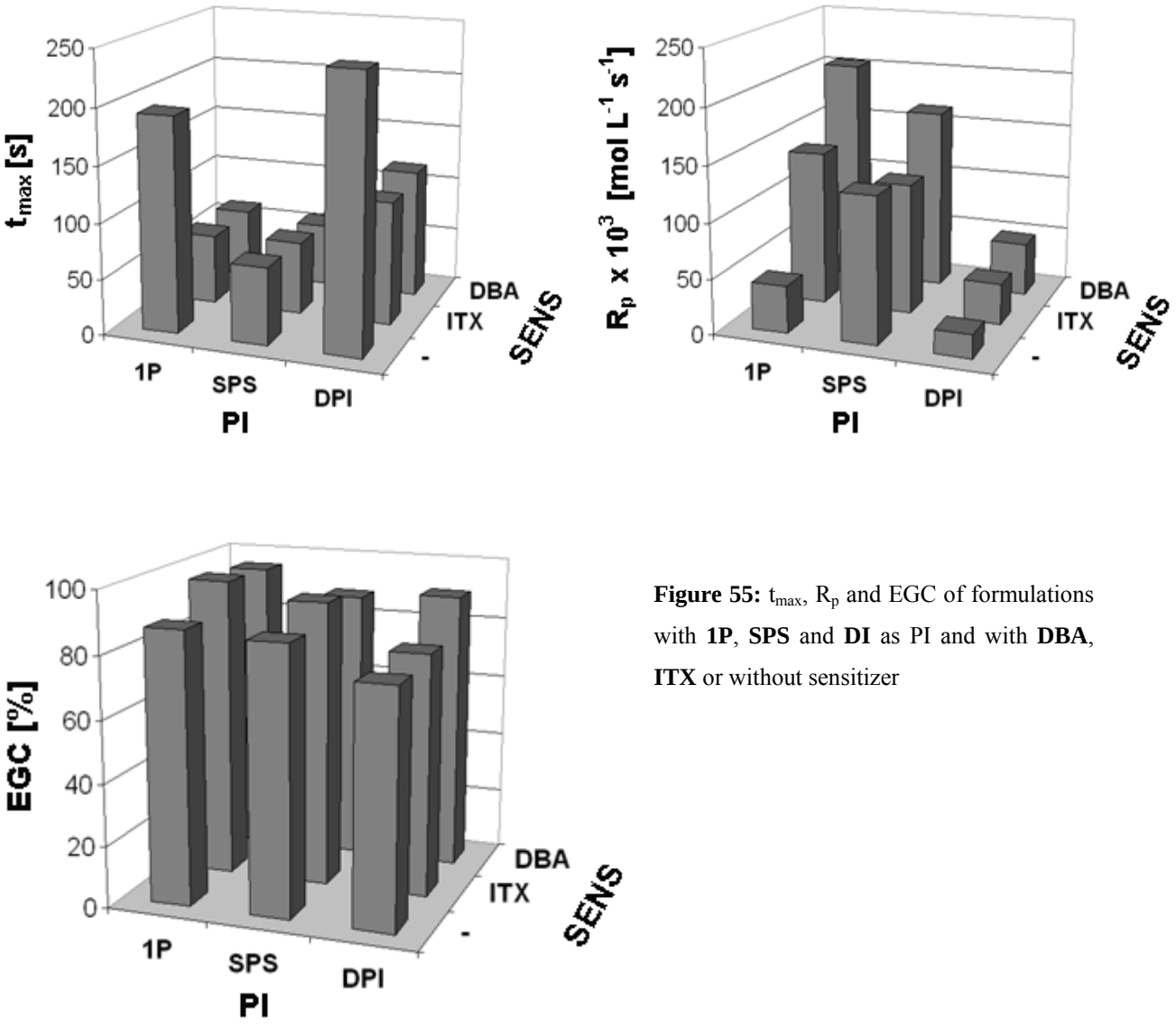

Figure 55: t_{max}, R_p and EGC of formulations with **1P**, **SPS** and **DI** as PI and with **DBA**, **ITX** or without sensitizer

According to the results of the study, **DBA** is a sensitizer that is quite comparable in reactivity to the frequently used sensitizer **ITX** in combination with all applied PIs. Concerning a comparison of the reactivity of the different PIs, it is apparent that the commercial initiator system **SPS** and **1P** show quite similar polymerization characteristics if a sensitizer is applied. t_{max} values for both PIs are almost identical and R_p is even higher for **1P**. Obviously, **1P** exhibits a very high reactivity but is limited in potential without a sensitizer due to a reduced light absorption compared to the bathochromic shifted sulfonium salt **SPS**. This fact is explicitly visualized by the low t_{max} and R_p of the sample without a sensitizer of **1P** compared to **SPS**. EGC values for all formulations, with or without sensitizer, are atypically high due to the long curing times that were applied and are therefore rather insignificant for comparisons of reactivity. However, in the applied experimental assembly **DI** shows by far the least reactivity in all polymerization characteristics including EGC although the base structure **DPI-P** exhibited a high reactivity in earlier experiments (Figures 47 and 48).

A possible reason for this discrepancy is a low dispensation of **DI** in the monomer. Although **DI** was completely dissolved, it can not be excluded that micro aggregates like micellar structures or fine dispersions were generated. In general, composition of cationic curing resigns is often more complicated than in radical polymerization, since PIs, but also sensitizers are often far less soluble in the monomers. In contrast to many other sensitizers, **DBA** possesses a good solubility in monomer formulations and is, unlike **ITX**, an effective sensitizer for both sulfonium and iodonium salts. Since **DBA** exhibits a tail out of absorption in the Vis region of the light spectrum similar to **ITX**, application in both Vis - and UV photo-curing is possible. **DBA** can undergo photo-bleaching and can be proposed as a very reactive sensitizer with a wide area of application.

Most sensitizers exhibit an optimal application concentration in a defined curing formulation. Due to the excellent results with **DBA** as sensitizer, the dependency of the enhancement of polymerization on the concentration of **DBA** was tested in a series of photo-DSC experiments. (Figure 56)

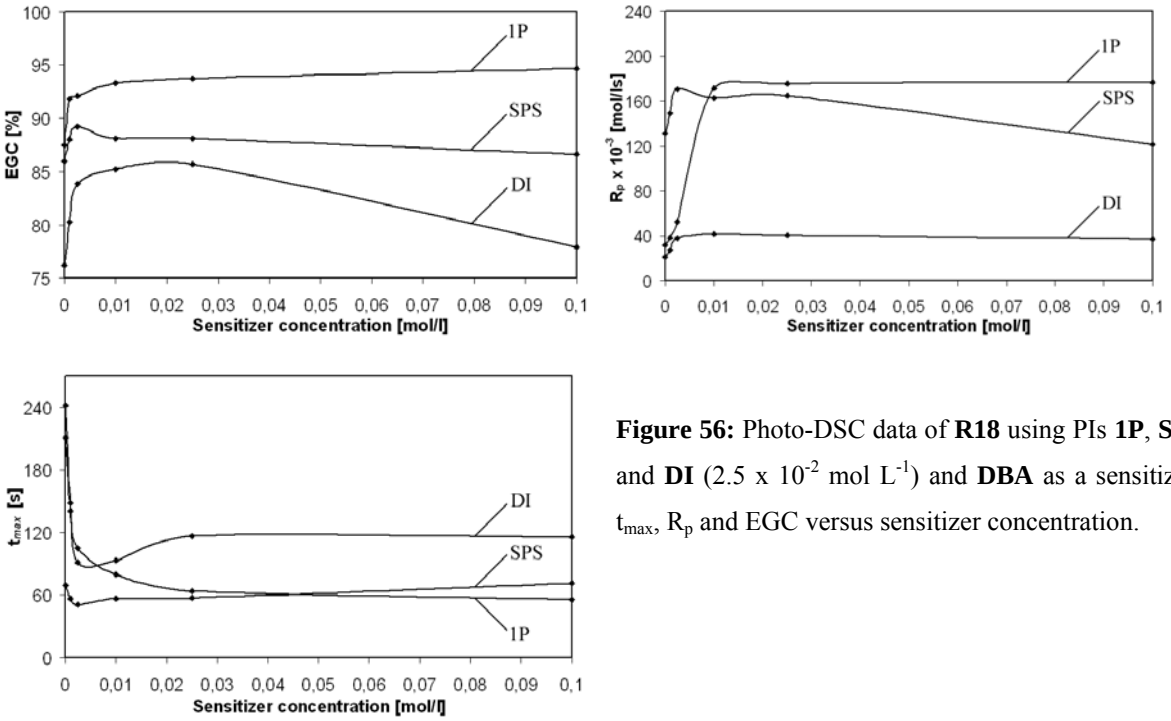

Figure 56: Photo-DSC data of **R18** using PIs **1P**, **SPS** and **DI** (2.5 x 10^{-2} mol L^{-1}) and **DBA** as a sensitizer: t_{max}, R_p and EGC versus sensitizer concentration.

At very low concentrations of sensitizer, both **DI** and **1P** exhibited a low reactivity compared to **SPS**. As was to be expected, the photo-reactivity of these PIs relies on a sufficient sensitization by **DBA** to a larger extent than **SPS**. However, **1P** showed an extraordinary high EGC independent of the **DBA** concentration. At sensitizer concentrations above 2.5 x 10^{-3} mol L^{-1} **1P** gave approximately the same polymerization characteristics as **SPS**, with about half the t_{max} and four times the R_p values of **DI**. Evidently, **1P** sensitized by **DBA** is a very reactive system, even compared to a commercial system that is maximized on reactivity like **SPS**. **DBA** exhibits an optimal application concentration for both **SPS** and **DI** between 1 x 10^{-2} and 1 x 10^{-3} mol L^{-1} in the applied formulation. Higher concentrations of **DBA** reduce the activity, possibly due to a filter effect. In case of **1P**, **DBA** obviously does not possess a defined concentration optimum, the polymerization parameters of the formulation increase with ascending sensitizer concentration up to 1 x 10^{-1} mol L^{-1}.

4. Bathochromic shifted and conjugated sulfonium salts

The phenyl(phenylethynyl) onium salts **1P** and **2P** exhibited a high reactivity as well as a high predisposition for sensitization compared to the aryl onium base structures **TPS-P** and **DPI-P**. However, both substances exhibit no absorbance in visible or near UV-light and a rather low absorbance of UV-B light. Therefore, these structures are dependent on coaction with a sensitizer system to develop a good performance in photocuring. In contrast to the phenyl(phenylethynyl) onium salts, the physical mixture of bathochromic shifted triarylsulfonium salts **SPS** displays an excellent reactivity even without application of a sensitizer. For this reason, it seems very promising to prepare derivatives of **1P** and **2P** that exhibit an enhanced innate absorption.

Since the base structure **2P** exhibits a thermal instability that is too high for the use of this initiator in most technical applications, efforts of system modifications should be concentrated on the sulfonium salt **1P**. As a main objective in alteration of the molecular system, the implementation of bathochromic groups modeled on **SPS** seems mandatory. As the physical mixture **SPS** is mainly composed of the double salt, an analogous double salt based on the sulfonium salt **1P**, (thiodi-4,1-ethynylphenylen)bis(diphenylsulfonium) dihexafluorophosphate (**4P**), should be synthesized. As a preliminary study, a bathochromic shifted single salt should be prepared. Since a thioether group should already be inserted in the double salt **4P**, implementation of a different bathochromic group for a comparison of the varied properties is an obvious choice. Because extension of the absorption by insertion of ether groups is also well known for triarylsulfonium salts,[104] diphenyl(p-methoxy-phenylethynyl)sulfonium triflate (**3P**) was chosen as an interesting new structure (Figure 57).

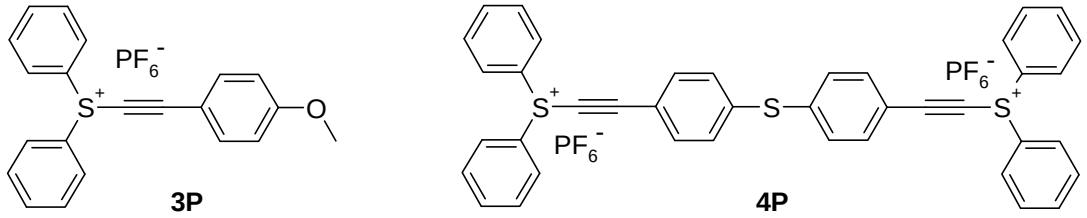

Figure 57: Bathochromic shifted phenyl(phenylethynyl) sulfonium salts **3P** and **4P**

A second possibility for a significant enhancement of the absorption behavior is the expansion of the conjugated system. This method is especially suited for phenyl(phenylethynyl) sulfonium salts which possess a phenylethynyl structure that can be easily expanded. The first, logical choice is to prepare a diethynylphenylen double salt, (1,4-diethynylphenylen)bis(diphenylsulfonium) dihexafluorophosphate (**5P**) which resembles the single salt **1P** (Figure 58).

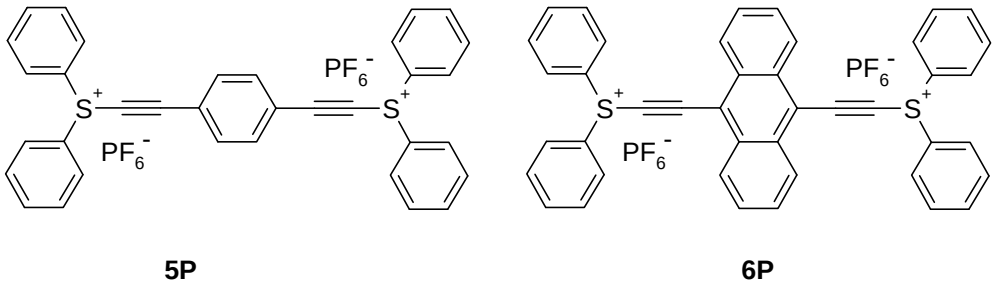

Figure 58: Conjugated phenyl(phenylethynyl) sulfonium double salts **5P** and **6P**

In theory, the conjugated system is expandable in any order. However, as anthracenes like **DBA** are established sensitizers, insertion of an anthracene structure could demonstrate interesting effects and the resulting diethynylanthracene sulfonium salt could be proposed to absorb visible light. It seems inevitable for a stable anthracene based sulfonium salt to block the reactive centers in position 9 and 10 of the anthracene system, which additionally proposes an inartificial synthetic route. Therefore, (9,10-diethynylanthracene)bis(diphenylsulfonium) dihexafluorophosphate **6P** was chosen as a second conjugated sulfonium salt based on the phenyl(phenylethynyl) sulfonium structure **1P**.

Apart from the expansion of the chromophore of sulfonium salts by incorporation of bathochromic groups or triple bonds, the implementation of double bonds is an obvious, logical alternative to achieve a significant bathochromic shift of the λ_{max} of the base structure. Exactly like phenylethynyl sulfonium salts, vinyl sulfonium salts represent conjugated systems which are significantly bathochromic shifted compared to the corresponding triarylsulfonium salts, but are rarely reported in literature for their use as PIs.[105] It has to be expected for most vinyl sulfonium salts that their reactivity as PIs in direct irradiation is reduced compared to their phenylethynyl analogons, since these structures might be able to deactivate their excited states by other mechanisms than photocleavage, for example by change of their configuration.

In general, (alkoxyphenylvinyl)-diphenylsulfonium salts with a broad variety of desirable properties like an enhanced solubility by insertion of aliphatic chains or as copolymerizable initiators by insertion of functional groups are easily accessible from **1P**. Furthermore, a comparison of the photoreactivity of these conjugated structures in direct excitation and especially sensitized polymerization with phenyl(phenylethynyl) sulfonium salts is certainly of high academic interest. For this reason (2-isopropoxy-2-phenyl-vinyl)-diphenylsulfonium hexafluorophosphate (**7P**) was chosen as a representative of this class of sulfonium salts for comparative photo-DSC experiments (Figure 59).

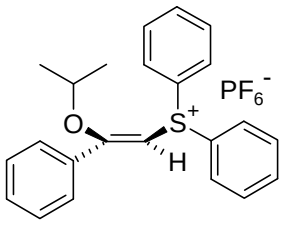

7P

Figure 59: Conjugated vinyl sulfonium salt **7P**

4.1 Synthesis of bathochromic shifted and conjugated sulfonium salts

Since a synthetic route was applied in the synthesis of **1P** that is in general transferable to other phenyl(phenylethynyl) sulfonium salts, the most suitable strategy for the synthesis of bathochromic shifted sulfonium salts like **3P** and **4P** is obviously an analogous preparation from *p*-substituted trimethylsilyl(phenyl)acetylene precursors and subsequent exchange of the counterion. The same synthetic strategy can be applied for the conjugated sulfonium salts **5P** and **6P**, provided a preparation of the trimethylsilylethynyl precursors is possible.

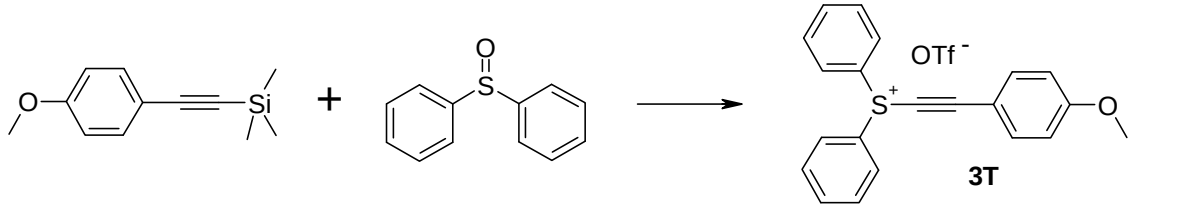

Structure: **4T**: R = 4,4'- 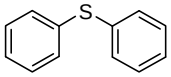 **5T**: R = 1,4-  **6T**: R = 9,10- 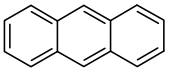

For the synthesis of these trimethylsilylethynyl reagents, coupling reactions of bromides or iodides with TMS-acetylene propose a short and uncomplicated synthetic pathway since the aromatic halogenides are commercially available or easily prepared with standard laboratory procedures.

In case of the vinyl-diphenylsulfonium salt **7P**, a direct synthetic preparation from the hexafluorophosphate **1P** by nucleophilic addition reaction of 2-propanol is obviously the most uncomplicated and promising synthetic route.

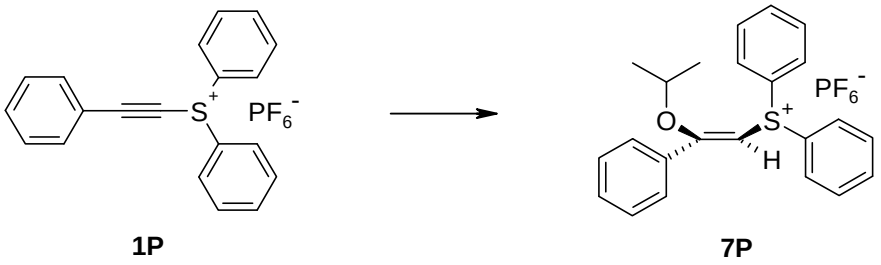

1P **7P**

4.1.1 Synthesis of precursors

Metalation of readily available acetylenes and subsequent reaction with trimethylsilylchloride (TMSCl) is a simple and straightforward synthetic method for the preparation of TMS-acetylenes as precursors in the synthesis of sulfonium salts.[106] Therefore, this synthetic method was applied in the synthesis of the precursor for the sulfonium salt **3P**.

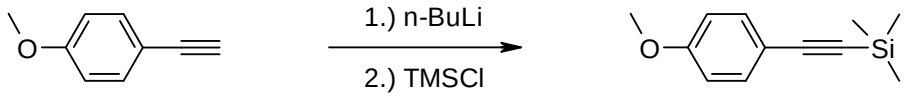

6

4-Methoxyphenylacetylenelithium was prepared by reaction of 4-methoxyphenylacetylene with n-butyllithium in THF and treated with trimethylsilylchloride. After extraction and column chromatography, **6** was received as a colorless oil in quantitative yield.

Sonogashira couplings[107] are another powerful tool in simple synthesis strategies for the preparation of conjugated or bathochromic shifted phenylethynyl sulfonium double salts like **4T - 6T**. Furthermore, all prerequisites are commercially available or easily accessible by synthesis, since the precursors for the performed reactions are aromatic dihalogenides, trimethylsilylacetylene (**7**) and rather simple palladium catalysts. Therefore, sonogashira couplings permit a short and uncomplicated synthetic route to the TMS-acetylene precursors that are the precondition for an analogous synthesis to **1P**.

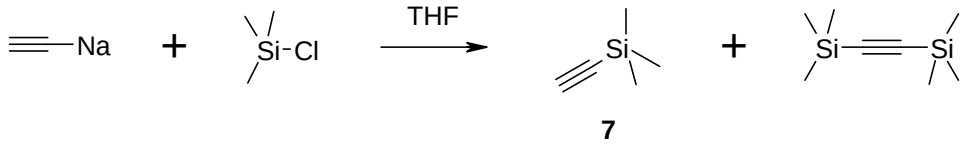

7

The acetylene **7** was prepared by reaction of a suspension of sodium acetylide in THF with trimethylsilylchloride at rt.[108] After extraction with xylene at 0 °C, the volatile product was received as a solution of trimethylsilylacetylene and 1,2-bis(trimethylsilyl)acetylene in THF by distillation. The percentage of reactive **7** (50 wt%) in the solution and the yield (47%) were determined by NMR analysis.

Biphasic aqueous / organic systems are an excellent medium for bromination reactions of water insoluble organic molecules. Since many unspecific reactions in the bromination can be dedicated to hydrogen bromine as a reactive intermediate, a biphasic reaction procedure permits a controlled process under mild conditions.[109]

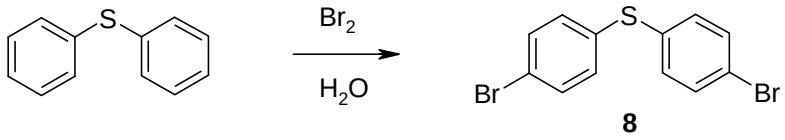

8

Diphenyl sulfide was brominated in a biphasic system of water and CH_2Cl_2 at rt. After extraction, the product was washed with petroleum ether to give pure para-substituted dibromide **8** as colorless crystals (81%).

These synthesized or commercially acquired coupling reagents were applied in the preparation of the precursor structures **9**-**11**.

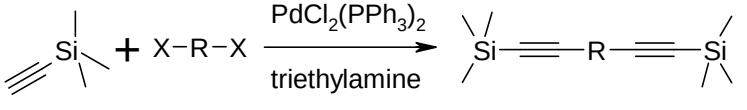

7

Structure: **9**: R = 4,4'- 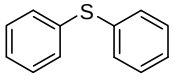 X = Br

10: R = 1,4-  X = I

11: R = 9,10- 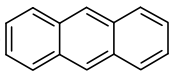 X = Br

The reactions were performed in degassed solutions of THF or toluene with triethylamine as base, dichlorobis(triphenylphosphine)palladium (II) ($PdCl_2(PPh_3)_2$) / copperiodide as catalyst system and the aromatic dihalogenides and acetylene **7** as coupling partners. Synthesis of 1,4-bis-(trimethylsilylethynyl)-benzene (**10**) from 1,4-diiodobenzene was performed at rt with 1 mol% catalyst within 1 h. For the synthesis of 4,4'-bis-(trimethylsilylethynyl)-diphenyl sulfide (**9**) and 9,10-(trimethylsilylethynyl)-anthracene (**11**) the less reactive dibromides 4,4'-dibromodiphenyl sulfide (**8**) and 9,10-dibromoanthracene were employed. Due to the narrow temperature-frame of the reaction caused by the low boiling point and high volatility of **7**, enhanced reaction times of 1 to several days and higher mol% of catalyst had to be used. As a consequence of the long reaction times at elevated temperature, additional doses of **7** and fresh catalyst had to be added sequentially to obtain maximal conversion. After extraction, column chromatography and washings with petroleum ether in case of **9** and **10** or methanol in case of **11**, the TMS-acetylenes were received as solids in yields of 57 - 89%.

4.1.2 Synthesis of sulfonium salts (3P - 5P, 6T and 7P)

Synthesis of the bathochromic shifted sulfonium triflates **3T** and **4T** and the conjugated sulfonium triflates **5T** and **6T** was performed analogue to **1P** by activation of diphenyl sulfoxide with trifluoromethanesulfonic acid anhydride and subsequent reaction with the TMS-acetylene **6** or **9**-**11**, respectively.

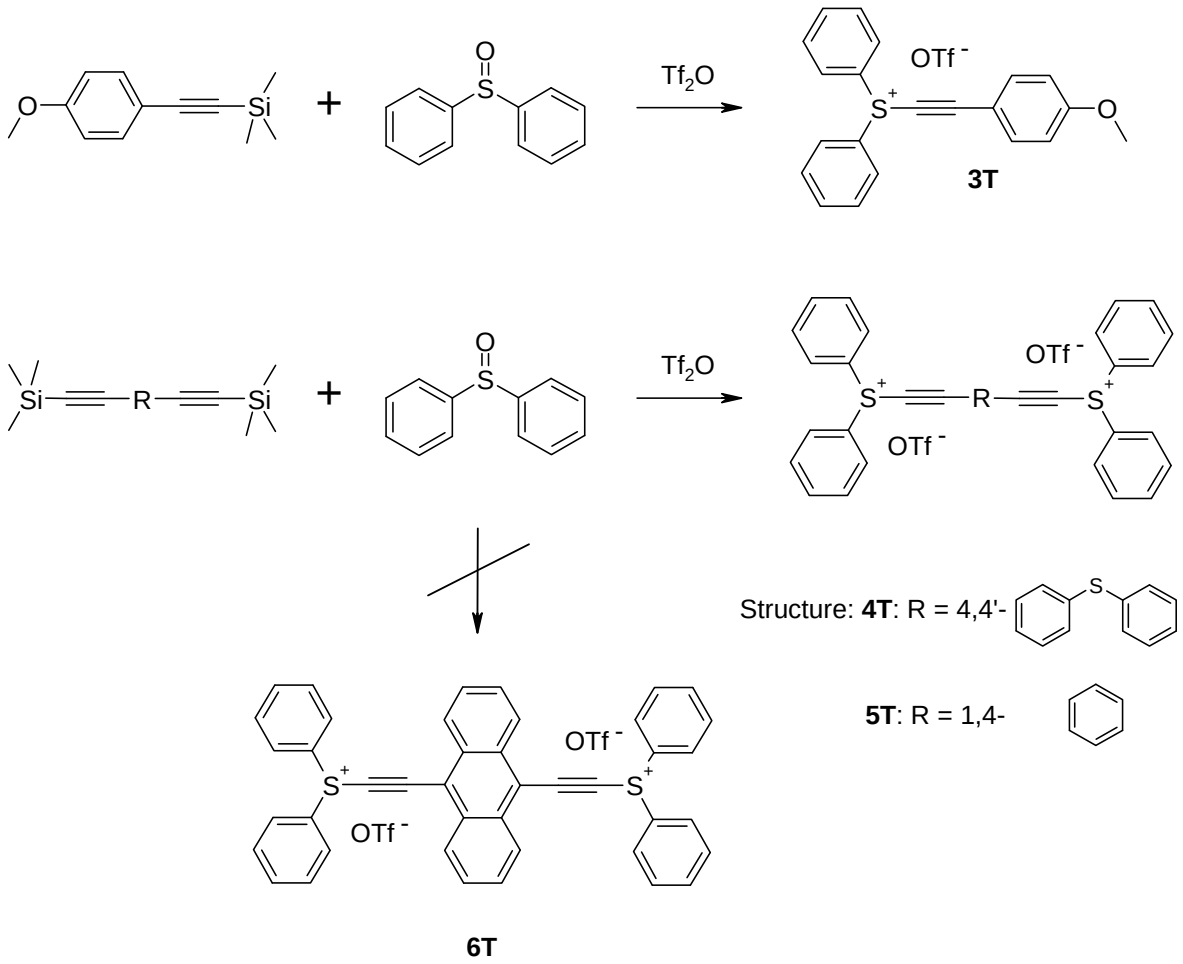

After extraction, washings with petroleum ether gave the bathochromic shifted sulfonium salts **3T** and **4T** as reddish oils in yields of 42 and 85% and washings with petroleum ether / CH_2Cl_2 (1:1) gave the conjugated sulfonium salt **5T** as colorless crystals in 55% yield. In the attempted synthesis of the diethynylanthracene disulfonium salt **6T**, a dark purple solid precipitated from the reaction mixture which was insoluble in common organic solvents for NMR analysis and laboratory use. An attempt of ion exchange to hexafluorophosphate, dispersion in monomer **R18** and a subsequent reactivity check by photo-DSC showed some limited ability to initiate polymerization, which was a strong indication for the formation of sulfonium salts in the raw product. However, due to the obvious insolubility of the precipitate in monomers and the impossibility to purify the sulfonium salt by washings, recrystallization or column chromatography, no further attempts were made to isolate **6T** for use as an initiator.

The sulfonium triflates **3T** - **5T** were conversed to the corresponding hexafluorophosphates **3P** - **5P** analogous to the procedure for **1P** in a two phase system of CH_2Cl_2 / 5 equiv. concentrated solution of potassium salt. The new PIs were received in yields from 89 to 95%. The degree of residual nucleophilic anions was analyzed by IR spectroscopy, in case of a concentration of triflate > 5 mol%, the ion exchange process was repeated.

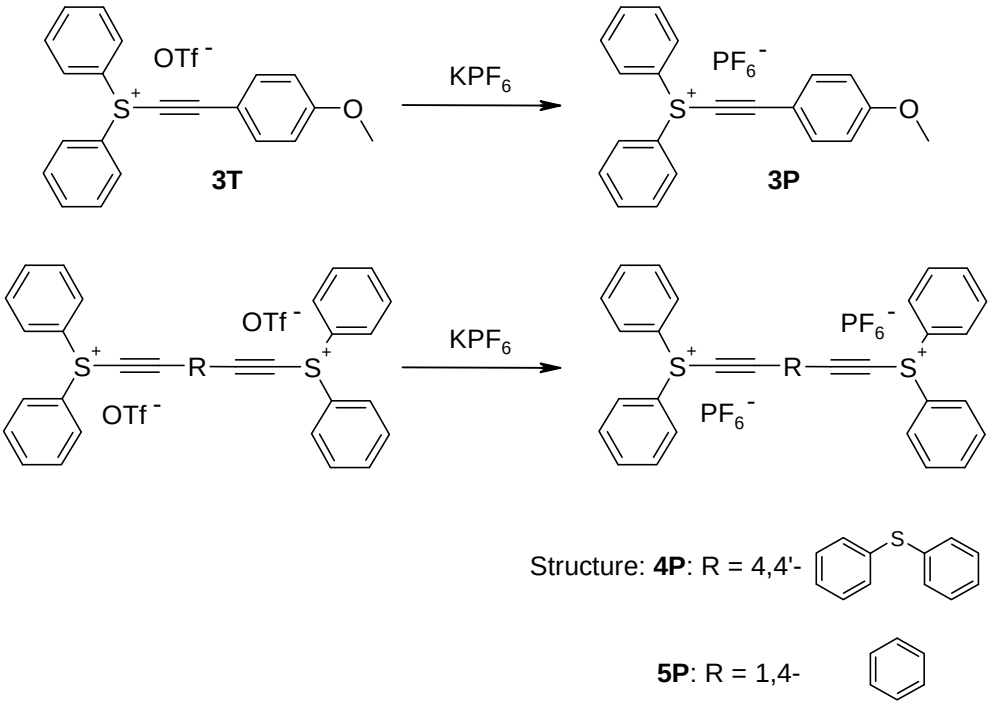

Synthesis of **7P** from **1P** was performed by thermal addition of 2-propanol as reactant and solvent during 12 h at reflux. After extraction, the residue was recrystallized from 2-propanol to give **7P** as colorless crystals (55%). NMR analysis in $CDCl_3$ gave a distribution of isomers of **6P** of **E** : **Z** = 1 : 16.

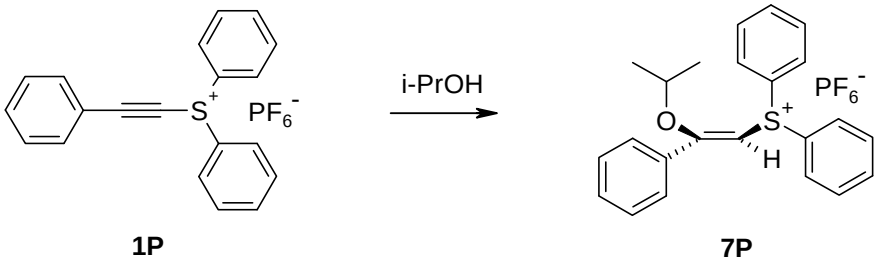

4.3 UV-Vis Spectroscopy

The UV-Vis absorption spectra of the new PIs were measured in the range of 1 x 10^{-3} to 1 x 10^{-6} mol L^{-1} in MeCN as solvent (Figures 60 and 61, Tables 10 and 11). The UV-Vis spectrum of the base structure **1P** is shown for comparison.

Bathochromic shifted sulfonium salts 3P and 4P:

Table 10: UV-Vis data in MeCN of PIs **1P**, **3P** and **4P** (10^{-5} M)

PI	λ_{max} [nm]	ε_{max} x 10^{-3} [L mol^{-1} cm^{-1}]
1P	274	16.9
	221	40.4
3P	301	14.2
	275	16.1
4P	322	18.2
	276	25.4

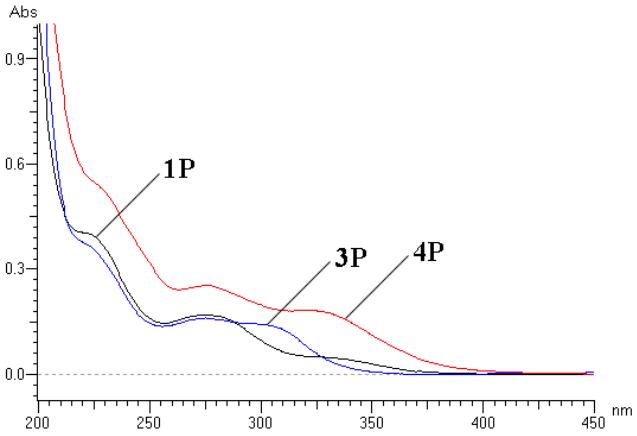

Figure 60: UV-Vis spectra of PIs **1P**, **3P** and **4P** in MeCN (1 x 10^{-5} mol L^{-1})

Due to the implementation of bathochromic groups, a significant red-shift in the absorption spectra of both phenylethynyl sulfonium salts **3P** and **4P** was observed. As expected for the incorporation of O and S, the λ_{max} of the new chromophore is shifted approximately for 25 nm for **3P** and 50 nm for **4P** in comparison to the λ_{max} of **1P** at 274 nm. Unfortunately, in case of **3P** tail out of the absorption was reduced from approximately 375 nm (**1P**) to approximately 350 nm. However, the ε_{max} of the salt **4P** which possesses 2 chromophores linked by a sulfide group was nearly doubled in comparison to **1P** as could be expected. Furthermore, tail out of the absorption was shifted to above 400 nm which is of significant importance for the direct excitation of the chromophore.

Conjugated sulfonium salts 5P and 7P:

Table 11: UV-Vis data in MeCN of PIs **1P**, **5P** and **7P** (10^{-5} M)

PI	λ_{max} [nm]	ε_{max} x 10^{-3} [L mol^{-1} cm^{-1}]
1P	274	16.9
	221	40.4
5P	297	26.7
7P	273	21.9
	202	35.1

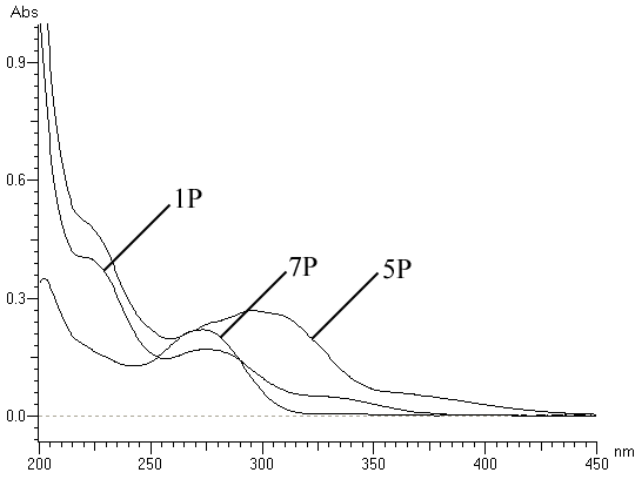

Figure 61: UV-Vis spectra of PIs **1P**, **3P** and **4P** in MeCN (1 x 10^{-5} mol L^{-1})

As expected for the extension of the conjugated system by a second triple bond, the λ_{max} of the conjugated sulfonium salt **5P** is red-shifted for approximately 25 nm compared to **1P**. Absorption tails out at above 400 nm and is shifted in comparison to **1P** for approximately 80 nm. Both **1P** and **7P** exhibit a λ_{max} at approximately the same wavelength. Obviously, the λ_{max} is hardly influenced by transfer of the acetylene bond into a vinyl bond by addition of 2-propanol. In contrast to the phenylethynyl sulfonium salts **1P** and **5P**, the vinyl sulfonium salt **7P** tails out rather sharp below 330 nm. Interestingly, absorption of **7P** between 200 and 250 nm is significantly reduced in comparison to the phenylethynyl sulfonium salts **1P** and **7P**.

4.4 Photo-DSC

A photo-DSC study was conducted to investigate the photo-reactivity of the bathochromic shifted onium salts **3P** and **4P** and the conjugated sulfonium salts **5P** and **7P** in comparison to **1P** and the commercial mixture of sulfonium salts **SPS**. Photo-DSC measurements were carried out with 5.7 ± 2 mg sample weight of 1,6-bis(2,3-epoxypropoxy)hexane (**R18,** UPPC) in isothermal mode at 30 °C under air.

Filtered UV-Vis light (1000 mW cm^{-2}; 250 - 450 nm) was applied by a light guide (Efos-Novacure). The given PI concentrations are related to reactive groups to permit a comparison of PIs with a different number of reactive centers within a molecule. All presented data was measured with a concentration of 2.5 x 10^{-2} mol reactive groups / L. The PIs were applied as 50 wt% formulations in propylene carbonate.

Bathochromic shifted sulfonium salts 3P and 4P:

If reactivity of the selected sulfonium salts as an initiator in direct excitation is primarily dependent on the degree of light absorption, **4P** should exhibit an excellent performance even compared to **SPS**. Unfortunately, this simplified theory was refuted by the results of the photo-DSC experiments in **R18** using bathochromic shifted PIs without a sensitizer (Figure 62, Table 12).

Table 12: Photo-DSC data of **R18** using **1P**, **SPS**, **3P** and **4P** as PI

PI	t_{max} [s]	R_p x 10^3 [mol $L^{-1}s^{-1}$]	EGC [%]
1P	193	43	88
SPS	70	131	86
3P	240	21	76
4P	113	31	93

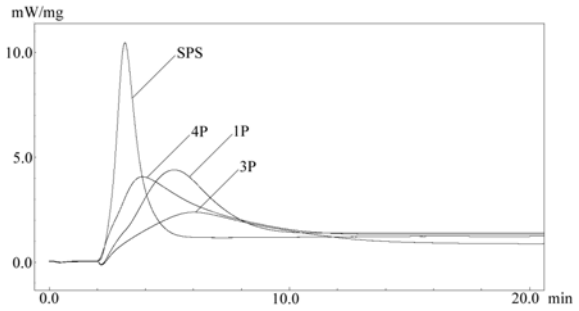

Figure 62: Photo-DSC of **R18** using **1P**, **SPS**, **3P** and **4P** as PI

In direct excitation of the chromophore, the bathochromic shifted sulfonium double salt **4P** showed at least a t_{max} value that was reduced by 40% in comparison to **1P**. However, **SPS** exhibited a t_{max} that was again only 60% of **4P** and a R_p of 4 times higher. Furthermore, Rp and DBC of **4P** were measurably decreased in comparison to **1P**. Interestingly, a direct correlation of absorption and reactivity as PI might exist for the comparison of the two bathochromic shifted phenylethynyl sulfonium salts **3P** and **4P**. The initiator **3P** which had a far lower bathochromic shifted absorption spectrum than **4P** was also less reactive, exhibiting only two third of the R_p, a lower EGC and approximately 2 times the t_{max} value of **4P**. In relation to the performance of **SPS**,

which showed a 3.5 times shorter t_{max} and a 6 times higher Rp value in combination with an enhanced EGC, the reactivity of **3P** was insignificant.

Anyhow, the low performance of the formulation containing **3P** can only to a minor part be caused by the early tail out of UV-Vis absorption in comparison with the other PIs. Another fact of great interest were the low Rp values of **3P** and especially **4P** which showed an improved t_{max} in regard to **1P**. The reduction of t_{max} was with reasonable certainty caused by an improved absorption, but in this connectivity, the low R_p would indicate a reduced reactivity of the sulfonium group or a secondary process after photocleavage that reduces the overall reactivity of the curing system. If one of these assumptions is correct, a reduction of the performance in combination with sensitizers of **3P** and **4P** in simile to **1P** is mandatory (Figures 63 and 64, Tables 13 and 14)

Table 13: Photo-DSC data of **R18** using **1P**, **SPS**, **3P** and **4P** as PI and **DBA** (2.5×10^{-2} mol L^{-1}) as sensitizer

PI	t_{max} [s]	$R_p \times 10^3$ [mol $L^{-1}s^{-1}$]	EGC [%]
1P	62	204	95
SPS	57	165	88
3P	92	42	82
4P	86	71	93

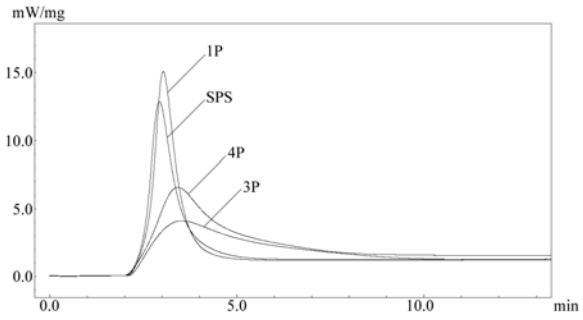

Figure 63: Photo-DSC of **R18** using **1P**, **SPS**, **3P** and **4P** as PI and **DBA** as sensitizer

Table 14: Photo-DSC data of **R18** using **1P**, **SPS**, **3P** and **4P** as PI and **ITX** (2.5×10^{-2} mol L^{-1}) as sensitizer

PI	t_{max} [s]	$R_p \times 10^3$ [mol $L^{-1}s^{-1}$]	EGC [%]
1P	63	139	97
SPS	65	119	92
3P	112	37	78
4P	89	78	91

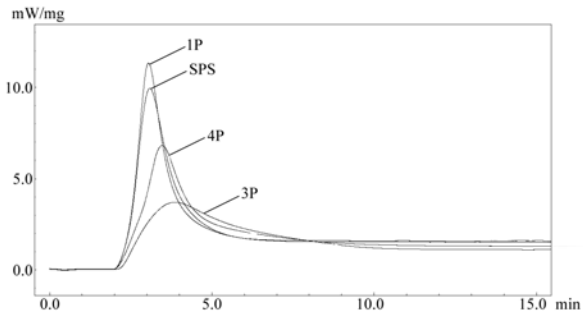

Figure 64: Photo-DSC of **R18** using **1P**, **SPS**, **3P** and **4P** as PI and **ITX** as sensitizer

In fact, the reactivity of the new bathochromic shifted systems in combination with **DBA** and **ITX** was significantly lower than the reactivity of **1P**. In combination with each of the sensitizers, t_{max} was approximately 1.5 - 2 times higher and R_p approximately 2.5 - 5 times lower than that of the reference initiator **1P** which exhibited a comparable performance to **SPS**. Similar to the experiments without a sensitizer, the performance of **3P** was significantly worse than that of **4P**, featuring only approximately half the R_p and a reduced EGC.

Conjugated sulfonium salts 5P and 7P:

The reduction of performance due to the alteration of the phenylethynyl system of **1P** to generate the bathochromic shifted salts **3P** and **4P** is not necessarily transferable to conjugated sulfonium salts like **5P** and **7P**. Therefore, again an increased performance of **5P** due to an enhanced light absorption was to be expected. In case of vinyl sulfonium salt **7P**, a marginal reactivity in direct irradiation was to be forecasted, since vinyl containing structures in general rather deactivate the absorbed excitation energy by mechanisms like E/Z-configuration change than by bond cleavage (figure 65, Table 15).

Table 15: Photo-DSC data of **R18** using **1P**, **SPS**, **5P** and **7P** as PI

PI	t_{max} [s]	$R_p \times 10^3$ [mol $L^{-1}s^{-1}$]	EGC [%]
1P	193	43	88
SPS	70	131	86
5P	118	48	95
7P	-	-	-

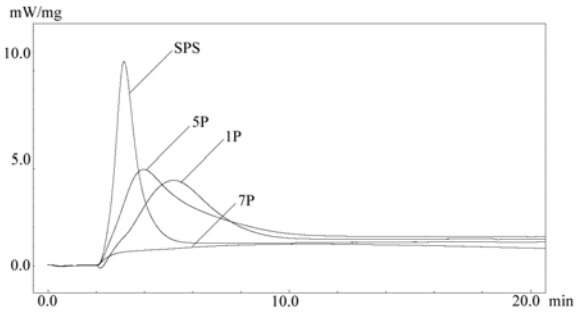

Figure 65: Photo-DSC of **R18** using **1P**, **SPS**, **5P** and **7P** as PI

In fact, initiation activity of **7P** was too low to start polymerization of **R18** in the conducted experiment. Obviously, deactivation of the absorbed energy by configuration change is far more prominent than bond cleavage (Figure 66).

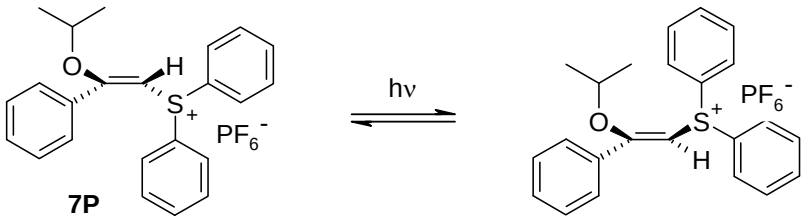

Figure 66: E/Z-configuration change of **7P**

In contrast to the vinyl sulfonium salt **7P**, the conjugated initiator **5P** exhibited an improved performance compared to **1P** with t_{max} of two third, a slightly improved R_p and a high EGC value. However, reactivity of the initiator system **SPS** exceeded **5P** significantly and displayed a t_{max} of approximately 60% and a R_p that was increased for a factor of approximately 2.5 in comparison to **5P**. Nevertheless, in case of **5P** extension of the conjugated system definitely enhanced the performance in direct irradiation compared with **1P**.

Since both sulfonium salts should display a susceptibility to sensitization, the corresponding photo-DSC experiments were conducted with **DBA** and **ITX** as sensitizers (Figures 67 and 68, Tables 16 and 17).

Table 16: Photo-DSC data of **R18** using **1P**, **SPS**, **5P** and **7P** as PI and **DBA** (2.5×10^{-2} mol L^{-1}) as sensitizer

PI	t_{max} [s]	$R_p \times 10^3$ [mol $L^{-1}s^{-1}$]	EGC [%]
1P	62	204	95
SPS	57	165	88
5P	88	90	96
7P	128	40	82

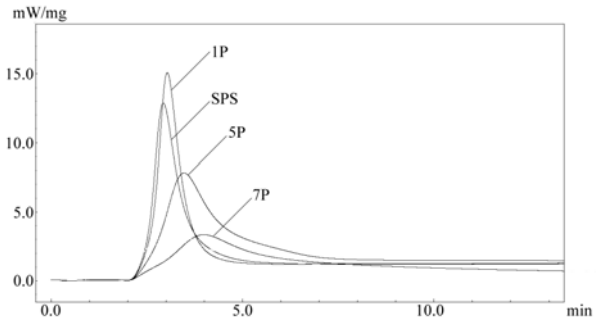

Figure 67: Photo-DSC of **R18** using **1P**, **SPS**, **5P** and **7P** as PI and **DBA** as sensitizer

Table 17: Photo-DSC data of **R18** using **1P**, **SPS**, **5P** and **7P** as PI and **ITX** (2.5×10^{-2} mol L^{-1}) as sensitizer

PI	t_{max} [s]	$R_p \times 10^3$ [mol $L^{-1}s^{-1}$]	EGC [%]
1P	63	139	97
SPS	65	119	92
5P	86	82	93
7P	-	-	-

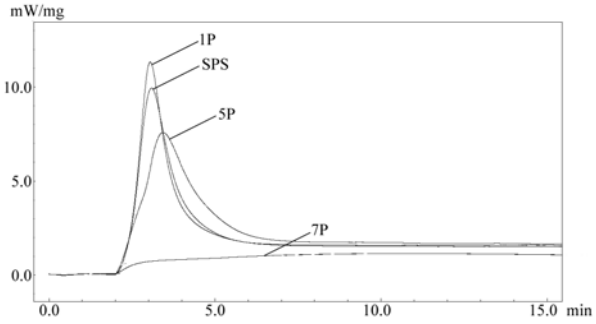

Figure 68: Photo-DSC of **R18** using **1P**, **SPS**, **5P** and **7P** as PI and **ITX** as sensitizer

The performance of the conjugated sulfonium salt **5P** in **R18** was only moderately enhanced by sensitization with **DBA** or **ITX**. The triarylsulfonium salt **SPS** and the base structure **1P** exhibited approximately a 1.5 times shorter time span to reach t_{max} and a 1.5 times higher R_p in combination with both sensitizers. Therefore, enhancement by sensitization was significantly lower for **5P** than for **1P**. A presumable explanation for this phenomenon is based on the assumption that **5P** displays an improved delocalization of electrons due to the extended conjugated system containing two sulfonium salt structures. Therefore, the double salt would exhibit an enhanced stability as a conjugated sulfonium-sulfonium radical cation compared to the isolated radical cation of **1P**. As a consequence, back-electron-transfer would evidently occur to a larger extent compared to **1P** and the probability for a PI / sensitizer complex to result in cleavage of the sulfonium salt would diminish (Figure 69).

In contrast to **5P**, the vinyl sulfonium salt **7P** was only sensitized by **DBA** and exhibited an insignificant reactivity compared to the reference initiators.

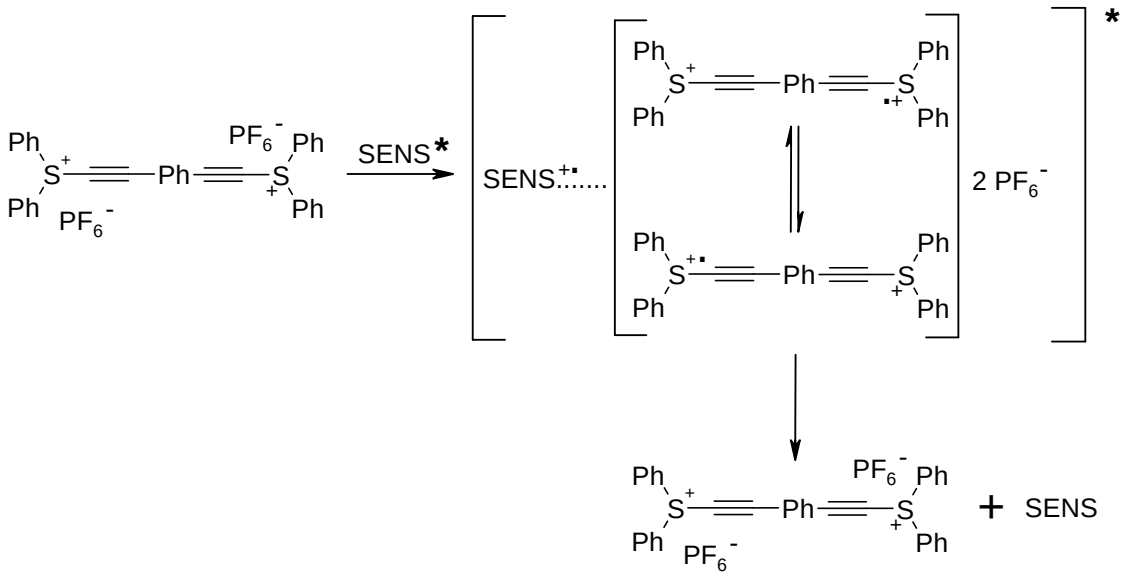

Figure 69: Back electron transfer in PI / sensitizer complex degradation of **5P**

The results of all photo-DSC experiments of both bathochromic shifted and conjugated sulfonium salts are displayed for better visualization and for comparison in Figure 70.

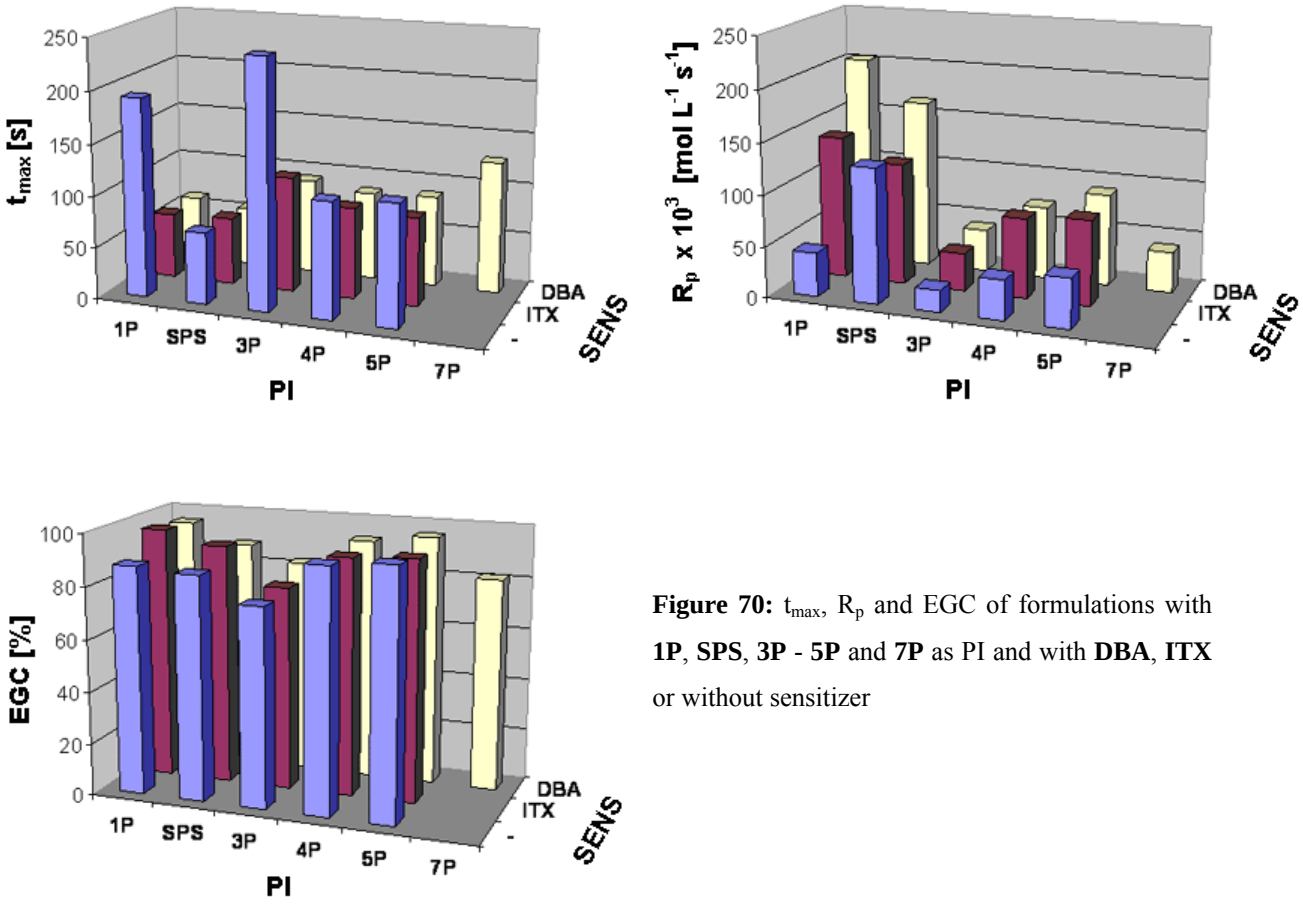

Figure 70: t_{max}, R_p and EGC of formulations with **1P**, **SPS**, **3P - 5P** and **7P** as PI and with **DBA**, **ITX** or without sensitizer

In general, the most significant value for a comparison of different photo-DSC measurements of the same monomer is t_{max}, since reactivity for the different PIs is usually displayed most explicitly. Anyhow, due to the effects observed with bathochromic and conjugated sulfonium salts, a comparison of t_{max} is of low convenience, since photo-DSC results with low t_{max}, but a dissatisfying overall performance occurred in several cases. However, in this special instance the R_p values are very significant and a comparison of the different initiators can be achieved at a glance. One of the most valuable properties of **1P** is the outstanding performance in combination with **DBA** and **ITX** which equals the photocuring properties of high reactive commercial initiators like **SPS**. Due to alteration of the base structure, this prominent ability was drastically reduced in all cases. By extension of the conjugated system, a slight improvement in direct excitation was achieved in case of **5P**. The implementation of bathochromic groups for the sulfonium salts **3P** and **4P** decreased reactivity under all applied conditions, probably due to several negative effects. Nevertheless, the phenylethynyl sulfonium salt **1P** is a very promising new base structure for cationic polymerization and alteration of this system for special applications seems to be a potential topic for further scientific research.

Experimental

Part 1: Oxygen scavengers

3. Synthesis of oxygen scavengers

3.1 Synthesis of 9,10-dibutyl-anthracene (1, DBA)

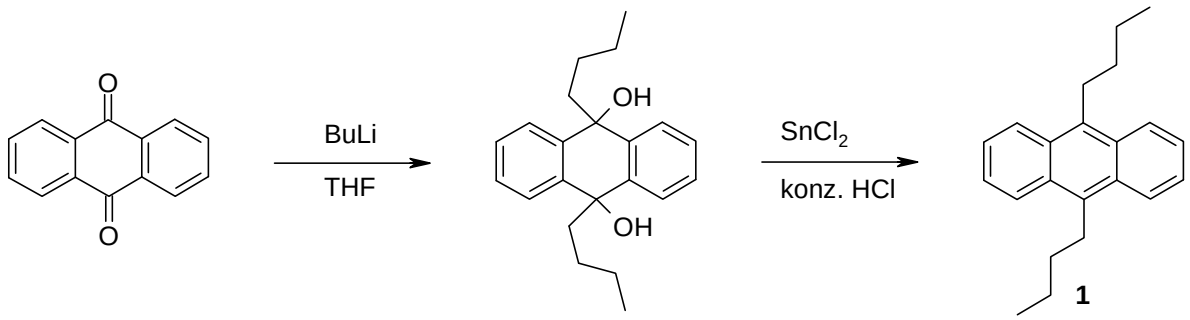

Reagents:	0.50 g	(2.40 mmol)	anthraquinone
	6.0 mL	(9.60 mmol)	n-butyllithium (1.6 M in hexane)
	32 mL		THF (abs.)
	4.07 g	(21.5 mmol)	tin dichloride
	7.0 mL		conc. HCl

N-butyllithium was added to a suspension of anthraquinone in dry THF (30 mL) under a nitrogen atmosphere at 0 °C and the mixture was stirred for 1h at rt. The solution was diluted with diethyl ether (100 mL) und quenched with sat. NH_4Cl solution (100 mL, 5 °C). The organic layer was washed with water (2 x 100 mL), brine (50 mL), dried over Na_2SO_4 and concentrated in vacuum. The residue was dissolved in petroleum ether, filtrated and the solvent was removed in vacuum.

A solution of tin dichloride in conc. HCl was added to the crude intermediate product in THF (2 mL) at rt under a nitrogen atmosphere and the reaction mixture was stirred for 24 h at 60 °C in the dark. The solution was diluted with diethyl ether (150 mL),

washed with water (2 x 150 mL), sat. $NaHCO_3$ solution (2 x 150 mL) and brine, dried over Na_2SO_4 and the solvent was removed in vacuum. Column chromatography (silica gel, petroleum ether) and subsequent recrystallization (methanol) gave 9,10-dibutyl-anthracene as pale yellow crystals.

Yield: 250 mg (36%) pale yellow crystals

$C_{22}H_{26}$	MW: 290.45 g/mol
TLC: (PE)	$R_f = 0.45$
Mp.: 104 °C	

^{1}H NMR ($CDCl_3$): δ (ppm) = 8.31 (dd, 4H, ar-H), 7.49 (dd, 4H, ar-H), 3.59 (t, 4H, ar-C$\underline{H}_2$-), 1.71-1.92 (m, 4H, ar-CH_2-C$\underline{H}_2$-), 1.48-1.70 (m, 4H, -C$\underline{H}_2$-CH_3), 1.03 (t, 6H, CH_3);
^{13}C NMR ($CDCl_3$): δ (ppm) = 133.97 (ar-C), 129.54 (ar-C), 125.37 (ar-C), 124.90 (ar-C), 33.72 (-CH_2-), 28.06 (-CH_2-), 23.61 (-$\underline{C}H_2$-CH_3), 14.24 ($\underline{C}H_3$)

3.2 Synthesis of symmetrically substituted furan derivatives

3.2.1 Synthesis of 2,5-dibromo-furan (2)

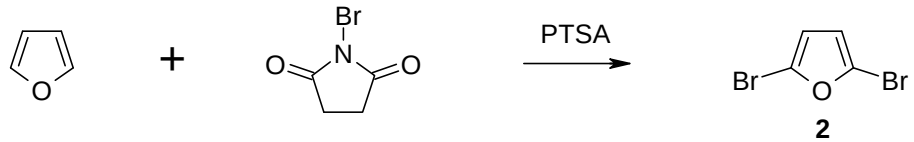

2

Reagents:	10.00 g	147.0 mmol	furan
	53.70 g	302.0 mmol	*N*-bromo-succinimide
	224 mg	1.30 mmol	toluene-4-sulfonic acid (PTSA)
	100 mL		carbon tetrachloride

Furan was added to a suspension of *N*-bromo-succinimide and PTSA in dry carbon tetrachloride and the reaction mixture was heated to reflux for 20 min until an exothermic reaction started. The mixture was stirred at reflux for additional 5 min, cooled to rt, diluted with chloroform (100 mL), washed with water (3 x 100 mL), sat. Na_2CO_3 solution (2 x 100 mL) and brine, dried over Na_2SO_4 and the solvent was removed in vacuum. Vacuum distillation and subsequent column chromatography (silica gel, petroleum ether) gave 2,5-dibromo-furan as a colorless oil.

Yield: 14.75 g (44%, Lit[66].: 39%) colorless oil

$C_4H_2Br_2O$ MW: 225.87 g/mol

TLC: (PE) $R_f = 0.86$

Bp.: 66 °C / 30 mbar (Lit.: 64 °C / 26 mbar)

^{1}H NMR ($CDCl_3$): δ (ppm) = 6.30 (s, 2H)

3.2.2 Synthesis of 4-*N*,*N*-dimethylaminophenyl boronic acid (3)

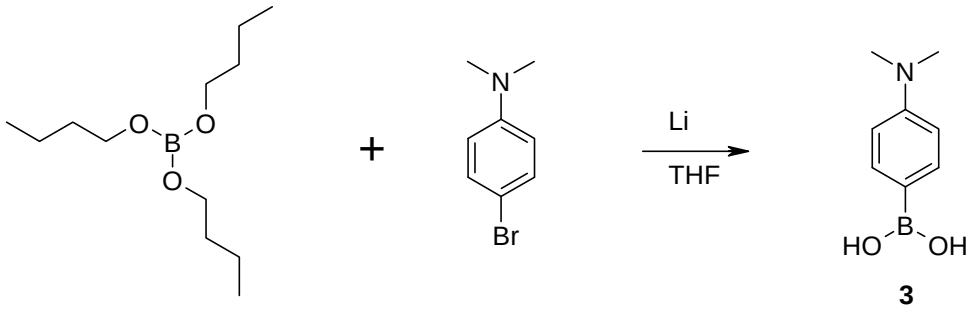

3

Reagents:	1.38 g	6.00 mmol	tributyl borate
	1.00 g	5.00 mmol	4-bromo-*N*,*N*-dimethylaniline
	70 mg	10.0 mmol	lithium (wire, sliced)
	60 mL		THF (abs.)

A solution of 4-bromo-*N*,*N*-dimethylaniline in THF (2.5 mL) was added within 5 min to a suspension of lithium in THF (7.5 mL) under an argon atmosphere and stirred for 2 h at 0 °C. The reaction mixture was filtered and added to a solution of tributyl borate in THF (50 mL) within 20 min at -78 °C under an argon atmosphere. The reaction mixture was stirred for 30 min at -78 °C, warmed to rt within 1 h under constant stirring and stirred over night at rt. The solution was poured on sat. NH_4Cl-solution (100 mL) and the aqueous layer was extracted with ethyl acetate (3 x 100 mL). The combined organic layers were washed with brine, dried over Na_2SO_4 and the solvent was removed in vacuum. Column chromatography (silica gel sat. with triethylamine, MeOH / CH_2Cl_2 = 1:25) and subsequent washing with diisopropyl ether gave 4-*N*,*N*-dimethylaminophenyl boronic acid as colorless crystals.

Yield: 400 mg (48%) colorless crystals

$C_8H_{12}BNO_2$ MW: 165.00 g/mol

TLC: (PE : EE = 1 : 1) R_f = 0.18

Mp.: 232-245 °C (Lit.: 230-250 °C)

^{1}H NMR ($CDCl_3$): δ (ppm) = 8.11 (d, 2H, Ar-H), 6.79 (d, 2H, Ar-H), 3.05 (s, 6H, CH_3)

3.2.3 Synthesis of 2,5-bis-[4-(*N*,*N*-dimethylamino)-phenyl]-furan (4)

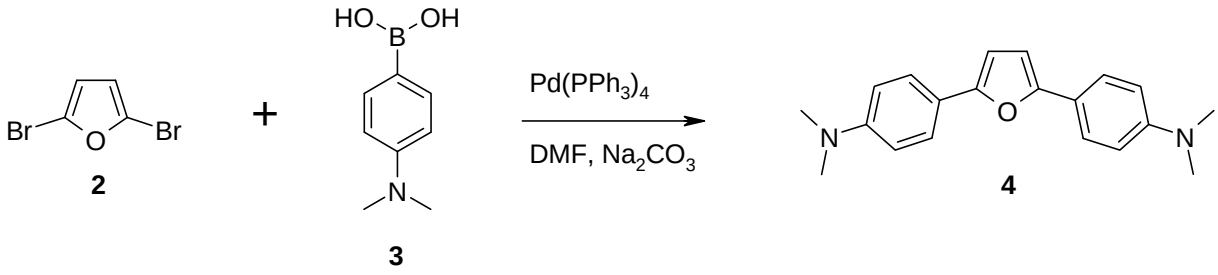

Reagents:	440 mg	2.67 mmol	4-*N*,*N*-dimethylaminophenyl boronic acid (**3**)
	150 mg	0.13 mmol	$Pd(PPh_3)_4$
	226 mg	1.00 mmol	2,5-dibromo-furan (**2**)
	20 mL		DMF
	5 mL		Na_2CO_3 solution (1 M)

4-*N*,*N*-Dimethylaminophenyl boronic acid (**3**) and $Pd(PPh_3)_4$ were added to a degassed mixture of 2,5-dibromo-furan (**2**) in DMF and aqueous 1 M Na_2CO_3 solution (5 mL) and the reaction mixture was stirred at 85 °C for 2 h under an argon atmosphere. The mixture was diluted with ethyl acetate (100 mL), washed with sat. Na_2CO_3 solution (2 x 50 mL), sat. NH_4Cl solution (1 x 50 mL), water (1 x 50 mL) and brine, dried over Na_2SO_4 and the solvent was removed in vacuum. Column chromatography (silicagel sat. with triethylamine, petroleum ether : ethyl acetate = 6 : 1) gave 2,5-bis-[4-(*N*,*N*-dimethylamino)-phenyl]-furan as yellow crystals.

Yield: 160 mg (52%) yellow crystals

$C_{20}H_{22}N_2O$	MW: 306.41 g/mol
TLC: (PE : EE = 6 : 1 + 2 dr. TEA)	$R_f = 0.28$
Mp.: 219-221 °C	

^{1}H NMR ($CDCl_3$): δ (ppm) = 7.62 (d, 4H, ar-$H^{2,2',6,6'}$), 6.76 (d, 4H, ar-$H^{3,3',5,5'}$), 6.50 (s, 2H, furan-$H^{3,4}$), 2.99 (s, 12H, CH_3)

^{13}C NMR ($CDCl_3$): δ (ppm) = 152.95 (furan-$C^{2,5}$), 149.55 (ar-$C^{4,4'}$), 124.66 (ar-$C^{2,2',6,6'}$), 120.18 (ar-$C^{1,1'}$), 112.51 (ar-$C^{3,3',5,5'}$), 104.23 (furan-$C^{3,4}$), 40.55 (CH_3)
MS: *m/z* = 306 (M^+), 291, 153, 77, 51

3.2.4 Synthesis of 2,5-bis-(phenylethynyl)-furan (5)

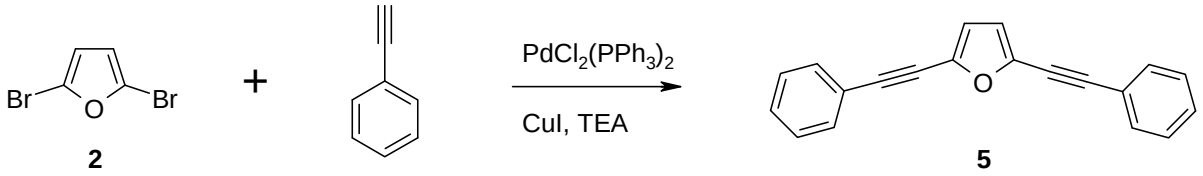

2 **5**

Reagents:	1.23 g	12.0 mmol	phenylacetylene
	1.13 g	5.00 mmol	2,5-dibromo-furan (**2**)
	38.0 mg	0.20 mmol	copper (I) iodide
	140.0 mg	0.20 mmol	$PdCl_2(PPh_3)_2$
	25 mL		triethylamine (abs.)

Copper (I) iodide, $PdCl_2(PPh_3)_2$, phenylacetylene and 2,5-dibromo-furan (**2**) were added to dry, degassed triethylamine and the reaction mixture was stirred for 2.5 h at 70 °C. The mixture was diluted with diethyl ether (100 mL), washed with water (100 mL), 0.5 M HCl (5 x 100 mL), water (2 x 100 mL) and brine, dried over Na_2SO_4 and the solvent was removed in vacuum. Column chromatography (silica gel, petroleum ether) and subsequent recrystallization from a small amount of petroleum ether gave 2,5-bis-(phenylethynyl)-furan as colorless crystals.

Yield: 1.00 g (75%) colorless crystals

$C_{20}H_{12}O$	MW: 268.32 g/mol
TLC: (PE)	R_f = 0.47
Mp.: 105 °C	

^{1}H NMR ($CDCl_3$): δ (ppm) = 7.47-7.58 (m, 4H, ar-$H^{2,2',6,6'}$), 7.31-7.41 (m, 6H, ar-$H^{3,3',4,4'5,5'}$), 6.67 (s, 2H, furan-$H^{3,4}$)

^{13}C NMR ($CDCl_3$): δ (ppm) = 138.01 (furan-$C^{2,5}$), 131.79 (ar-$C^{2,2',5,5'}$), 129.24 (ar-$C^{4,4'}$), 128.77 (ar-$C^{3,3',5,5'}$), 122.28 (ar-$C^{1,1'}$), 116.65 (furan-$C^{3,4}$), 94.42 (ar-$C^{1,1'}$-C≡C), 79.57 (furan-$C^{2,5}$-C≡C)

MS: *m/z* = 268 (M^+), 239, 213, 129, 119

Elem. Anal. Calcd. for $C_{20}H_{12}O$: C 89.53%; H 4.51%; Found: C 89.24%; H 4.79%

4. Storage stability

Oxygen Scavengers (OSs) that react with singlet oxygen in [4 + 2] cycloaddition reactions are inevitably capable to undergo thermally induced cycloadditions with C=C double bonds. Since the OSs were chosen for the application in acrylic or methacrylic UV-Vis curable formulations, a sufficient stability towards cycloaddition with these functional groups is inevitable. Furthermore, OSs should be stable against thermally induced oxidation reactions with triplet oxygen, although they should exhibit the utmost reactivity towards light induced oxidation.

For storage stability experiments, solutions of the OSs **DPF**, **DBA**, **4** and **5** (1×10^{-3} mol L^{-1}) were stored in the dark in MeCN and MeCN + dodecyl acrylate (1×10^{-2} mol L^{-1}) at rt under air and under an argon atmosphere for 30 days. After 0, 1, 3, 7, 14, 21 and 30 days, the samples were investigated for decomposition and reaction products by HPLC analysis. Furthermore, the obtained signals were integrated and compared to chromatograms of the samples drawn at point zero and the reference sample.

6. Sensitized Steady State Photooxidation (SSSP)

Since oxygen is able to diffuse into the surface of a polymerizing radiation curable formulation, an extraordinary high reaction rate of the OS is inevitable to constantly keep the oxygen level of the formulation at low values. Therefore, determination of the reaction rate towards singlet oxygen by SSSP experiments is a perfect preliminary test for a first estimation of the potential of a new OS.

Kinetic measurements of solutions of OSs (1 x 10^{-3} mol L^{-1}) and sensitizers (1 x 10^{-4} mol L^{-1}), in MeCN (HPLC grade) were carried out in a 50-mL three-necked flask fitted with a septum, a gas inlet, and a quartz quick-fit (cone / screw thread adaptor) closed on one end with a quartz window. A light guide was attached to the window and the samples were magnetically stirred and irradiated with filtered UV-Vis light (400 - 500 nm) at an intensity of 1000 mW cm^{-2} (instrument setting of EFOS-Novacure) at rt for 5 min. The solution was constantly purged with air before and during irradiation. (Figure 71)

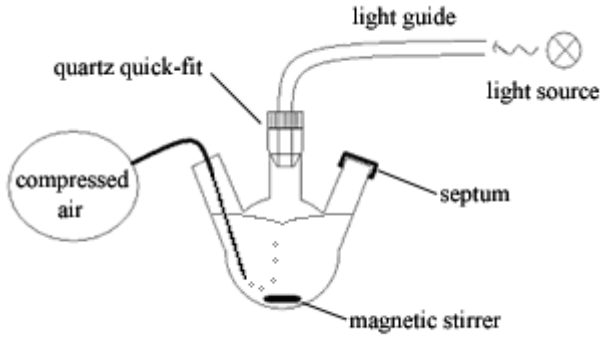

Figure 71: Standardized arrangement of SSSP experiments

In case of SSSP experiments without a sensitizer, the same experimental approach discussed above, but UV-Vis light in the region of 320 - 500 nm at an intensity of 1000 mW cm^{-2} was used. A quantitative analysis was carried out by HPLC with samples taken before saturation of the solution with compressed air (reference sample 1), before start of the irradiation (reference sample 2) and after 10, 30, 60, 90, 120, 180 and 300 s of the start of the photochemical reaction. The samples were investigated for photooxidation products by HPLC analysis and quantitative analysis of the degree of

photooxidation was obtained by integration of the DAD signal of the OS and comparison to the area in the chromatogram of reference sample 2. The reference sample 1 was used to exclude the occurrence of thermally induced side reactions which would adulterate the results of the SSSP experiments. The HPLC method 1 was used for the analysis of the photooxidation of furans, method 2 was employed for the anthracene **DBA**. (Table 18)

Table 18: Parameters of HPLC methods

	method 1	method 2
flow [mL / min]	0.8	0.8
injection volume [µl]	10	10
oven temperature [°C]	30	30
start	3 min 97% H_2O	30 min 100% MeCN
gradient	20 min auf 97% MeCN	/
post operation	2 min auf 97% MeCN	/
reset	5 min auf 97% H_2O	/
post run [min]	6	6

A concentration / reaction time graph was drawn of the results of the SSSP experiments. The linear scope of the obtained graphs was used for approximation of the reaction rate ($R_v = [SF]/dt$).

7. Photopolymerization

Thin film polymerization

Thin film polymerization with subsequent ATR FTIR spectroscopy of radiation curable formulations containing OSs is a perfect tool for an evaluation under practical conditions. With ATR FTIR spectroscopy, the double bond conversion of the surface layer can be easily quantified due to the low depth of penetration of this technology.

Coatings of monomer films (60 µm) of 1,6-bis(methacryloxy-2-ethoxycarbonylamino)-2,4,4-trimethylhexane (**UDMA**) containing 1 wt% of a 1:1 mixture of camphorquinone (**CQ**) / ethyl 4-(dimethylamino)benzoate (**DMAB**) (each 27.8 mmol L^{-1}) as a photoinitiator (PI) system and different OSs (45.0 mmol L^{-1}) on alumina sheets were polymerized under a medium pressure mercury lamp (50 W cm^{-1}, 15 cm distance). Samples with curing times of 2, 3, 4, 5, 6, 7 and 10 min were investigated by ATR FTIR spectroscopy and compared to reference samples without OS cured under nitrogen or air, respectively.

Analysis was performed by integration of characteristic absorption bands of functional groups in FTIR which vanish during polymerization. The most important absorption bands used for analysis were the C=O stretching vibration band at approximately 1706 cm^{-1} and the signal of the CH_2 - torsion vibration at 815 cm^{-1} as well as the C=C stretching vibration band at 1638 cm^{-1} of the methacrylic double bond. For the determination of the DBC, the CH_2 - torsion vibration (795 - 835 cm^{-1}) was set in relation to the partial integral (1706 - 1800 cm^{-1}) of the C=O stretching vibration band, which was defined as a constant factor and used as an internal standard. The baseline was always placed between the points 795 cm^{-1} und 2150 cm^{-1} and the integral in the area 795 - 835 cm^{-1} was defined as 0 for 100% DBC. (Figure 72)

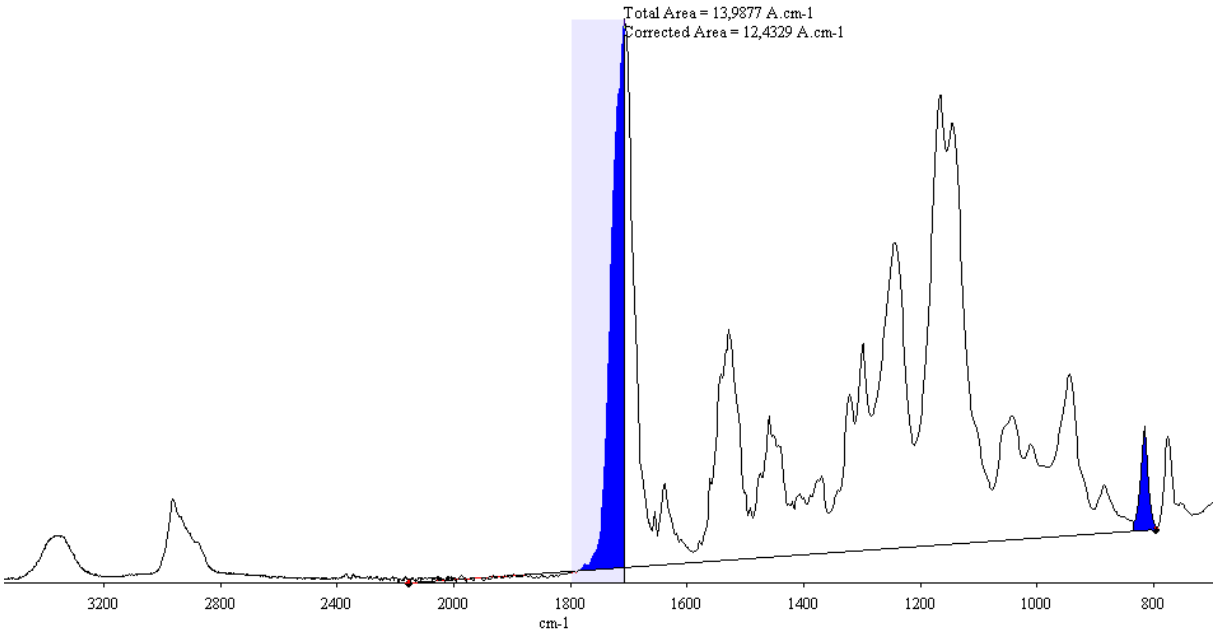

Figure 72: Integration areas in ATR FTIR analysis

An exact knowledge of the systematic and statistic errors of this relative analytical method is inevitable to obtain a useful evaluation. The most important options to reduce the error in the analytical process are:

- The light path and the mirrors have to be purged with argon before each series of measurements to remove dust and to keep the background signal at the lowest values possible.
- A background spectrum has to be taken before each measurement and has to be electronically subtracted from the sample spectrum.
- The contact pressure applied on the samples during the measurements has to be standardized.
- The chosen integral areas have to be kept exactly constant for the evaluation of all spectra.
- The position of the baseline should be kept as constant as possible for all spectra.

The statistic error for the presented results of this analytical method is approximately ± 2% with 6 measurements on different spots of the same sample. The effect of the systematic error on the obtained values is obviously much higher. Due to the definition of integral in the area 795 - 835 cm^{-1} as 0 for 100% DBC, a significant error was accepted for high DBCs. However, the reproducibility of the obtained values in the region of 30 - 50% DBC is very high, which is the amount of DBC were the consistence of the surface layer of the **UDMA** films changes from sticky and therefore insufficiently cured to hard. For this reason, the significant error for a DBC above 50% was accepted without further adaptation of the method.

Photo-DSC

Differential scanning photocalorimetry (Photo-DSC) is a unique method for obtaining a fast indication of the reactivity of a UV-curing system. The method is based upon the

measurement of the temperature difference of a sample of photo-curable formulation and a reference sample with a differential scanning calorimeter (DSC). In concurrent irradiation by a light source, the heat release caused by the progressing polymerization of the photo-curable formulation is significantly higher than the heat release of the reference sample. The time to reach the peak maximum (t_{max}) reveals information about the reactivity of the formulation, especially the activity of the PI. Furthermore, the double bond conversion (DBC) or epoxy group conversion (EGC) as well as initial rates of polymerization (R_P) can be calculated from the DSC plot. The measurements can be exclusively compared with results obtained by exactly the same analytical arrangement since different instruments exhibit varying values, for instance, for the heat release between the sample and the measuring cell. Furthermore, day light, room temperature, the performance of the light source, the condition of the instruments and, in case of cationic polymerization, humidity have a significant influence on the results of the measurements. Therefore, a relative comparison with reference formulations or standards is inevitable for exact statements.

Photo-DSC measurements of formulations of **UDMA** containing **CQ** as initiator and coinitiators (each 27.8 mmol L^{-1}) were conducted with a modified Shimadzu DSC 50 equipped with a home-made aluminum cylinder (height 6.8 cm).[110] The filtered UV-Vis light (320 - 500 nm) was applied by a light guide (EFOS-Novacure) attached to the top of the aluminum cylinder. The distance between the end of the light source and the sample was standardized at 32.0 mm. The light intensity at the level of the surface of the cured samples was measured by an EIT Uvicure® high energy UV integrating radiometer. A light intensity of 13.83 mW cm^{-2} at the surface of the sample, corresponding to 1000 mW cm^{-2} at the tip of the light guide, was used for standard conditions. The exact instrumental arrangement is presented in Figure 73 below.

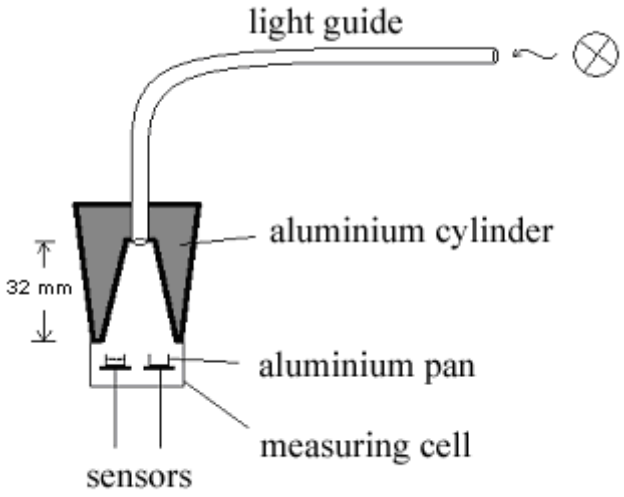

Figure 73: Instrumental arrangement for Shimadzu DSC 50

The measurements were carried out in an isothermal mode at room temperature under air and the mass of the samples was 6.5 ± 0.2 mg. Before each series of measurements, a calibration of the thermal sensors was performed by manual adjustment of the light guide. A temperature difference of 0.2 mW between the two sensors was regarded as negligible.

From the obtained data, the time to reach the peak maximum t_{max} [s], the area of the peak ΔH_P [J/g] and the height of the peak h [mW/mg] were determined. The t_{max} is directly accessible from the photo-DSC plot (Figure 74).

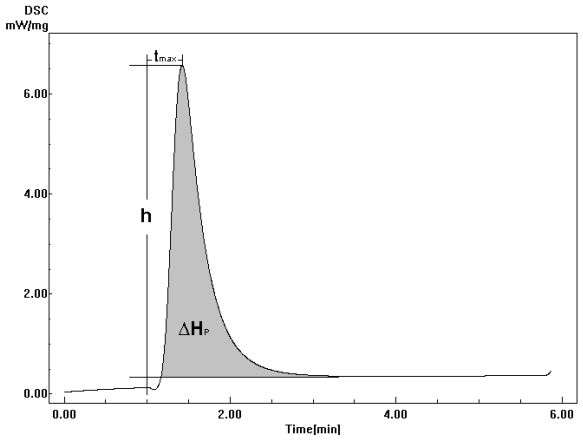

Figure 74: Photo-DSC analysis

The DBC was calculated from the overall heat evolved (ΔH_P), where $\Delta H_{0,P}$ is the theoretical heat obtained for 100% conversion (eq. 1).

$$DBC = \frac{\Delta H_P \times M_M}{\Delta H_{0,P}} \quad (1)$$

M_M is the molecular weight of the monomer. Initial rates of polymerization R_p [mol L^{-1} s^{-1}] were calculated from the height of the maximum of the plots h and the density of the monomer ρ following eq. 2.

$$R_P = \frac{h \times \rho}{\Delta H_{0,P}} \quad (2)$$

In Table 19 the values used for the calculations are listed.

Table 19: Values for the photo-DSC calculations

	MW [g/mol]	***ρ [g/l]***	***ΔH$_{0,P}$ [J/mol]***
UDMA	470.57	1094	100000 [111]

Part 2: Cationic initiators

2. Onium salt base structures

2.1 Synthesis of onium salts as reference initiators (TPS-T)

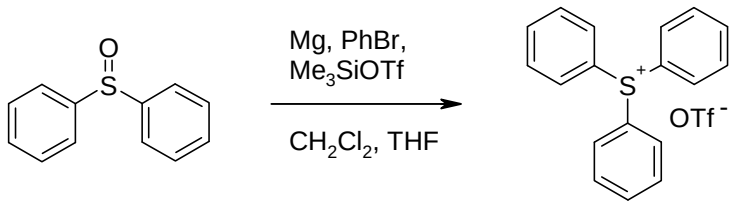

TPS-T

Reagents:	2.00 g	12.7 mmol	bromobenzene
	0.33 g	14.0 mmol	magnesium (swarf)
	15 mL		THF (abs.)
	0.96 g	4.75 mmol	diphenyl sulfoxide
	1.33 g	6.00 mmol	trimethylsilyl triflate
	10 mL		CH_2Cl_2 (abs.)

Preparation of reagent A:

Grignard reaction of a suspension of magnesium in THF (5 mL) was started by addition of a few drops of pure bromobenzene at reflux under an argon atmosphere. A solution of bromobenzene in THF (10 mL) was added to the suspension within 15 min and the reaction mixture was stirred for 2 h at reflux.

Preparation of reagent B:

Trimethylsilyl triflate was added to a solution of diphenyl sulfoxide in CH_2Cl_2 at -78 °C under an argon atmosphere within 15 min. The reaction mixture was warmed to rt and stirred for 15 min.

Reagent A was filtered and added to reagent B at -78 °C under an argon atmosphere within 15 min. The solution was stirred for 5 h at rt, aqueous trifluoromethane sulfonic acid (2%, 15 mL) was added and the solution was extracted with chloroform (2 x 50 mL). The combined organic layers were dried over molecular sieve (4Å), the solvent was removed in vacuum and the residue was recrystallized from a mixture of Et_2O : $CHCl_3$ = 5 : 1.

Yield: 960 mg (49%) colorless crystals

$C_{18}H_{15}S$. CF_3SO_3 MW: 412.45 g/mol
Mp.: 129-132 °C (Lit.: 135-137 °C)

^1H NMR ($CDCl_3$): δ (ppm) = 7.81-7.64 (m, 15H)
IR (ATR, cm^{-1}): 3076, 1478, 1448, 1262, 1226, 1149, 1069, 1031, 998, 938, 842, 752, 701

2.2 Synthesis of diphenyl(phenylethynyl)sulfonium salts (1T)

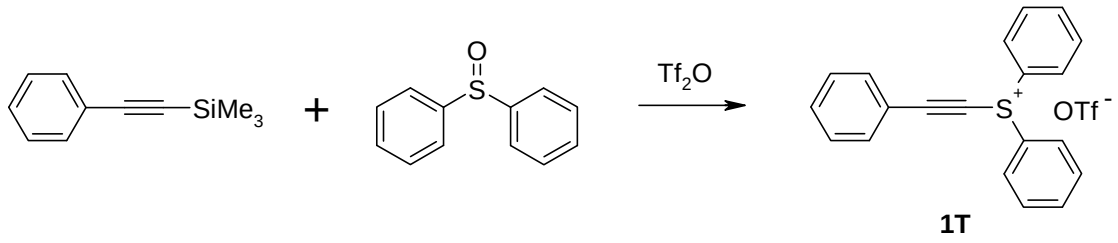

1T

Reagents:	2.16 g	7.65 mmol	trifluoromethanesulfonic acid anhydride (Tf_2O)
	1.56 g	7.65 mmol	diphenyl sulfoxide
	1.35 g	7.65 mmol	trimethylsilyl(phenyl)acetylene
	65 mL		CH_2Cl_2 (abs.)

Freshly distilled Tf_2O was added dropwise to a solution of diphenyl sulfoxide in dry CH_2Cl_2 (45 mL) at -50 ºC under argon and the reaction mixture was stirred for 45 min. A solution of trimethylsilyl(phenyl)acetylene in dry CH_2Cl_2 (10 mL) was added within 5 min at -50 ºC and the resulting mixture was stirred for 5 h at -10 to -20 ºC. The reaction mixture was diluted with CH_2Cl_2 (50 mL), washed with water (3 × 50 mL) and the combined aqueous layers were extracted with CH_2Cl_2 (2 x 20 mL). The combined organic layers were dried over molecular sieve (4Å) and concentrated in vacuum. Column chromatography (CH_2Cl_2 : MeCN = 3 : 1) and subsequent washing with petroleum ether gave **1T** as a yellow oil which crystallized partially within 12 month at -25 °C.

Yield: 1.9 g (57%) yellow oil

$C_{20}H_{15}S$. CF_3SO_3 MW: 436.48 g/mol

^{1}H NMR ($CDCl_3$): δ (ppm) = 8.27-8.14 (m, 3H), 7.87-7.38 (m, 12H)
^{13}C NMR ($CDCl_3$): δ (ppm) = 135.7, 134.5, 134.0, 132.6, 131.2, 130.3, 129.9, 128.5, 117.5, 112.2, 63.5
IR (ATR, cm^{-1}): 3067, 2185, 1687, 1580, 1477, 1447, 1259, 1224, 1151, 1068, 1030, 999, 932, 873, 746

2.3 Synthesis of phenyl(phenylethynyl)iodonium salts (2T)

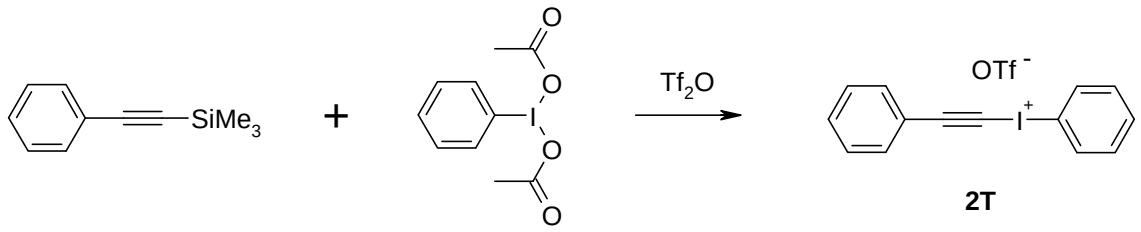

2T

Reagents:	2.54 g	9.00 mmol	trifluoromethanesulfonic acid anhydride (Tf_2O)
	2.90 g	9.00 mmol	(diacetoxyiodo)benzene
	2.38 g	13.5 mmol	trimethylsilyl(phenyl)acetylene
	25 mL		CH_2Cl_2 (abs.)

Freshly distilled Tf_2O was added dropwise to a suspension of (diacetoxyiodo)benzene in dry CH_2Cl_2 at 0 °C under argon and the reaction mixture was stirred for 30 min. Trimethylsilyl(phenyl)acetylene was added at -40 °C and the solution was stirred for 4 h at -15 °C. The reaction mixture was diluted with CH_2Cl_2 (50 mL), washed with water (2 × 50 mL) and the combined aqueous layers were extracted with CH_2Cl_2 (2 x 20 mL). The combined organic layers were dried over molecular sieve (4Å) and concentrated in vacuum at 0 °C. **2T** crystallized at -20 °C within several days and was thoroughly washed with ether (5 x 5 mL, 0 °C).

Yield: 2.65 g colorless crystals (65%)

$C_{14}H_{10}I$. CF_3SO_3 MW: 454.21 g/mol

Mp.: decomposed at 60 °C

^{1}H NMR ($CDCl_3$): δ (ppm) = 8.33 (d, 2H), 7.76-7.29 (m, 8H)

^{13}C NMR ($CDCl_3$): δ (ppm) = 137.2, 134.8, 132.6, 132.1, 131.3, 131.0, 129.1, 119.5, 119.1, 102.3

IR (ATR, cm^{-1}): 3084, 2172, 1775, 1564, 1490, 1472, 1447, 1291, 1216, 1162, 1065, 1022, 988, 928, 849, 818, 760, 741

2.4 Ion exchange

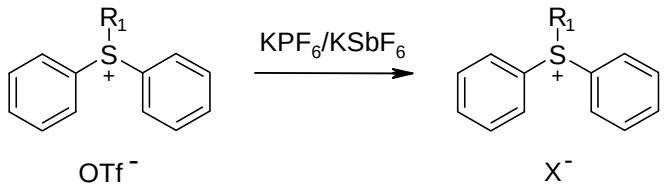

1P: $R_1 = C_8H_5$, X = PF_6

1Sb: $R_1 = C_8H_5$, X= SbF_6

TPS-P: $R_1 = C_6H_5$, X = PF_6

TPS-Sb: $R_1 = C_6H_5$, X= SbF_6

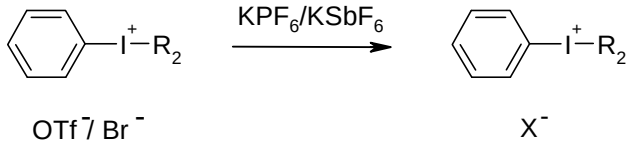

2P: $R_2 = C_8H_5$, X = PF_6

2Sb: $R_2 = C_8H_5$, X= SbF_6

DPI-P: $R_2 = C_6H_5$, X = PF_6

DPI-Sb: $R_2 = C_6H_5$, X= SbF_6

Product	Reagent	Procedure
TPS-P	0.96 g (2.33 mmol) Triphenylsulfonium triflate (**TPS-T**)	A
TPS-Sb	0.40 g (0.97 mmol) Triphenylsulfonium triflate (**TPS-T**)	A
DPI-P	1.00 g (2.77 mmol) Diphenyliodonium bromide	A
DPI-Sb	0.50 g (1.38 mmol) Diphenyliodonium bromide	A
1P	1.90 g (4.35 mmol) Diphenyl(phenylethynyl)sulfonium triflate (**1T**)	B
1Sb	0.50 g (1.15 mmol) Diphenyl(phenylethynyl)sulfonium triflate (**1T**)	B
2P	0.50 g (1.10 mmol) Phenyl(phenylethynyl)iodonium triflate (**2T**)	B
2Sb	0.50 g (1.10 mmol) Phenyl(phenylethynyl)iodonium triflate (**2T**)	B

Procedure A:

The onium salt was suspended in a saturated solution of 10 equiv. of potassium hexafluorophosphate (93 g/L) or potassium hexafluoroantimonate in distilled water and the mixture was thoroughly stirred for 2 h at rt. The residue was filtrated and washed with water.

Procedure B:

A 0.1 M solution of the onium salt in CH_2Cl_2 was added to a saturated solution of 5 equiv. of potassium hexafluorophosphate (93 g/L) or potassium hexafluoroantimonate in distilled water and the mixture was thoroughly stirred for 30 min at rt. The aqueous layer was extracted with CH_2Cl_2 and the combined organic layers were dried over molecular sieve (4Å) and concentrated in vacuum. In case of **2P** and **2Sb** all steps of the procedure were performed at 0 °C.

Purification:

TPS-P, **TPS-Sb**, **DPI-P and DPI-Sb** were recrystallized from i-PrOH. **1P** and **1Sb** crystallized at -20 °C within several days and were thoroughly washed with PE. In case of a residual concentration (FT IR) of onium triflate (> 5 mol%) the ion exchange process was repeated.

Yield	Product
0.81 g (84%) colorless crystals	**Triphenylsulfonium hexafluorophosphate (TPS-P)** $C_{18}H_{15}S$. PF_6 MW: 408.34 g/mol 1H NMR ($CDCl_3$): δ (ppm) = 7.81-7.64 (m, 15H) IR (ATR, cm^{-1}): 3076, 1478, 1448, 1183, 1069, 1027, 998, 938, 821, 748
0.42 g (87%) colorless crystals	**Triphenylsulfonium hexafluoroantimonate (TPS-Sb)** $C_{18}H_{15}S$. SbF_6 MW: 499.12 g/mol ^{1}H NMR ($CDCl_3$): δ (ppm) = 8.00-7.52 (m, 15H) IR (ATR, cm^{-1}): 3103, 1478, 1450, 1319, 1268, 1182, 1068, 1024, 999, 926, 842, 749
0.76 g (64%) colorless crystals	**Diphenyliodonium hexafluorophosphate (DPI-P)** $C_{12}H_{10}I$. PF_6 MW: 426.08 g/mol ^{1}H NMR ($CDCl_3$): δ (ppm) = 8.21 (d, 4H), 7.61 (t, 2H), 7.47 (t, 4H) IR (ATR, cm^{-1}): 3100, 1563, 1471, 1446, 1269, 1011, 985, 818, 732

0.65 g (93%) colorless crystals	**Diphenyliodonium hexafluoroantimonate (DPI-Sb)** $C_{12}H_{10}I$. SbF_6 MW: 516.86 g/mol ^{1}H NMR (DMSO): δ (ppm) = 8.20 (d, 4H), 7.62 (t, 2H), 7.47 (t, 4H) IR (ATR, cm^{-1}): 1564, 1471, 1446, 1328, 1265, 1180, 1093, 1065, 1012, 988, 916, 833, 734
1.50 g (80%) colorless crystals	**Diphenyl(phenylethynyl)sulfonium hexafluorophosphate (1P)** $C_{20}H_{15}S$. PF_6 MW: 432.37 g/mol Mp: 120-123 °C ^{1}H NMR ($CDCl_3$): δ (ppm) = 8.17-8.02 (m, 4H), 7.85-7.76 (m, 2H), 7.74-7.63 (m, 6H), 7.50-7.39 (m, 3H) ^{13}C NMR ($CDCl_3$): δ (ppm) = 135.3, 133.9, 133.4, 132.1, 129.4, 129.2, 127.5, 116.7, 112.0, 62.2 IR (ATR, cm^{-1}): 3074, 2192, 1478, 1448, 1183, 1166, 1067, 1027, 999, 931, 872, 821, 748
0.57 g (95%) reddish oil	**Diphenyl(phenylethynyl)sulfonium hexafluoroantimonate (1Sb)** $C_{20}H_{15}S$. SbF_6 MW: 523.15 g/mol ^{1}H NMR ($CDCl_3$): δ (ppm) = 8.15-7.97 (m, 4H), 7.86-7.76 (m, 2H), 7.76-7.37 (m, 9H) IR (ATR, cm^{-1}): 3069, 2185, 1687, 1597, 1477, 1448, 1268, 1224, 1182, 1068, 1030, 999, 930, 873, 745
0.30 g (60%) colorless crystals	**Phenyl(phenylethynyl)iodonium hexafluorophosphate (2P)** $C_{14}H_{10}I$. PF_6 MW: 450.10 g/mol Mp.: decomposed at 50 °C ^{1}H NMR ($CDCl_3$): δ (ppm) = 8.33 (d, 2H, Ar-H), 7.76-7.29 (m, 8H, Ar-H) ^{13}C NMR ($CDCl_3$): δ (ppm) = 137.6, 134.3, 133.3, 132.8, 132.6, 131.6, 128.8, 119.7, 117.1, 107.9 IR (ATR, cm^{-1}): 3100, 2170, 1470, 1447, 1030, 987, 924, 829, 759, 738

	Phenyl(phenylethynyl)iodonium hexafluoroantimonate (2Sb)
0.39 g	$C_{14}H_{10}I$. SbF_6 MW: 540.88 g/mol
(66%)	^1H NMR ($CDCl_3$): δ (ppm) = 8.35 (d, 2H), 7.78-7.28 (m, 8H)
yellow oil	IR (ATR, cm^{-1}): 3066, 2161, 1687, 1564, 1460, 1471, 1446, 1283, 1233, 1166, 1069, 1025, 987, 922, 814, 760, 735

2.5 Quantification of ion exchange by IR spectroscopy

Residual nucleophilic counterions, like triflate ions, inevitably have an impact on the performance of the PI system in cationic polymerization. In general, a sufficient quantification of the residual concentration of the nucleophilic anion is usually not possible by standard analytical methods used for substance verification like NMR, HPLC or GC MS. However, many counterions, including triflates, possess strong absorptions in IR. In Figure 75 the strong absorption bands of the triflate anion at 1259, 1224, 1151 and 1030 cm^{-1} and the hexafluorophosphate anion at 822 cm^{-1} in the spectra of **1T** and **1P** are shown for illustration.

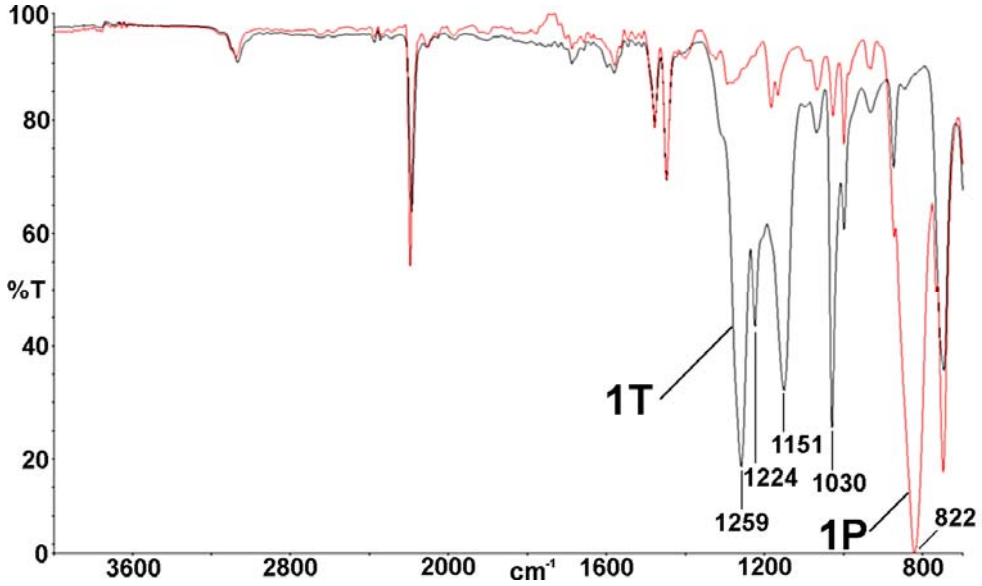

Figure 75: FT IR spectra of **1T** and **1P**

Due to the strong absorption bands of the inorganic counterions, IR spectroscopy is a powerful tool for the analysis of cationic PIs. ATR FTIR spectroscopy is a very fast and accurate method for the accommodation of IR data and was used for the monitoring of the proceeding of the ion exchange process. However, this method is no good choice for the quantification of small residues of nucleophilic counterions due to a low resolution of the spectrum compared to IR spectroscopy in liquid systems. For this reason, a final FT IR spectroscopy of the dissolved PI combined with a mathematical peak deconvolution of the spectrum[112] was performed to verify the completion of the ion exchange process. In FT IR spectroscopy in liquid systems, the choice of the solvent plays a key role for the quality of the obtained spectrum. A possible solvent for IR spectroscopy must exhibit a good solubility for the cationic PI and must not be able of any chemical reactions with the PI. Furthermore, the solvent must not possess any strong absorption bands in the area of the spectrum that is needed for the quantification. Therefore, methylene chloride (CH_2Cl_2), which meets all mentioned prerequisites for the analysis of onium hexafluorophosphates, -antimonates and triflates was chosen as solvent.

ATR FTIR spectra with ATR correction were recorded on a Biorad FTS 135 FTIR spectrometer with Golden Gate ATR unit and utilized for a first estimation of the degree of ion exchange. Before each measurement, the light path and the mirrors were purged with argon to remove dust and reduce the background signal. A new background signal was recorded before each measurement and electronically subtracted from the spectrum. The residual concentration of triflate was estimated using the strong absorption bands at 1259, 1151 and 1030 cm^{-1} in conjunction with the C≡C band (2183 cm^{-1}) as an internal standard. The ion exchange process with subsequent ATR FTIR analysis was repeated until no remnant concentration of nucleophilic counterions could be verified any longer.

The completion of the ion exchange process was examined by FT IR spectroscopy in CH_2Cl_2 in a sealed cell with NaCl windows on a Perkin Elmer System 2000 FT IR spectrometer. The residual concentration of triflate was determined by mathematical peak deconvolution of the IR spectra with the software program “PeakFit™” V4.12

(SYSTAT). In Figure 76 the deconvolution of IR spectra in the synthesis of **1P** from **1T** using the C≡C band (2183 cm^{-1}) as an internal standard is displayed for illustration.

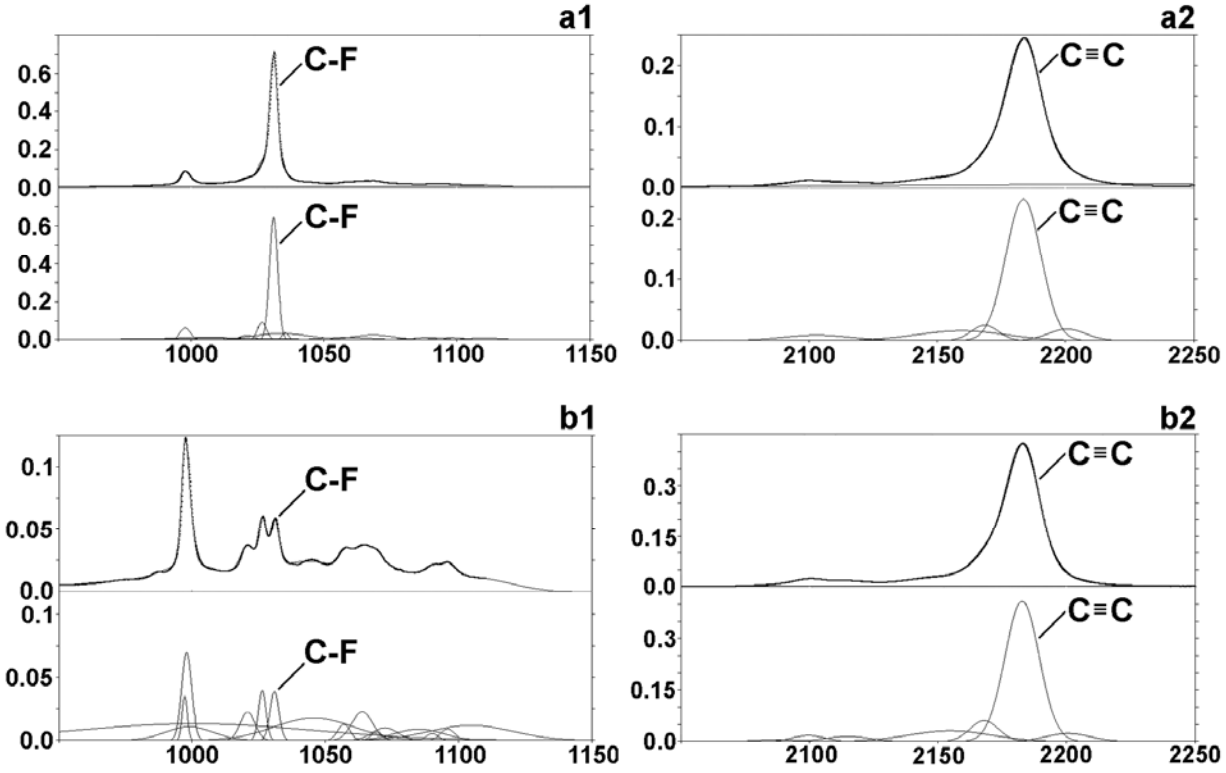

Figure 76: Mathematical peak deconvolution with PeakFit™ of spectra sections of **1T** (a) and **1P** (b) of the C-F band of **1T** at 1031 cm^{-1} (1) and the C≡C reference band at 2183 cm^{-1} (2)

The amount of residual triflate **1T** was calculated from the ratio of the area of the corresponding gauss curves of the C-F band of **1T** at 1031 cm^{-1} to the C≡C band. The ion exchange was not entirely completed in the example above, the residual concentration of **1T** was about 4 - 5 mol% of the PI.

2.7 Photolysis and thermal decomposition

Steady state photolysis combined with reversed phase HPLC with UV detection and GC MS analysis for the identification and quantification of the corresponding

photoproducts is an excellent method to draw conclusions on the photodecomposition pathway of aryl sulfonium and aryl iodonium salts. However, residues of aryl onium salts as well as the strong acids that are formed by the photodecomposition interfere with the chromatographical methods and must be separated before analysis.

Photolysis experiments of solutions of the phenylethynyl sulfonium and -iodonium salts (1 x 10^{-2} mol L^{-1}) in MeCN and CH_2Cl_2 (10 mL) were carried out in a 25-mL three-necked flask fitted with a septum, a gas inlet, and a quartz quick-fit (cone / screw thread adaptor) closed on one end with a quartz window. A light guide was attached to the window and the samples were magnetically stirred and irradiated with filtered UV-Vis light (250 - 400 nm) at an irradiation intensity of 1000 mW cm^{-2} at the tip of the light guide (instrument setting of EFOS-Novacure) at rt. In case of photolysis in MeCN, Residues of the PIs, acids and ionic compounds were separated by column chromatography (silica gel, 3g) with MeCN as mobile phase (HPLC grade, 20 mL). The eluate was directly used for HPLC and GC MS analysis. As it could not be excluded that important photolysis products were lost by this separation technique, an identical photolysis of the PIs was carried out in CH_2Cl_2 with subsequent removal of ions and acids by extraction with water (3 x 15 mL).
Thermal decomposition of **2P** was carried out within 30 min in a 50 wt% solution in trifluoromethane sulfonic acid at rt under argon in a 5-mL flask fitted with a septum. After the reaction mixture was diluted with CH_2Cl_2 and extracted with water, analysis of the photodecomposition products was performed analogous to the photodecomposition experiments.

For the qualitative analysis of the photodecomposition products, gas chromatography / mass spectrometry was performed on a Hewlett-Packard 5890/5970 B system using fused silica capillary columns (Supelco, SPB-5, 60 m x 0.25 mm as well as Perkin-Elmer, 25 m x 0.32 mm). MS spectra were recorded with EI ionization (70 eV) and a quadrupole analyzer. Benzene, phenylacetylene, diphenylsulfide, diphenyl sulfoxide, iodobenzene, phenyl(phenylethynyl) sulfide, phenyl(phenylethynyl) sulfoxide, phenylethynyl iodide, dibenzothiophene, thiophenol, biphenyl and 1,2-diphenylacetylene were used as external standards. All photochemical and thermal

decomposition products of the phenylethynyl sulfonium and -iodonium salts were detectable with the methods listed below. (Table 20)

Table 20: Parameters of GC MS methods

	method 1	method 2
column	Perkin-Elmer, 25 m x 0.32 mm	Perkin-Elmer, 25 m x 0.32 mm
column head pressure [kPa]	60	60
solvent delay [min]	2.5	2.5
injection temperature [°C]	300	300
initial temperature [°C]	60	80
initial time [min]	2	2
rate [°C / min]	10	15
final temperature [°C]	300	300
final time [min]	20	20

The quantitative analysis was performed on a revers-phase HP-1100 high-performance liquid chromatography (HPLC) system with a diode array detector (DAD). UV-Vis spectra of all photodecomposition products were accessible by the DAD detector. All separations were carried out on a Waters XTerra MS C18 column (particle size = 5 µm, 150 × 3.9-mm i.d.). The photodecomposition and thermal decomposition products as well as all external standards listed above for GC MS analysis were detectable with the methods listed below. (Table 21)

Table 21: Parameters of HPLC methods

	method 1	method 2
flow [mL / min]	0.8	0.8
injection volume [µl]	10	10
oven temperature [°C]	30	30
start	3 min 97% H_2O	5 min 20% MeCN / 80% H_2O
gradient	20 min to 97% MeCN	20 min to 97% MeCN
post operation	2 min to 97% MeCN	7 min to 97% MeCN
reset	5 min to 97% H_2O	5 min to 20% MeCN / 80% H_2O
post run [min]	6	6

2.7.1 Synthesis of decomposition products

2.7.1.1 Synthesis of phenyl(phenylethynyl) sulfide (F_2)

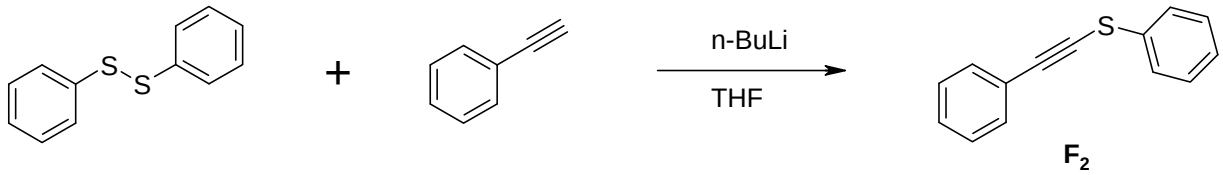

Reagents:	2.04 g	20.0 mmol	phenylacetylene
	4.37 g	20.0 mmol	diphenyl disulfide
	9.42 g	21.0 mmol	n-butyllithium (2.23 M in hexane)
	60 mL		THF (abs.)

N-butyllithium was added to a solution of phenylacetylene in THF (50 mL) at -78 °C within 10 min under a nitrogen atmosphere. The reaction mixture was stirred at -40 °C for 30 min and diphenylsulfide in THF (10 mL) was added within 10 min at -78 °C. The solution was stirred at 0 °C for 1 h, poured on sat. Na_2CO_3-solution (100 mL) and extracted with ether (3 x 75 mL). The combined organic layers were washed with sat. Na_2CO_3 solution (3 x 50 mL), water (3 x 50 mL) and brine, dried over Na_2SO_4 and the solvent was evaporated in vacuum to give pure phenyl(phenylethynyl) sulfide as a yellowish oil.

Yield: 4.20 g (99%, Lit[98].: 91%) yellowish oil

$C_{14}H_{10}S$	MW: 210.30 g/mol
TLC: (PE)	$R_f = 0.58$

^{1}H NMR ($CDCl_3$): δ (ppm) = 7.63-7.50 (m, 4H, Ar-H), 7.46-7.22 (m, 6H, Ar-H)

^{13}C NMR ($CDCl_3$): δ (ppm) = 133.0 (Ar-C), 131.8 (Ar-C), 129.3 (Ar-C), 128.7 (Ar-C), 128.4 (Ar-C), 126.6 (Ar-C), 126.2 (Ar-C), 122.9 (Ar-C), 98.0 (C≡C), 75.5 (C≡C)

2.7.1.2 Synthesis of phenyl(phenylethynyl) sulfoxide ($F_{2,OX}$)

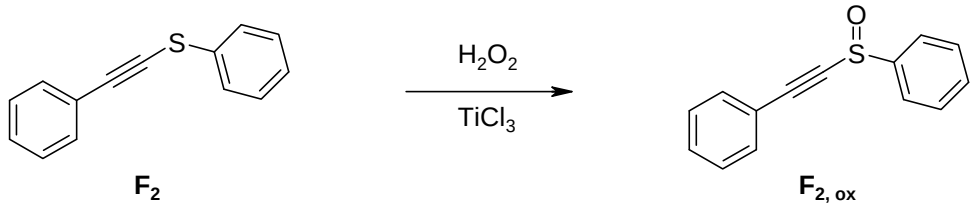

Reagents:	2.10 g	10 mmol	phenyl(phenylethynyl) sulfide
	2.31 g	15 mmol	titan (III) chloride
	10 mL	100 mmol	hydrogen peroxide (35 wt%)
	210 mL		methanol
	40 mL		water

A mixture of hydrogen peroxide and methanol (40 mL) was added to a solution of titan (III) chloride and phenyl(phenylethynyl) sulfide in water (40 mL) and methanol (170 mL) within 5 min at 0 °C. The reaction mixture was stirred for 2 h at 5 °C, poured on water (250 mL) and extracted with ether (3 x 200 mL). The combined organic layers were washed with sat. Na_2CO_3-solution (150 mL), water (3 x 100 mL) and brine, dried over Na_2SO_4 and the solvent was evaporated in vacuum. Column chromatography (silica gel, PE : EE = 8 : 1) gave phenyl(phenylethynyl) sulfoxide as a colorless oil.

Yield: 2.00 g (89%) colorless oil

$C_{14}H_{10}OS$	MW: 226.30 g/mol
TLC: (PE : EE = 8 : 1)	R_f = 0.26

^{1}H NMR ($CDCl_3$): δ (ppm) = 7.70-7.20 (m, 10H, Ar-H)

2.8 Photo-DSC

Photo-DSC experiments in 3,4-epoxycyclohexenylmethyl-3',4'-epoxycyclohexenyl carboxylate (**ECHC**) were conducted with a Netzsch DSC 204 F1 Phoenix with autosampler and UV-Vis irradiation device (EXFO Omnicure 2001, 280 - 450 nm, 3 W cm^{-2}, double light guide 3 mm). The measurements were carried out in an isothermal mode at 30 °C under a nitrogen atmosphere. The mass of the samples was 10.0 ± 0.2 mg.

Photo-DSC measurements of 1,6-bis(2,3-epoxypropoxy)hexane (**R18**) using light sources with a broader emission spectrum (250 - 450 nm) were conducted with a modified Shimadzu DSC 50 equipped with a home-made aluminum cylinder. The filtered UV-Vis light was applied by a light guide (EFOS-Novacure) attached to the top of the aluminum cylinder. The light intensity at the level of the surface of the cured samples was measured by an EIT Uvicure® high energy UV integrating radiometer. A light intensity of 13.83 mW cm^{-2} at the surface of the sample, corresponding to 1000 mW cm^{-2} at the tip of the light guide, was used for standard conditions. A nitrogen purge (20 mL/min) was used for a minimum of 10 min to eliminate remaining humidity before the irradiation. The measurements were conducted in an isothermal mode at 30 °C. The mass of the samples was 5.0 ± 0.2 mg.

Additional information on Photo-DSC, including instructions on the analysis of the obtained data is described in “Part 1: Oxygen Scavengers; 6. Photopolymerization”. Instead of a DBC, the EGC was calculated from the overall heat evolved (ΔH_P), where $\Delta H_{0,P}$ is the theoretical heat obtained for 100% conversion and M_M is the molecular weight of the monomer (eq. 3).

$$EGC = \frac{\Delta H_P \times M_M}{\Delta H_{0,P}} \tag{3}$$

In Table 22 the values used for the calculations are listed.

Table 22: Values for the photo-DSC calculations

	MW [g/mol]	*ρ [g/l]*	*$\Delta H_{0,P}$ [J/mol]*
ECHC	252.31	1170	146100 [113]
R18	230.31	1070	151000 [114]

3. Broad band irradiation experiments

Purification of commercial sulfonium salts

Mixture of diphenyl(4-phenylthio)phenyl sulfonium and (thiodi-4,1-phenylene)bis(diphenylsulfonium) hexafluorophosphate (SPS)

Column chromatography (silica gel, CH_2Cl_2 : MeOH = 15 : 1) and subsequent evaporation of the solvent in vacuum gave **SPS** as a colorless foam with a molar distribution of single to double salt of approximately 1 : 3 (^{1}H NMR analysis).

(4-dodecyl)bis(diphenyliodonium) hexafluoroantimonate (**DI**)

Column chromatography (silica gel, CH_2Cl_2 : MeOH = 100 : 1) and subsequent evaporation of the solvent in vacuum gave **DI** as a colorless oil.

4. Bathochromic shifted and conjugated sulfonium salts

4.1 Synthesis of bathochromic shifted and conjugated sulfonium salts

4.1.1 Synthesis of precursors

4.1.1.1 Synthesis of 4-methoxyphenyl trimethylsilyl acetylene (6)

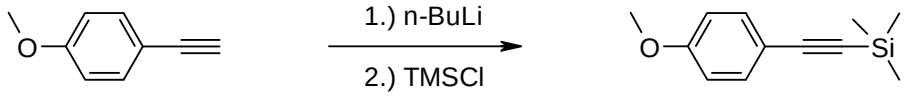

6

Reagents:	500 mg	3.78 mmol	p-methoxyphenylacetylene
	2.12 mL	4.73 mmol	n-butyllithium (2.23M in hexane)
	514 mg	4.73 mmol	trimethylsilylchloride
	25 mL		THF (abs.)

n-Butyllithium was added to p-methoxyphenylacetylene in THF (20 mL) within 5 min at -70 °C under an argon atmosphere and the reaction mixture was stirred for 30 min at -20 °C. Trimethylsilylchloride in THF (5 mL) was added within 5 min at -80 °C, the solution was stirred for 30 min at -80 °C and warmed to rt within 1 h. The reaction mixture was poured on sat. NH_4Cl solution (50 mL, 5 °C) and extracted with ether (2 x 50 mL. The combined organic layers were washed with water (50 mL) and brine, dried over Na_2SO_4 and the solvent was evaporated in vacuum. Column chromatography (silica gel, PE : EE = 99 : 1) gave 4-methoxyphenyl trimethylsilyl acetylene as a colorless oil.

Yield: 770 mg (99%) colorless oil

$C_{12}H_{16}OSi$ MW: 204.35 g/mol

TLC: (PE : EE = 30 : 1) $R_f = 0.7$

^{1}H NMR ($CDCl_3$): δ (ppm) = 7.40 (d, 2H, Ar-H), 6.81 (d, 2H, Ar-H), 3.80 (s, 3H, O-Me), 0.24 (s, 9H, Si-Me)

4.1.1.2 Synthesis of trimethylsilylacetylene (7)

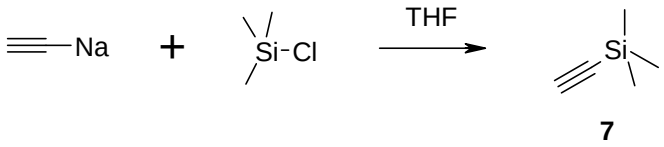

7

Reagents:	7.15 g	149 mmol	sodium acetylide
	17.1 g	149 mmol	trimethylsilylchloride
	45 mL		THF (abs.)

Trimethylsilylchloride in THF (15 mL) was added to a suspension of sodium acetylide in THF (30 mL) within 15 min at rt and the reaction mixture was stirred for 18 h at rt. The solution was poured on ice water (100 mL) and extracted with xylene (100 mL). The organic layer was washed with water (6 x 100 mL, 0 °C) and brine, dried over Na_2SO_4 and distilled (52 - 56 °C) to give a 50 wt% (NMR analysis) solution of trimethylsilylacetylene in THF.

Yield: 12.48 g (47%, Lit[108].: 75%) solution, 50 wt% in THF

$C_5H_{10}Si$ MW: 98.22 g/mol

^{1}H NMR ($CDCl_3$): δ (ppm) = 2.37 (s, 1H, C≡C-H), 0.19 (s, 9H, Si-Me),

^{13}C NMR ($CDCl_3$): δ (ppm) = 93.2 (C≡C-H), 68.1 (C≡C-H), -0.16 (Si-Me)

4.1.1.3 Synthesis of 4,4'-dibromodiphenyl sulfide (8)

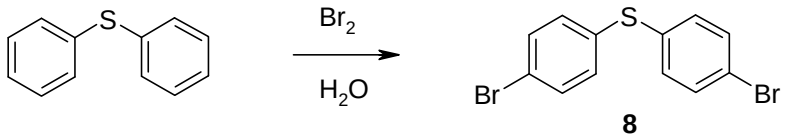

8

Reagents:	5.59 g	30.0 mmol	diphenyl sulfide
	9.59 g	60.0 mmol	bromine
	100 mL		CH_2Cl_2
	100 mL		water

Bromine was added to diphenyl sulfide in CH_2Cl_2 and water within 5 min at rt and the reaction mixture was stirred for 18 h at rt. The aqueous layer was extracted with CH_2Cl_2 (30 mL) and the combined organic layers were washed with sat. Na_2CO_3 solution (2 x 50 mL), water (50 mL) and brine, dried over Na_2SO_4 and the solvent was evaporated in vacuum. The crude product was washed with petroleum ether (2 x 20 mL) to give 4,4'-dibromodiphenyl sulfide as colorless crystals.

Yield: 8.4 g (81.4%, Lit[109].: 87%) colorless crystals

$C_{12}H_8Br_2S$ MW: 344.07 g/mol

TLC: (PE) $R_f = 0.50$

MP: 110-112 °C (Lit.: 112 °C)

^{1}H NMR ($CDCl_3$): δ (ppm) = 7.45 (d, 4H, Ar-H), 7.20 (d, 4H, Ar-H)

4.1.1.4 Sonogashira couplings for the synthesis of TMS-acetylene precursors (9-11)

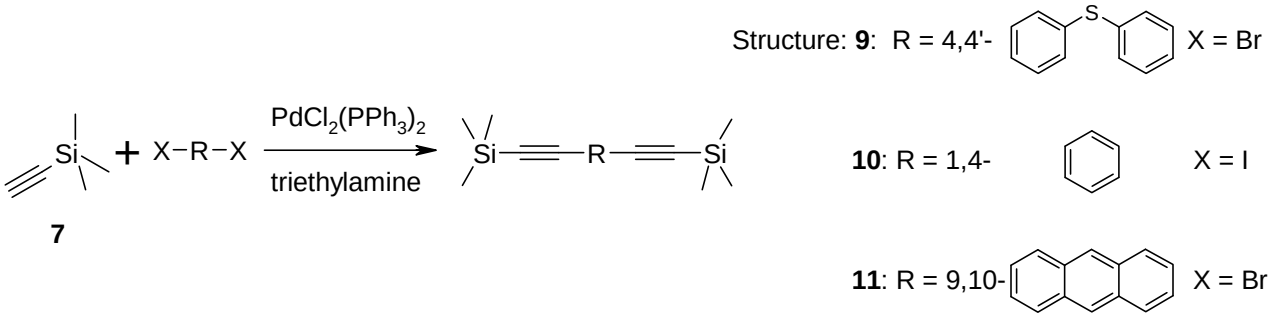

Reagents	9	10	11
7 (50 wt% solution)	1.97 g (10.0 mmol)	3.93 g (20.0 mmol)	1.97 g (10.0 mmol)
X-R-X	1.43 g (4.17 mmol)	3.00 g (9.09 mmol)	1.53 g (4.55 mmol)
$PdCl_2(PPh_3)_2$	0.15 g (0.21 mmol)	65 mg (0.09 mmol)	0.32 g (0.46 mmol)
copper (I) iodide	79 mg (0.42 mmol)	35 mg (0.18 mmol)	0.17 g (0.91 mmol)
triethylamine	1.85 g (18.2 mmol)	3.69 g (36.4 mmol)	1.85 g (18.2 mmol)
THF (abs.)	20 mL	20 mL	-
toluene (abs.)	-	-	50 mL

Procedure	9	10	11
Reaction time [h]	16 h	1 h	100 h
Temperature [°C]	50 °C	25 °C	40 °C
$PdCl_2(PPh_3)_2$ added: [g] at [h] reaction time	0.15 g at 14 h	-	0.10 g at 3 h 0.10 g at 27 h
7 added: [g] at [h] reaction time	1.97 g at 14 h	-	0.64 g at 27 h

$PdCl_2(PPh_3)_2$, X-R-X and trimethylsilylacetylene solution (**7**) were added to a degassed suspension of copper (I) iodide and triethylamine in THF or toluene at rt under an argon atmosphere. After the reaction was completed, the solution was poured on water (50 mL) and extracted with ether (50 mL). The organic layer was washed with sat. NH_4Cl solution (3 x 50 mL), water (3 x 50 mL) and brine, dried over Na_2SO_4 and the solvent was evaporated in vacuum.

4,4'-Bis-(trimethylsilylethynyl)-diphenyl sulfide (9)

Purification: Column chromatography (silica gel, PE) gave **9** as colorless crystals that were washed with petroleum ether (2 mL, 5 °C).

Yield: 900 mg (57%) colorless crystals

$C_{22}H_{26}SSi_2$ MW: 378.69 g/mol
TLC: (PE) $R_f = 0.25$
Mp.: 128-129 °C

^{1}H NMR ($CDCl_3$): δ (ppm) = 7.36 (d, 4H, Ar-H), 7.20 (d, 4H, Ar-H), 0.22 (s, 18H, Si-Me)
^{13}C NMR ($CDCl_3$): δ (ppm) = 136.2 (Ar-C), 132.9 (Ar-C), 130.8 (Ar-C), 122.2 (Ar-C), 104.5 (C≡C), 95.6 (C≡C), 0.1 (Si-Me)
IR (ATR, cm^{-1}): 2963, 2905, 2157, 1485, 1398, 1248, 1220, 1081, 1014, 844, 818, 756

1,4-Bis-(trimethylsilylethynyl)-benzene (10)

Purification: Column chromatography (silica gel, PE) gave **10** as colorless crystals that were washed with petroleum ether (4 mL, 5 °C).

Yield: 2.19 g (89%) colorless crystals

$C_{16}H_{22}Si_2$ MW: 270.53 g/mol
TLC: (PE) $R_f = 0.40$
Mp: 154-155 °C (Lit.: 122 °C)

^{1}H NMR ($CDCl_3$): δ (ppm) = 7.39 (s, 4H, Ar-H), 0.24 (s, 18H, Si-Me)

9,10-(Trimethylsilylethynyl)-anthracene (11)

Purification: The crude product was washed with methanol (2 x 10 mL) to give **11** as orange crystals.

Yield: 1.00 g (59%) orange crystals

$C_{24}H_{26}Si_2$	MW: 370.65 g/mol
TLC: (PE)	$R_f = 0.33$
Mp: 224 °C (Lit.: 225 °C)	

^{1}H NMR ($CDCl_3$): δ (ppm) = 8.50-8.40 (m, 4H, Ar-H), 7.54-7.42 (m, 4H, Ar-H), 0.30 (s, 18H, Si-Me)

4.1.2 Synthesis of sulfonium salts (3P - 5P, 6T and 7P)

4.1.2.1 Synthesis of sulfonium triflates (3T-5T)

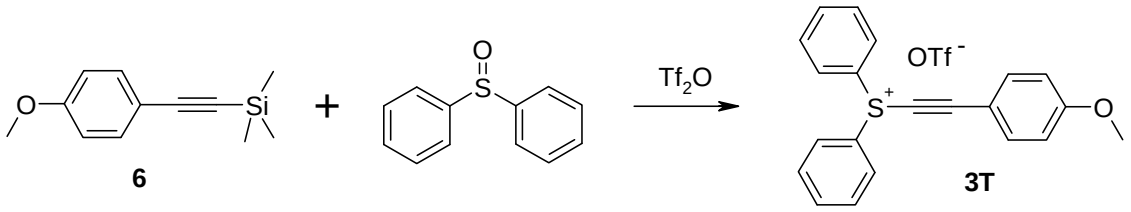

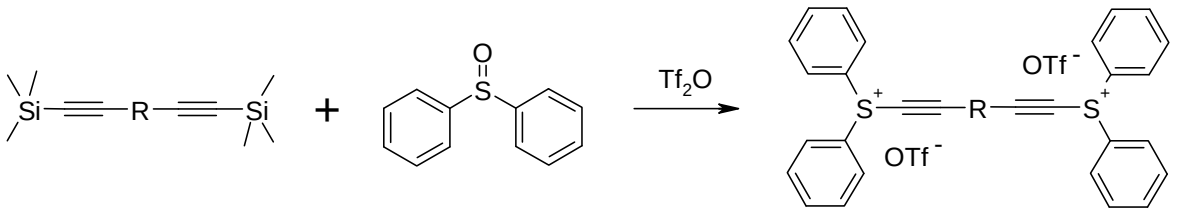

Structure: **4T**: R = 4,4'-

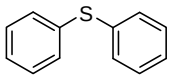

5T: R = 1,4-

Reagents	3T	4T	5T
diphenyl sulfoxide	0.52 g (2.55 mmol)	0.33 g (1.62 mmol)	0.52 g (2.55 mmol)
Tf_2O	0.72 g (2.55 mmol)	0.46 g (1.62 mmol)	0.72 g (2.55 mmol)
6	0.52 g (2.55 mmol)	-	-
9	-	0.31 g (0.81 mmol)	-
10	-	-	0.33 g (1.20 mmol)

Trifluoromethanesulfonic acid anhydride (Tf_2O) was added to a solution of diphenyl sulfoxide in dry CH_2Cl_2 (15 mL) within 10 min under argon at -70 °C and the reaction mixture was stirred at -30 °C for 30 min. The trimethylsilyl acetylene precursor (**6, 9-11**) in dry CH_2Cl_2 (5 mL) was added at -70 °C and the reaction mixture was stirred at -10 to -20 °C for 5 h. The reaction mixture was diluted with CH_2Cl_2 (50 mL),

washed with water (3 × 50 mL) and the combined aqueous layers were extracted with CH_2Cl_2 (2 x 20 mL). The combined organic layers were dried over molecular sieve (4Å) and concentrated in vacuum.

Diphenyl(p-methoxyphenylethynyl)sulfonium triflate (3T)

Purification: washed with petroleum ether (3 x 4 mL)

Yield: 505 mg (42%) reddish oil

$C_{21}H_{17}OS$. CF_3SO_3 MW: 466.50 g/mol

^{1}H NMR (DMSO-d_6): δ (ppm) = 8.13-7.38 (m, 12H, Ar-H), 7.00-6.84 (m, 2H, Ar-H), 3.83 (s, 3H, O-Me)
IR (ATR, cm^{-1}): 3073, 2175, 1602, 1511, 1477, 1448, 1259, 1224, 1150, 1030, 1000, 879, 783, 744

(Thiodi-4,1-ethynylphenylen)bis(diphenylsulfonium) dihexafluorophosphate (4T)

Purification: washed with petroleum ether (3 x 4 mL)

Yield: 623 mg (85%) orange oil

$C_{40}H_{28}S_3$. CF_3SO_3 MW: 903.00 g/mol

^{1}H NMR ($CDCl_3$): δ (ppm) = 8.10-7.06 (m, 28H)
IR (ATR, cm^{-1}): 3069, 2187, 1686, 1586, 1479, 1447, 1401, 1260, 1224, 1151, 1085, 1030, 999, 873, 824, 817, 744

(1,4-Diethynylphenylen)bis(diphenylsulfonium) dihexafluorophosphate (5T)

Purification: washed with a mixture of CH_2Cl_2 and petroleum ether (1:1)

Yield: 520 mg (55%) colorless crystals

$C_{34}H_{24}S_2 . (CF_3SO_3)_2$ MW: 794.84 g/mol

Mp.: decomposes at 180 °C

^{1}H NMR (DMSO-d_6): δ (ppm) = 8.10-7.72 (m, 20H), 7.64 (bs, 4H)

IR (ATR, cm^{-1}): 3102, 2197, 1477, 1454, 1406, 1258, 1224, 1152, 1029, 999, 873, 746

4.1.2.2 Ion exchange

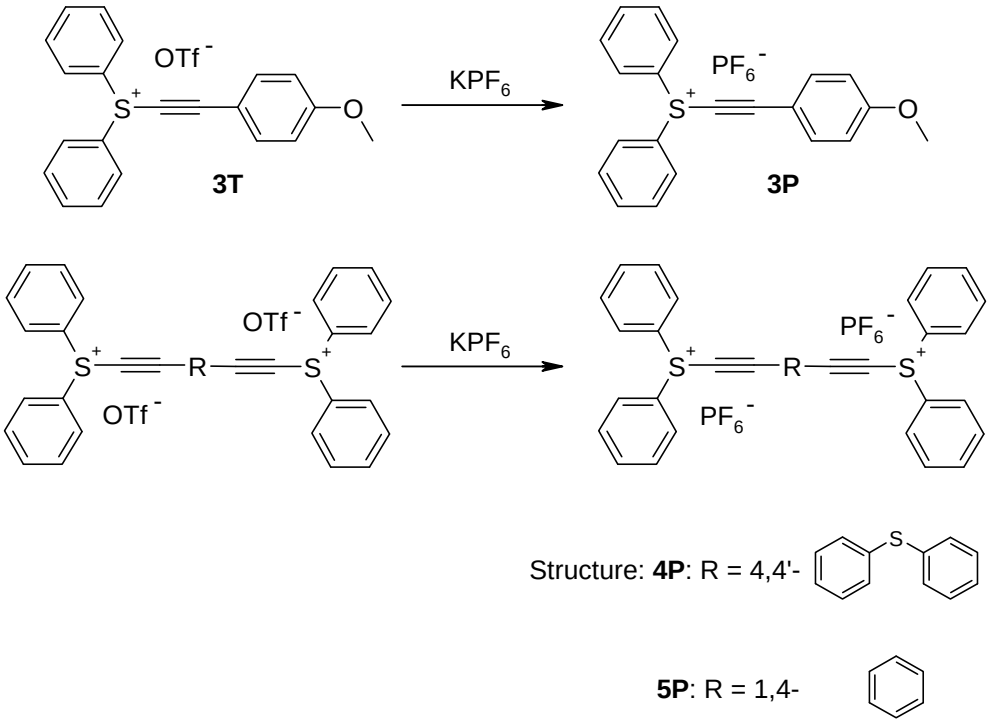

Product	Reagent
3P	0.50 g (1.07 mmol) Diphenyl(p-methoxyphenylethynyl)sulfonium triflate (**3T)**
4P	0.61 g (0.68 mmol) (Thiodi-4,1-ethynylphenylen)bis(diphenylsulfonium) triflate **(4T)**
5P	0.50 g (0.63 mmol) (1,4-Diethynylphenylen)bis(diphenylsulfonium) triflate **(5T)**

Procedure:

A 0.1 M solution of the onium salt in CH_2Cl_2 was added to a concentrated solution of 5 equiv. of potassium hexafluorophosphate and the mixture was thoroughly stirred for 30 min at rt. The aqueous layer was extracted with CH_2Cl_2 and the combined organic layers were dried over molecular sieve (4Å) and concentrated in vacuum.

Purification:

3P and **4P** were washed with petroleum ether. **5P** was washed with a mixture of CH_2Cl_2 and petroleum ether (1:1). In case of a residual concentration (FT IR) of onium triflate (> 5 mol%) the ion exchange process was repeated.

Yield	Product
0.47 g (95%) reddish oil	**Diphenyl(p-methoxyphenylethynyl)sulfonium hexafluorophosphate (3P)** $C_{21}H_{17}OS$. PF_6 MW: 462.39 g/mol ^{1}H NMR ($CDCl_3$): δ (ppm) = 8.11-7.40 (m, 12H, Ar-H), 7.02-6.88 (m, 2H, Ar-H), 3.85 (s, 3H, O-Me) ^{13}C NMR ($CDCl_3$): δ (ppm) = 136.3, 135.1, 132.0, 131.1, 129.7, 129.2, 128.1, 115.0, 108.2, 61.0, 55.8 IR (ATR, cm^{-1}): 3073, 2175, 1602, 1511, 1477, 1448, 1305, 1176, 1070, 1024, 1000, 879, 825, 744
0.58 g (89%) orange oil	**(Thiodi-4,1-ethynylphenylen)bis(diphenylsulfonium) hexafluorophosphate (4P)** $C_{40}H_{28}S_3$. $(PF6)_2$ MW: 894.78 g/mol ^{1}H NMR (DMSO-d_6): δ (ppm) = 8.13-7.09 (m, 28H) Due to low solubility, no ^{13}C NMR could be measured. IR (ATR, cm^{-1}): 3071, 2187, 1686, 1586, 1479, 1447, 1401, 1224, 1085, 1030, 999, 824, 744
0.45 g (92%) colorless crystals	**(1,4-Diethynylphenylen)bis(diphenylsulfonium) hexafluorophosphate (5P)** $C_{34}H_{24}S_2$. $(PF_6)_2$ MW: 786.62 g/mol ^{1}H NMR (DMSO-d_6): δ (ppm) = 8.12-7.76 (m, 20H), 7.69 (bs, 4H) ^{13}C NMR (DMSO-d_6): δ (ppm) = 142.3, 134.8-128.7, 125.6 IR (ATR, cm^{-1}): 3103, 2196, 1477, 1453, 1407, 1019, 999, 973, 818, 745

4.1.2.3 Synthesis of (2-isopropoxy-2-phenyl-vinyl)-diphenyl-sulfonium hexafluorophosphate (7P)

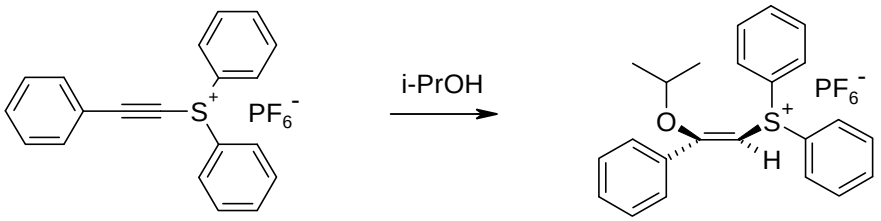

1P **7P**

Reagents:	660 mg	1.57 mmol	diphenyl(phenylethynyl)sulfonium hexafluorophosphate (**1P**)
	60 mL		2-propanol

1P was suspended in 2-propanol, the reaction mixture was stirred for 12 h at reflux and the solvent was evaporated in vacuum. The reaction mixture was diluted with CH_2Cl_2 (20 mL), washed with water (3 × 20 mL) and the combined aqueous layers were extracted with CH_2Cl_2 (2 x 10 mL). The combined organic layers were dried over molecular sieve (4Å) and concentrated in vacuum. The residue was recrystallized from 2-propanol to give **7P** as colorless crystals. ^{1}H NMR analysis in $CDCl_3$ gave a distribution of isomers of **7P** of **E** : **Z** = 1 : 16.

Yield: 425 mg (55%) colorless crystals

$C_{23}H_{23}OS$. PF_6 MW: 492.47 g/mol

Mp.: 132-136 °C

^{1}H NMR ($CDCl_3$): δ (ppm) = 7.89-7.77 (m, 4H [**Z**+**E**], Ar-H), 7.72-7.65 (m, 8H [**Z**+**E**], Ar-H), 7.54-7.42 (m, 3H [**Z**+**E**], Ar-H), 6.10 (s, 0.06H [**E**], C=C-H), 6.04 (s, 0.94 [**Z**], C=C-H), 5.08 (sept. 0.06H [**E**], C-H), 4.51 (sept. 0.94H [**Z**], C-H), 1.43 (d, 0.36H [**E**], CH_3), 1.21 (d, 5.64H [**Z**], CH_3)

^{13}C NMR ($CDCl_3$): δ (ppm) = **Z**: 173.0 (C=<u>C</u>-O), 134.2 (Ar-H), 132.6 (Ar-H), 131.7 (Ar-H), 130.5 (Ar-H), 129.6 (Ar-H), 129.5 (Ar-H), 128.3 (Ar-H), 128.1 (Ar-H), 91.4 (C=<u>C</u>-S^+), 77.1 (<u>C</u>-CH_3), 22.1 (CH_3)

IR (ATR, cm^{-1}): 3090, 2986, 1596, 1562, 1480, 1450, 1310, 1225, 1183, 1081, 1026, 1001, 932, 878, 823, 740

Materials and Methods

Reagents and solvents were - unless otherwise noted - all applied in a quality that is common for organic synthesis and - if necessary - purified. All solvents were distilled before use. Anhydrous solvents were dried with common procedures. **UDMA** was received from Ivoclar Vivadent AG, **ECHC** from Bodo Möller Chemie GmbH and **R18** from UPPC GmbH as gifts.

For **thin layer chromatography (TLC)** aluminum foils, coated with silicagel 60 F_{254} from the company Merck were applied. Column chromatography was performed using silicagel 60 (Merck, 40-60 µm).

ATR FTIR spectra were measured with an ATR-arrangement using a Biorad FTS-135 IR device. **FT IR spectra** were measured with a Perkin Elmer System 2000 FT IR spectrometer.

Photo-DSC experiments were conducted with a Netzsch DSC 204 F1 Phoenix with autosampler and UV-Vis-irradiation device (EXFO Omnicure 2001, 280 - 450 nm, 3 W cm^{-2}, double light guide 3 mm) or with a modified Shimadzu DSC 50 device and filtered UV-Vis light that was applied by the aid of a light guide (EFOS-Novacure, 250 - 450 nm or 320 - 500 nm, 13.83 mW cm^{-2}) and a self-made aluminum block.

^{1}H NMR and **^{13}C NMR** spectra were measured with a BRUKER AC-E-200 FT NMR spectrometer.
The chemical shift is displayed in ppm (s = singlet, d = duplet, t = triplet, q = quartet, m = multiplet, dd = duplet on duplet, bs = broad signal). Deuterated chloroform ($CDCl_3$) and deuterated dimethyl sulfoxide (d_6-DMSO) were used as solvents (deuteration grade 99.5% and 99.8%).

The preparation and analysis of photosensitive compounds or mixtures was performed in a **red light laboratory**. Adhesive filter foils from the company IFOHA (Art. Nr. 11356) were used to cover the windows and the fluorescent lamps.

HPLC analysis was performed on a Hewlett Packard Series 1100 Chemstation high-performance liquid chromatography system with a Waters XTerra MS C18 column (particle size = 5 μm, 150 × 3.9-mm i.d.) and a diode array detector.

GC MS spectrometry was performed on a Hewlett Packard 5890A gas chromatograph with a 5970B series mass selective detector with HP 7673A automatic sampler and fused silica capillary columns (Supelco, SPB-5, 60 m x 0.25 mm as well as Perkin-Elmer, 25 m x 0.32 mm). MS spectra were recorded with EI ionization (70 eV) and a quadrupole analyzer.

UV-Vis spectra

The range of wavelength applied for UV-Vis curing systems in technical applications is usually in the region of 250 to 500 nm. UV-Vis spectroscopy is an important tool to gain an overview of the range of wavelength a photoinitiator (PI), sensitizer or oxygen scavenger (OS) is able to absorb, and thus to form electronically excited states. A high light absorption and thus a high extinction coefficient is not necessarily an indication for a good quantum yield. Therefore, it is not possible to draw conclusions from spectral data obtained by UV-Vis spectroscopy on the efficiency of the light absorbing system as a photo-reactive compound. However, a good adjustment of the light absorbing systems and the emission spectrum of the light source is a crucial factor for an optimal performance of a UV-Vis curing system.

The 3 prerequisites for solvents that can be applied in UV-Vis spectroscopy are:

- A good solubility of the substance that has to be analyzed.
- No absorption of the solvent in the chosen wavelength range.
- No chemical reaction between the substance that has to be analyzed and the solvent.

In the presented work, all UV-Vis spectra were recorded in acetonitrile (HPLC grade) which has no light absorption above 200 nm.

The most important values gained by UV-Vis spectroscopy are the wavelengths of maximum absorption (λ_{max}) which are directly accessible from the spectrum and the corresponding extinction coefficients which can be calculated from the Beer-Lambert law. (eq. 4)

$$A = \varepsilon \times c \times l \qquad (4)$$

ε	extinction coefficient [L mol^{-1} cm^{-1}]
l	path length [cm]
c	concentration [mol L^{-1}]
A	absorption

The concentration of the measured solutions were in the range of 1 x 10^{-3} to 1 x 10^{-6} mol L^{-1}. UV-Vis spectra were recorded on a Hitachi U-2001 spectrophotometer with the following instrument settings:

path length	1 cm
wavelength area	500-200 nm
scan speed	100 nm/s
lamp change	400 nm

Melting points were determined on a Zeiss Axioskop microscope with a heating system of the company Leitz and are uncorrected.

Conclusion

In the present work, two different approaches to minimize the undesired effect of oxygen inhibition in radiation curable coatings are investigated. In a first approach, the photosensitized generation of singlet oxygen and subsequent scavenging of this species by selective singlet oxygen trappers was presented as a straightforward method to reduce the oxygen inhibition in radical photocuring of methacrylate formulations. For a possible application of this technique without use of colored sensitizers in UV-Vis curing, the structures **4** and **5** were synthesized as examples of bathochromic shifted and conjugated furan-based systems.

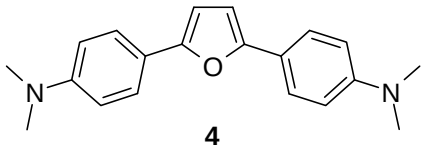

4

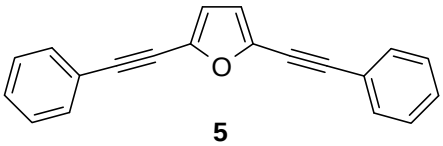

5

Storage stability tests proved a sufficient shelf life towards methacrylates and ground state oxygen for a possible application in radical curing formulations. However, in comparison with the highly reactive oxygen scavengers diphenylfuran (**DPF**) and 9,10-dibutylanthracene (**DBA**), the new furan based systems exhibited a reduced reactivity to undergo cycloaddition reactions with singlet oxygen in sensitized steady state photooxidations (SSSP). In particular the conjugated furan **5** showed a significantly reduced reactivity due to the incorporation of triple bonds into the diphenylfuran base structure in all performed steady state photooxidations. In contrast to **5**, the bathochromic shifted furan **4** exhibited an over all reaction rate that was very well comparable with **DPF** in steady state photooxidations without application of a sensitizer due to an improvement of the absorption behavior. Unfortunately, no positive effect of both new structures as oxygen scavengers could be verified in thin film polymerization. In contrast to **5**, which obviously exhibited a too low reactivity towards singlet oxygen to reduce the oxygen inhibition, the furan **4** was found to interfere with the applied **CQ** / **DMAB** photoinitiator system in Photo-DSC experiments.

In a second approach, cationic polymerization is used as an option to completely evade the problem of inhibition by oxygen in thin film applications of UV-Vis curing. Since most base structures of photoinitiators for cationic polymerization are limited to absorption of light in UV-C, scientific work on new initiators with an improved light absorption or utilization of sensitizers is mandatory for an application of this technique in UV-Vis curable coatings. Therefore, two new base structures, diphenyl(phenylethynyl)sulfonium and phenyl(phenylethynyl)iodonium salts capable of photo-acid-generation are presented and simple, straightforward synthetic routes to the hexafluorophosphate salts **1P** and **2P** of these structures as photoinitiators for cationic polymerization are described.

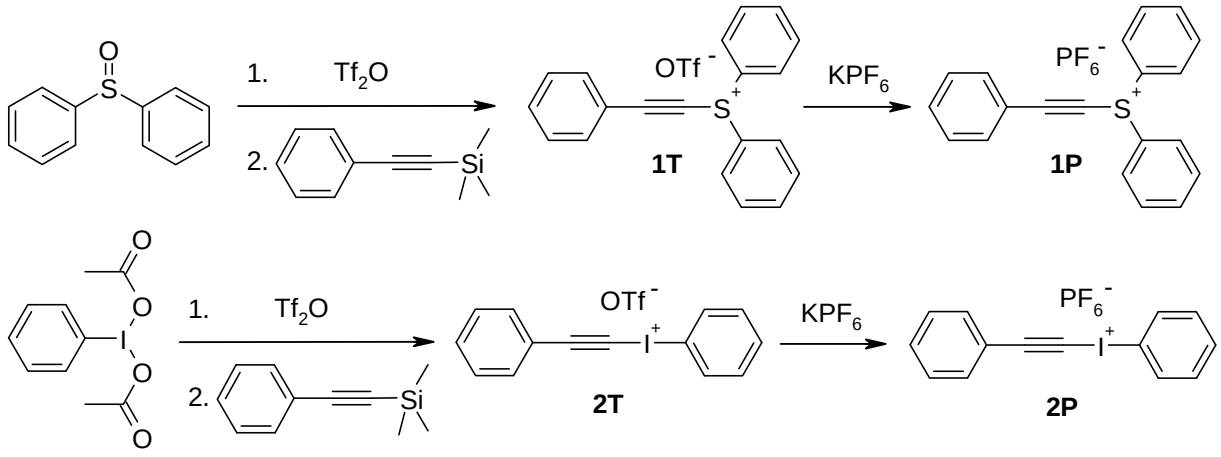

FT IR spectroscopy with subsequent mathematical peak deconvolution was employed as a plain and accurate method for analysis of the completeness of the counterion exchange, that is easily adaptable for a broad variety of onium salt initiators. Steady state photolysis with subsequent GC MS and HPLC analysis was applied to determine the photodecomposition products. Diphenyl sulfide and phenyl(phenylethynyl) sulfide in a ratio of 8 : 1 in case of **1P** and iodobenzene for **2P** were found to be the main photoproducts. No products formed by reactions of phenyl radicals, including benzene, were detectable. In photo-DSC experiments, the activity of **1P** and **2P** as photoinitiators in cationic photopolymerization was demonstrated. The high reactivity of the phenyl(phenylethynyl) onium salts in direct irradiation and sensitized initiation with **DBA**, 2-isopropylthioxanthone (**ITX**) and benzophenone (**BP**) was confirmed by comparison with their corresponding phenyl onium salts diphenyliodonium

hexafluorophosphate (**DPI-P**) and triphenylsulfonium hexafluorophosphate (**TPS-P**). In contrast to most other onium salts, a capability of **ITX** and **BP** to act as sensitizers for **1P** and **2P** was shown.

In these photo-DSC experiments, **DBA** was introduced as a new, photo-bleaching sensitizer for UV-Vis curing that exhibited an excellent activity as a sensitizer comparable to the well established **ITX**. In contrast to the thioxanthone **ITX**, the anthracene **DBA** was proved to be able to sensitize common phenyl sulfonium base structures like **TPS-P**. Due to this promising results, **DBA** was examined in more detail in broad band irradiation photo-DSC experiments as a new sensitizer for the well known onium salt initiators (4-dodecyl)bis(diphenyliodonium) hexafluoroantimonate (**DI**) and a commercial mixture of diphenyl(4-phenylthio)phenyl sulfonium and (thiodi-4,1-phenylene)bis(diphenylsulfonium) hexafluorophosphate (**SPS**). In all conducted photo-DSC experiments in broad band irradiation, the anthracene **DBA** exhibited a superior activity as a sensitizer compared to **ITX** and optimal application concentrations of **DBA** were determined for the commercial photoinitiators.

Based on the phenyl(phenylethynyl) onium salt structure **1P**, the bathochromic shifted and conjugated sulfonium salts **3P - 5P** were prepared using an analogue procedure for the formation of the sulfonium structure from TMS-acetylene precursors. Furthermore, the conjugated vinyl-sulfonium salt **7P** was obtained by thermal addition of 2-propanol to **1P**.

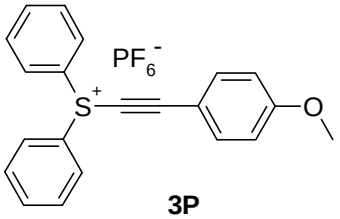

3P

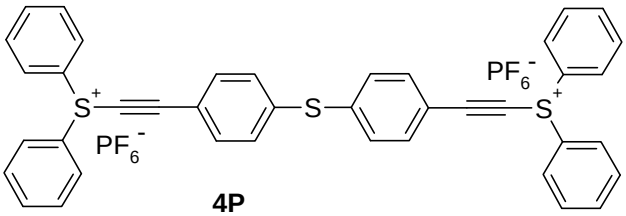

4P

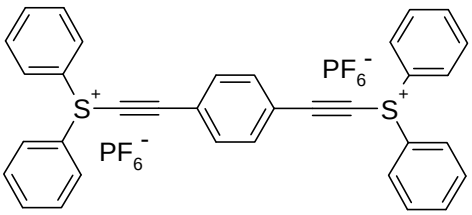

5P

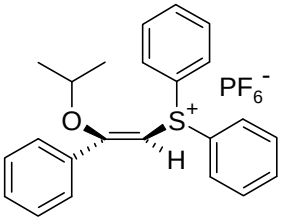

7P

UV-Vis spectroscopy was applied to show a significant improvement of the absorption behavior of **4P** and **5P** in comparison to the base structure **1P**. Both new sulfonium salts exhibit absorptions up to and above 400 nm, a prerequisite for a possible application in near visible light polymerization. Comparative Photo-DSC experiments of the sulfonium salts proved a reduction of the reactivity as initiators of the bathochromic shifted structures **3P**, **4P** and the vinyl-sulfonium salt **7P** compared to **1P** in both direct irradiation and sensitized initiation. In case of the conjugated sulfonium salt **5P**, a significant increase of the performance as an initiator in direct irradiation compared to **1P** could be verified although a decrease of activity in combination with sensitizers in comparison to **1P** was noted.

Abbreviations

ATR IR	Attenuated Total Reflectance Infrared Spectroscopy
BP	benzophenone
CQ	camphorquinone
DAD	Diode Array Detector
DBA	9,10-dibutyl-anthracene
DBC	double bond conversion
DI	(4-dodecyl)bis(diphenyliodonium) hexafluoroantimonate
DMA	9,10-dimethyl-anthracene
DMAB	ethyl 4-(dimethylamino)benzoate
DMF	dimethylformamide
DMSO	dimethyl sulfoxide
DPBF	2,5-diphenyl-isobenzofuran
DPF	2,5-diphenylfuran
ε	extinction coefficient
ECHC	3,4-epoxycyclohexenylmethyl-3',4'-epoxycyclohexenyl carboxylate
EGC	epoxy group conversion
FT IR	Fourier Transform Infrared Spectroscopy
GC MS	Gas Chromatography - Mass Spectrometry
h	height of the peak (DSC)
HPLC	High Pressure Liquid Chromatography
ΔH_P	heat of polymerization
$\Delta H_{0,P}$	theoretical heat of polymerization
i-PrOH	propan-2-ol
ITX	2-isopropylthioxanthone
λ_{max}	wavelength of maximum absorption
MB	methylene blue
MeCN	acetonitrile
M_M	molecular weight of the monomer

n-BuLi	n-butyllithium
NMR	Nuclear Magnetic Resonance
OS	oxygen scavenger
PE	petroleum ether
photo-DSC	Differential Scanning Photocalorimetry
PTSA	toluene-4-sulfonic acid
R_p	rate of polymerization
rt	room temperature
R_v	rate of decomposition
R18	1,6-bis(2,3-epoxypropoxy)hexane
SPS	mixture of diphenyl(4-phenylthio)phenyl sulfonium and (thiodi-4,1-phenylene)bis(diphenylsulfonium) hexafluorophosphate
SSSP	Sensitized Steady State Photooxidation
Tf_2O	trifluoromethanesulfonic acid anhydride
THF	tetrahydrofuran
TLC	Thin Layer Chromatography
t_{max}	time to reach the peak maximum
TMSCl	trimethylsilylchloride
UDMA	1,6-bis(methacryloxy-2-ethoxycarbonylamino)-2,4,4-trimethylhexane

References

[1] Rehse, G. *"Development of inks"* Farbe und Lack; 1970; **76** (12); 1222-1225.

[2] Herz, C. P.; Eichler, J.; Neisius, K. H.; Ohngemach, J. *"UV Radiation curing, Part2"* Kontakte; 1980; **3**; 15-20.

[3] Allen, N. S.; Edge, M. *"UV and elektron beam curing"* J. Oil Colour Chem. Assoc.; 1990; **73** (11); 438-445.

[4] Bett, S. J.; Dworjanyn, P. A.; Garnett, J. L. *"UV and EB [electron beam] curing"* J. Oil Colour Chem. Assoc.; 1990; **73**; 446-453.

[5] Senich, G. A.; Florin, R. E. *"Radiation curing of coatings"* JMS-Rev. Macromol. Chem. Phys.; 1984; **C 24** (2); 239-324.

[6] Kirchmayr, R.; Berner, G.; Rist, G. *"Photoinitiators for UV curing of paints"* Farbe und Lack; 1980; **86** (3); 224-230.

[7] Shahidi, I. K.; Powanda, T. M. *"Ultraviolet curing. Review of the technologie"* Am. Ink Maker; 1975; **53** (1); 20-26.

[8] Davis, M.; Doherty, J.; Godfrey, A. A.; Green, P. N.; Young, J. R. A.; Parrish, M. A. *"The UV-curing behavior of some photoinitiators and photoactivators"* J. Oil Colour Chem. Assoc.; 1978; **61** (7); 256.

[9] Kinstle, James F. *"Polymerization by uv radiation. II. Free radical homopolymerization in liquid systems."* Journal of Radiation Curing; 1974; **1** (2); 2-18, 25.

[10] Pappas, S. P. *"Photochemical aspects of uv curing"* Progr. Org. Coatings; 1974; **2** (4); 333-347.

[11] Osborn, C. L. *„Photoinitiation systems and their role in UV-curable coatings and inks"* J. Rad. Curing.; 1976; **3** (3); 2-3, 5-11.

[12] Ledwith, A. *"Photoinitiation by aromatic carbonyl compounds"* J. Oil Colour Chem. Assoc.; 1976; **59** (5); 157.

[13] Davidson, R. S.; Orton, S. P. *"Photo-induced electron-transfer reactions. Fragmentation of 2-aminoethanols"* J. Chem. Soc., Chem. Comm.; 1974; 209.

[14] Oster, G.; Yang, N. L. *"Photopolymerization of vinyl monomers"* Chem. Rev.; 1968; **68** (2); 125.

[15] McGinnis, V. D.; Dusek, J. M. *"Comparative kinetics of ultraviolet curable coating systems"* J. Paint Technology; 1974; **46**; 23-30.

[16] Gruber, H. F. *"Photoinitiators for free radical polymerization"* Prog. Polym. Sci.; 1992; **17** (6); 953-1044.

[17] Bonamy, A.; Fouassier, J. P.; Lougnot, D. J.; Green, P. N. *"Novel and efficient water-soluble photoinitiator for polymerization"* J. of Polymer Science, Polymer Letters Edition; 1982; **20** (6); 315-320.

[18] Dietliker, K. In Chemistry & Technology of UV & EB Formulation for Coatings, Inks & Paints Vol. 3; *"Photoinitiators for Free Radical and Cationic Polymerisation"*; SITA Technology Ltd.; London UK (**1991**).

[19] Fouassier, J. P. In Radiation curing in polymer sience and technology; Elsevier Appl. Sci. Vol.II: Photoinitiating Systems; 717ff; (**1993**).

[20] Jakubiak, J.; Rabek, J. F. *"Photoinitiators for visible light polymerization"* Polimery; 1999; 7-8; 447-461.

[21] Rees, M. T. L.; Russel, G. T.; Zammit, M. D.; Davis, T. P. *„Visible Light Pulsed-OPO-Laser Polymerisation at 450 nm Employing a Bis(acylphosphine oxide) Photoinitiator"* Macromolecules; 1998; **31** (6); 1763-1772.

[22] Studer, K.; Decker, C.; Beck, E.; Schwalm, R. *"Overcoming oxygen inhibition in UV-curing of acrylate coatings by carbon dioxide inerting, Part I."* Progress in Organic Coatings; 2003; **48** (1); 92-100.

[23] Fouassier, J.-P. In Photoinitiation, Photopolymerization, and Photocuring: Fundamentals and Applications; Hanser/Gardner: Cincinnati, Ohio, 1995.

[24] Hoyle, C. E. *"An overview of oxygen inhibition in photocuring."* Technical Conference Proceedings - UV & EB Technology Expo & Conference, Charlotte, NC, United States, May 2-5, 2004, 892-899.

[25] Gou, L.; Opheim, B.; Scranton, A. B. *"The effect of oxygen in free radical photopolymerization"* Recent Research Developments Polymer Science; 2004; **8**; 125-141.

[26] Crivello, J. V.; Dietliker, K. In Photointiators for free Radikal Cationic & Anionic Photopolymerisation, 2nd Edition; Bradley, G., ed.; Wiley, New York, 1999.

[27] Studer, K.; Decker, C.; Beck, E.; Schwalm, R. *"Overcoming oxygen inhibition in UV-curing of acrylate coatings by carbon dioxide inerting: Part II."* Progress in Organic Coatings; 2003; **48** (1); 101-111.

[28] Bolon, D. A.; Webb, K.K. *"Barrier coats versus inert atmospheres. The elimination of oxygen inhibition in free-radical polymerizations"* Journal of Applied Polymer Science; 1978; **22** (9); 2543-51.

[29] Ali, M. Z. *"High Speed Photopolymerzable with Initiator in a Topcoat."* US.Pat.Appl.; US 4988607; 1991

[30] Bradley, G.; Davidson, R. S. *"Some aspects of the role of amines in the photoinitiated polymerisation of acrylates in the presence and absence of oxygen"* Recl. Trav. Chim. Pay-Bas; 1995, **114**, 528-533.

[31] Selli, E.; Bellobono, I. R. *"Photopolymerization of Multifunctional Monomers: Kinetic Aspects."* In Radiation Curing in Polymer Science and Technology; Fouassier, J.-P., Rabek, J. F., Eds.; Elsevier Applied Science: London, 1993. Vol. 3 : Polymerization Mechanisms

[32] Allen, N. S., Johnson, M. A., Oldring, P. K. T., Salim, M. S. In Chemistry & Technology of UV & EB Formulation for Coatings, Inks & Paints, Oldring, P. K. T., ed., SITA Technology: London, 1991, Vol. 2: Prepolymers and Reactive Diluents for UV and EB Curable Formulations

[33] Schaefer, F. C.; Zimmermann, W. D. *"Dye-sensitized photochemical autoxidation of aliphatic amines in nonaqueous media."* J. Org. Chem.; 1970; **35** (7); 2165-74.

[34] Miller, C. W.; Jonsson, S.; Hoyle, C. E.; Yang, D.; Kuang, W. F.; Kess, R.; Iijima, T.; Nason, C.; Ng, L.-T. In Experience the World of UV/EB, RadTech 2000: The Premier UV/EB Conference & Exhibition, Baltimore, MD, US, Apr 9-12, 2000, 754-772.

[35] Schwetlick, K. *"Mechanisms of antioxidant action of organic phosphorus compounds."* Pure and Applied Chemistry; 1983; **55** (10); 1629-36.

[36] Kuang, W.; Hoyle, C.E.; Vishwanathan, K.; Jonsson, S.; *"Oxygen scavening effects of phosphorus compounds in photopolymerization."* RadTech North America 2002 Conf.Proc.; 2002; 292-299.

[37] Krongauz, V. V.; Chawla, C. P. *"Revisting aromatic thiols effects on radical photopolymerization"* Polymer; 2003; **44**; 3871-3876.

[38] Cokbaglan, L.; Arsu, N.; Yagci, Y.; Jockusch, S.; Turro, N. J. *"2-Mercaptothioxanthone as a Novel Photoinitiator for Free Radical Polymerization"* Macromolecules; 2003; **36**; 2649-2653.

[39] Davidson, R. S.; Goodin, J. W. *"Some studies on the photoinitiated cationic polymerization of epoxides."* European Polymer Journal; 1982; **18** (7); 589-595.

[40] Crivello, J. V.; Lam, J. H. W. *"Photoinitiated cationic polymerisation wtih triarylsulfonium salts"* J. Polym. Sci. Part A: Polym. Chem.; 1979; **17** (4); 977-999.

[41] Dektar, J. L.; Hacker, N. P. *"Triphenylsulfonium salt photochemistry. New evidence for triplet excited state reactions."* J. Org. Chem.; 1988; **53** (8); 1833-1835.

[42] Welsh, K. M.; Dektar, J. L.; Hacker, N. P.; Turro, N. J. *"Photo-CIDNP and nanosecond flash photolysis studies on the photodecomposition of triarylsulfonium and diarylhalonium salts."* Polym. Mater. Sci. Eng.; 1989; **61**; 181-184.

[43] Crivello, J. V.; Radiaton Curing Workshop, ACS Meeting, Dallas; (**1989**)

[44] Crivello, J. V.; Lam, J. H. W. *"Dye-sensitized photoinitiated cationic polymerization."* J. Polym. Sci., Polym. Chem. Ed.; 1978; **16** (10); 2441-2451.

[45] Pappas, S.P. In Photopolymerization and Photoimaging Science and Technology; Allen, N.S.; Ed.; Elsevier Applied Science: London 1989, 55.

[46] Bachofner, H. E.; Beringer, F. M.; Meites, L. *"Diaryliodonium salts. V. The electroreduction of diphenyliodonium salts."* J. Am. Chem. Soc.; 1958; **80**; 4269-4274.

[47] McKinney, P. S.; Rosenthal, S. *"Electrochemical reduction of the triphenyl-sulfonium ion."* Journal of Electroanalytical Chemistry and Interfacial Electrochemistry; 1968; **16** (2); 261-270.

[48] Adams, W. R. *"Reaktionen unter Sauerstoffaufnahme (Photooxidatio*n)" in Houben-Weyl, Methoden der Organischen Chemie, Georg Thieme Verlag Stuttgart; 4. Auflage; 1975; VIb; 1465-99.

[49] Mazur, S.; Foote, C. S. *"Chemistry of singlet oxygen. IX. Stable dioxetane from photooxygenation of tetramethoxyethylene."* J. Am. Chem. Soc.; 1970; **92** (10); 3225-6.

[50] Sawaki, Y.; Foote, C. S. *"Mechanism of photoepoxidation of olefins with α-diketones and oxygen."* J. Org. Chem.; 1983; **48** (25); 4934-40.

[51] Decker, C. *"A novel Method for Consuming Oxygen Instantaneously in Photopolymerizable Films"* Macromolecular Chemistry; 1979; **180**; 2027-2030.

[52] Gou, L.; Opheim, B.; Coretsopoulos, C.; Scranton, A. B. **"***Consumption of the molecular oxygen in polymerization systems using photosensitized oxidation of dimethylanthracene.***"** Chemical Engineering Communications; 2006; **193** (5); 620-627.

[53] Gou, L.; Coretsopoulos, C. N.; Scranton, A. B. *"Reduction of oxygen inhibition in free-radical photopolymerization."* Polymer Preprints (American Chemical Society, Division of Polymer Chemistry); 2004; **45** (2); 39-40.

[54] Gou, L.; Scranton, A. *"A photochemical method to eliminate oxygen inhibition in photocured systems."* Technical Conference Proceedings - UV & EB Technology Expo & Conference, Charlotte, NC, United States, May 2-5; 2004; 230-241.

[55] Gou, L.; Coretsopoulos, C. N.; Scranton, A. B. *"Measurement of the dissolved oxygen concentration in acrylate monomers with a novel photochemical method."* Journal of Polymer Science, Part A: Polymer Chemistry; 2004; **42** (5); 1285-1292.

[56] Klemm, E.; Hoerhold, H. H.; Doms, I. *"Light-curing dental materials for crowns and bridges"* Ger. (East); DD 215699; 1984

[57] Scranton, A. B.; Gou, L. *"Photochemical method to eliminate oxygen inhibition of free radical polymerizations."* PCT Int. Appl; WO 2004062781; 2004

[58] Hoefer, M.; Moszner, N.; Liska, R. *"Oxygen scavengers and sensitizers for reduced oxygen inhibition in radical photopolymerization"* Journal of Polymer Science, Part A: Polymer Chemistry; 2008; **46** (20); 6916-6927.

[59] Howard, J. A.; Mendenhall, G. D. *"Autoxidation and photooxidation of 1,3-diphenylisobenzofuran. Kinetic and product study."* Canadian Journal of Chemistry; 1975; **53** (14); 2199-2201.

[60] Young, R. H.; Martin, R. L.; Chinh, N.; Mallon, C.; Kayser, R. H. *"Substituent effects in dye-sensitized photooxidation reactions of furans."* Canadian Journal of Chemistry; 1972; **50** (6); 932-938

[61] Clark, K. J. "*Preparation of 9,10-disubstituted anthracenes."* J. Chem. Soc.; 1956; 1511-1515.

[62] Benn, R.; Bogdanovic, B.; Bruening, M.; Grondey, H.; Herrmann, W.; Kinzelmannm, H. G.; Seevogel, K. *"Preparation and characterization of inner complexes of anthrylenemagnesium."* Chemische Berichte; 1993; **126** (1); 225-237.

[63] Barba, F.; Desamparados V. M.; Guirado, A. *"Synthesis of 2,5-diarylfurans from phenacyl bromides."* Synthesis; 1984; **7**; 593-595.

[64] Nowlin, G. *"Furanization and cleavage of 1,4-diketones by use of polyphosphoric acid."* J. Am. Chem. Soc.; 1950; **72**; 5754-5756.

[65] Vachal, P.; Toth, L. M. *"General facile synthesis of 2,5-diarylheteropentalenes."* Tetrahedron Letters; 2004; **45** (38); 7157-7161.

[66] Prugh, J. D.; Huitric, A. C.; McCarthy, W. C. *"The Synthesis and Proton Magnetic Resonance Spectra of Some Brominated Furans"* J. Org. Chem.; 1964; **29**; 1991-1993.

[67] Long, R. S.; Pretka, J. E. (American Cyanamid Co.). "2,5-Bis(p-aminophenyl)furan azo derivatives." US 2852503; Sept 9, 1958.

[68] Gollnick, K.; Griesbeck, A. *"Singlet oxygen photooxygenation of furans. Isolation and reactions of (4 + 2)-cycloaddition products (unsaturated sec.-ozonides)."* Tetrahedron; 1985; **41** (11); 2057-2068.

[69] Crivello, J. V. *"Photoinitiated cationic polymerization."* Ann. Rev. Mater. Sci.; 1983; **13**; 173-190.

[70] Beringer, F. M.; Drexler, M.; Gindler, E. M.; Lumpkin, C. C. *"Diaryliodonium salts. I. Synthesis."* J. Am. Chem. Soc.; 1953; **75**; 2705-2708.

[71] Beringer, F. M.; Bachofner, H. E.; Falk, R. A.; Leff, M. *"Diaryliodonium salts. VII. Di-2-thienyl- and phenyl-2-thienyliodonium salts."* J. Am. Chem. Soc.; 1958; **80**; 4279-4281.

[72] Beringer, F. M.; Falk, R. A.; Karniol, M.; Lillien, I.; Masulio, G.; Mausner, M.; Sommer, E. *"Diaryliodonium salts. IX. Synthesis of substituted diphenyliodonium salts."* J. Am. Chem. Soc.; 1959; **81**; 342-351.

[73] Beringer, F. M.; Nathan, R. A. *"Diaryliodonium salts from aryllithium reagents with trans-chlorovinyliodoso dichloride."* J. Org. Chem.; 1969; **34** (3); 685-689.

[74] Beringer, F. M.; Nathan, R. A. *"Iodonium salts from organolithium reagents with transchlorovinyliodoso dichloride."* J. Org. Chem.; 1970; **35** (6); 2095-2096.

[75] Beringer, F. M.; Dehn, J. W.; Winicov, M. *"Diaryliodonium salts. XIV. Reactions of organometallic compounds with iodosobenzene dichlorides and with iodonium salts."* J. Am. Chem. Soc.; 1960; **82**; 2948-2952.

[76] Gronowitz, S.; Holm, B. *"Inverted reactivity of aryllithium derivatives. IV. The reaction of thienyl-aryliodonium chlorides with nucleophiles."* Tetrahedron; 1977; **33** (5); 557-561.

[77] Pitt, H. M.; *"Sulfonium compounds."* U.S. Patent 2807648 to Stauffer Chemical Company; 1957

[78] Crivello, J. V.; Lam, J. H. W. *"A new preparation of triarylsulfonium and -selenonium salts via the copper(II)-catalyzed arylation of sulfides and selenides with diaryliodonium salts."* J. Org. Chem.; 1978; **43** (15); 3055-3058.

[79] Wildi, D. S.; Taylor, S. W.; Potratz, H. A. *"Preparation of triarylsulfonium halides by the action of aryl Grignard reagents on diphenyl sulfoxide."* J. Am. Chem. Soc.; 1951; **73**; 1965-1967.

[80] Smiles, S.; Le Rossignol, R. *"Aromatic sulfonium bases."* J. Chem. Soc.; 1906; **89**; 696-708.

[81] Dougherty, G.; Hammond, P. D. *"Synthesis of aryl sulfonium salts."* J. Am. Chem. Soc.; 1939; **61**; 80-81.

[82] Crivello, J. V.; Lam, J. H. W. *"Diaryliodonium salts. A new class of photoinitiators for cationic polymerization."* Macromolecules; 1977; **10** (6); 1307-1315.

[83] Makarova, L. G.; Nesmeyanov, A. N. *"The decomposition and formation of onium salts and the synthesis of organoelemental compounds through onium compounds. I. Two types of decomposition of diphenyliodonium salts."* Bull. Acad. Sci., U.S.S.R. Classe sci. chim., 617-625 (1945); Chem. Abstr. *40*, 4686 (1946)

[84] Caserio, M. C.; Glusker, D. L.; Roberts, J. D. *"Hydrolysis of diaryliodonium salts."* J. Am. Chem. Soc.; 1959; **81**; 336-342.

[85] Dektar, J. L.; Hacker, N. P. *"A new mechanism for photodecomposition and acid formation from triphenylsulfonium salts."* J. Chem. Soc., Chem. Commun.; 1987; **20**; 1591-1592.

[86] Dektar, J. L.; Hacker, N. P. *"Photochemistry of diaryliodonium salts."* J. Org. Chem.; 1990; **55** (2); 639-647.

[87] Crivello, J. V.; Lee, J. L. *"Complex triarylsulfonium salt photoinitiators."* Polymer Photochemistry; 1982; **2** (3); 219-226.

[88] Crivello, J. V.; Lam, J. H. W. *"Photoinitiated cationic polymerization by dialkylphenacylsulfonium salts."* J. Polym. Sci. Part A: Polym. Chem.; 1979; **17** (9); 2877-2892.

[89] Ochiai, M.; Nagaoka, T.; Sueda, T.; Yan, J.; Chen, D.; Miyamoto, K. *"Synthesis of 1-alkynyl(diphenyl)onium salts of group 16 elements via heteroatom transfer reaction of 1-alkynyl(phenyl)-λ^3-iodanes"* Organic & Biomolecular Chemistry; 2003; **9** (1); 1517-1521.

[90] Koser, G. F.; Rebrovic, L.; Wettach, R. H. *"Functionalization of Alkenes and Alkynes with [Hydroxy(tosyloxy)iodo]benzene. Bis(tosyloxy)alkanes, Vinylaryliodonium Tosylates, and Alkynylaryliodonium Tosylates"* J. Org. Chem.; 1981; **46** (21); 4324-4326.

[91] Ochiai, M.; Kunishima, M.; Sumi, K.; Nagao, Y.; Fujita, E.; Arimoto, M.; Yamaguchi, H. *"Reaction of alkynyltrimethylsilanes with a hypervalent organoiodine compound: a new general synthesis of alkynyliodonium salts."* Tetrahedron Letters; 1985; **26** (37); 4501-4504.

[92] Kitamura, T.; Kotani, M.; Fujiwara, Y. *"An alternative synthesis of alkynyl(phenyl)iodonium triflates using (diacetoxyiodo)benzene and alkynylsilanes"* Synthesis; 1998; 1416-1418.

[93] Pirguliyev, N. Sh.; Brel, V. K.; Akhmedov, N. G.; Zefirov, N. S. *"An efficient ligand exchange reaction of (E)-[β -(trifluoromethanesulfonyloxy)ethenyl](phenyl)iodonium triflates with aryl- and alkynyllithium reagents leading to diaryl- and alkynyliodonium triflates."* Synthesis; 2000; **1**; 81-83.

[94] Yoshida, M.; Osafune, K.; Hara, S. *"Facile synthesis of iodonium salts by reaction of organotrifluoroborates with p-iodotoluene difluoride."* Synthesis; 2007; **10**; 1542-1546.

[95] Miller, R. D.; Renaldo, A. F.; Ito, H. *"Deoxygenation of sulfoxides promoted by electrophilic silicon reagents: preparation of aryl-substituted sulfonium salts"* J. Org. Chem.; 1988; **53**; 5571-5573.

[96] Nenajdenko, V. G.; Vertelezkij, P. V.; Balenkova, E. S. *"Synthesis of β-Dimethylsulfonium- and β-Methylthio-Substituted Vinyl Triflates by Reaction of Acetylenes with Dimethyl Sulfide Ditriflate"* Synthesis; 1997; **3**; 351-355.

[97] Bieber, L. W.; da Silva, M. F.; Menezes, P. H. *"Short and efficient preparation of alkynyl selenides, sulfides and tellurides from terminal alkynes"* Tetrahedron Letters; 2004; **45**; 2735-2737.

[98] Glass, R. S.; Guo, Q.; Liu, Y. *"Neighboring Tin Effect in the Oxidation of a-Stannyl Phenyl Vinyl Sulfides"* Tetrahedron; 1997; **53** (36); 12273-12286.

[99] Foote, C. S.; Peters, J. W. *"Chemistry of singlet oxygen. XIV. Reactive intermediate in sulfide photooxidation."* J. Am. Chem. Soc.; 1971; **93** (15); 3795-3796.

[100] Watanabe, Y.; Numata, T.; Oae, S. *"Mild and facile preparation of sulfoxides from sulfides using titanium(III) chloride/hydrogen peroxide"* Synthesis; 1981; 204-206.

[101] Kitamura, T.; Tanaka, T.; Taniguchi, H. *"Photolysis of alkynyl(phenyl)iodonium salts. Remarkable solvent effect and generation of acids."* Chemistry Letters; 1992; **11**; 2245-2248.

[102] Bonesi, S. M.; Manet, I.; Freccero, M.; Fagnoni, M.; Albini, A. *"Photosensitized Oxidation of Sulfides: Discriminating between the Singlet-Oxygen Mechanism and Electron Transfer Involving Superoxide Anion or Molecular Oxygen"* Chemistry--A European Journal; 2006; **12** (18); 4844-4857.

[103] Pappas, S. P. *"Photogeneration of acid: Part 6 - A review of basic principles for resist imaging applications."* Journal of Imaging Technology; 1985; **11** (4); 146-157.

[104] Akhtar, S. R.; Crivello, J. V.; Lee, J. L.; Schmitt, M. L. *"New synthesis of aryl-substituted sulfonium salts and their applications in photoinitiated cationic polymerization."* Chemistry of Materials; 1990; **2** (6); 732-737.

[105] Jaeger, U.; Beck, E.; Nuyken, O.; Vogel, R. *"Alkenylsulfonium salts, their preparation and use as photoinitiators."* Ger. Offen.; DE 4305332; 1993

[106] Page, P. C. Bulman, C.; Rosenthal, S. *"Simple preparation of α -bromoacylsilanes, α -ketoacylsilanes, and α-ketoesters from silyl acetylenes."* Tetrahedron; 1990; **46** (7); 2573-86.

[107] Takalo H., Kankare J., Hänninen E. *"Synthesis of some substituted dimetyl and diethyl 4-(Phenylethynyl)-2,6-pyridinedicarboxylates"* Acta Chemica Scandinavica B; 1988; **42**; 448-454.

[108] Plater, M. J.; Aiken, S.; Bourhill, G. *"A new synthetic route to donor-acceptor porphyrins."* Tetrahedron; 2002; **58** (12); 2405-2414.

[109] Bravo, A.; Dordi, B.; Fontana, F.; Minisci, F. *"Oxidation of Organic Sulfides by Br_2 and H_2O_2. Electrophilic and Free-Radical Processes"* Journal of Organic Chemistry; 2001; **66** (9); 3232-3234.

[110] Liska, R.; Herzog, D. *"New photocleavable structures. II. α-cleavable photoinitiators based on pyridines."* J. Polym. Sci. Part A: Polym. Chem.; 2004; 42 (3); 752-764.

[111] Ganster, B.; Fischer, U. K.; Moszner, N.; Liska, R. *"New Photocleavable Structures. Diacylgermane-Based Photoinitiators for Visible Light Curing."* Macromolecules; 2008; **41** (7); 2394-2400.

[112] Dworak, C.; Kopeinig, S.; Hoffmann, H.; Liska, R. *"Photoinitiating monomers based on Di- and triacryloylated hydroxylamine derivatives."* J. Polym. Sci. Part A: Polym. Chem.; 2009; **47** (2); 392-403.

[113] Ito, H.; Kidokoro, N.; Ishikawa, H. *"Differential photocalorimetric study of cationic photopolymerization."* Journal of Photopolymer Science and Technology; 1992; **5** (2); 235-246.

[114] Hansen, C. M.; Skaarup, K. *„Three-dimensional solubility parameter-key to paint component affinities. III. Independent calculation of the parameter components."* Journal of Paint Technology; 1967; **39** (511); 511-14.